Recovery, Specification, and Consistency *

Ngoc-Khanh Tran† Shixiang Xia‡ Guofu Zhou§

May 4, 2026

Abstract

Recovering market beliefs, time and risk preferences from asset prices requires specifying a subjective state space for the pricing model. Recovery results are unique to each specification but differ cross specifications and can only be mutually consistent when each specification extracts identical price information. Finer specifications do not improve the recovery consistency because they require more price information, and hence, are also more sensitive to information distortion. Using option price data, analytical methods and neural network analysis, we show that recovery inconsistencies are common and economically significant. Our findings suggest that a fully consistent recovery framework remains difficult to achieve.

Keywords: Preference recovery, Inconsistency, Specification, Information loss, Perturbative analysis.

*We are very grateful to Jack Bao, Gurdip Bakshi, Tyler Beason, Jaroslav Borovička, Peter Carr, Hui Chen, John Cochrane, Ric Colacito, Darrell Duffie, Philip Dybvig, Stefano Giglio, Ravi Jagannathan, Scott Joslin, Leonid Kogan, Raman Kumar, Anh Le, Hong Liu, Andrew MacKinlay, Asaf Manela, Ian Martin, Thomas Maurer, Jun Pan, Brad Paye, Marcel Rindisbacher, Matt Ringgenberg, Steve Ross, Ivan Shaliastovich, Ken Singleton and Andrea Vedolin for many comments and suggestions.

†Pamplin College, Virginia Tech, Email: nktran7@vt.edu.

‡Department of Economics and Finance, City University of Hong Kong, Email: shixiang.xia@cityu.edu.hk.

§Olin Business School, Washington University in St. Louis, Email: zhou@wustl.edu.

1 Introduction

Recovering market participants' rational characteristics, such as risk preferences, time preferences, and beliefs, from traded asset prices is a fundamental problem in financial economics. However, it is challenging because of a basic identification issue: even in a complete and frictionless market, different combinations of preferences and beliefs can generate the same set of asset prices. In his path-breaking paper, Ross (2015) provides the first recovery theorem that addresses this challenge by establishing sufficient conditions under which unique recovery is possible. While conceptually elegant, the practical applicability of this theorem, as well as many subsequent studies, depends on whether these uniquely recovered characteristics can be reliably obtained under the identified conditions.

This paper examines the implementability of recovery from a consistency perspective, centered on a key observation: the market's underlying state space, which is an essential input for formulating and implementing recovery, is unobserved ex ante and whose specifications are highly consequential for the recovery results. The consistency question asks whether the uniquely recovered characteristics under different subjective state space specifications are reconcilable, given that they all describe the same underlying true pricing model. By linking each specification to the price information required for recovery, the consistency problem becomes one of whether information is lost when moving from one specification to another. This connection underlies all of our findings below.

We derive a necessary and sufficient condition for recovery consistency across different subjective state space specifications. This condition requires that the underlying characteristics (marginal utilities and transition probabilities) be identical for any states that differentiate the subjective specifications. Intuitively, consistency is preserved only when switching between specifications involves states with indistinguishable fundamentals, thereby preventing information distortion. This condition is highly restrictive, indicating that a consistent recovery framework remains elusive.

We show that price information is distorted across different specifications, and that substantial distortion persists even between closely related ones. This reveals that recovery consistency problems are prevalent, significant, and persistent. The issue affects not only the original Recovery Theorem setting but also its major extensions, including best-fit, continuous-time, arbitrage-based, and generalized formulations, even in frictionless markets with perfect price

data. The reason is a misspecification: in almost all cases, the true state space is unobserved, and the specification one proposes is likely unable to capture it fully, which significantly affects the recovery process. Through qualitative, quantitative, and empirical analyses, we provide new insights into the practical limits of the recovery framework.

Quantitatively, we develop a perturbation analysis to characterize the recovery consistency problem analytically. A central tradeoff arises in choosing the subjective state space: although a finer specification appears to better capture the underlying market structure, it also produces a larger recovery system and demands substantially more price data. In contrast to the original recovery framework, where results are fully determined by the dominant eigenspace of the Arrow-Debreu (AD) price matrix, our perturbation analysis shows that the entire eigenspectrum governs the degree of inconsistency. When the spectrum is dense, higher-order eigenvalues lie close to the dominant one. The recovered characteristics - driven by the dominant eigenspace - then become highly sensitive to specification changes because they are strongly influenced by the nearby higher eigenspaces and their changes. As the full AD price matrix encodes all pricing information used in recovery, perturbations across the entire eigenspectrum accumulate and compound into the recovered characteristics when the specification changes. Consequently, even a minor adjustment in the pricing information embedded in the AD matrix can generate substantial changes in recovery results, explaining why inconsistencies persist rather than vanish as the specification becomes increasingly refined.

Empirically, we document robust recovery inconsistencies based on a set of option data. The results confirm the critical role of state space specification in the recovery process, as predicted by our theoretical perturbation analyses. Given the sparsity of option price data, we first apply a neural network method to construct stable implied volatility surfaces and the corresponding AD price matrices. We then implement recovery under alternative specifications and evaluate several measures of inconsistency. These measures increase systematically as the necessary and sufficient condition for consistency is more severely violated, providing direct evidence that specification input drives the magnitude of recovery inconsistencies. A complementary simulation analysis, in which the true underlying market model is known by construction, reinforces this result by showing that the gap between the true and recovered characteristics becomes larger as the analyst's subjective specification deviates further from the consistency condition. A simple calibration to the U.S. aggregate consumption and stock market dynamics further illustrates the direction (i.e., overshooting or undershooting) of recovery inconsistencies in the presence of

adverse economic states.

We further illustrate how the inherently subjective nature of state space specification impacts broader applications of recovery theory. Specifically, we show that this subjectivity (i) generates consistency issues in the continuous-time and other versions of the recovery framework and (ii) affects the evaluation of a well-known bound on the equity market risk premium.

In the continuous-time recovery setting, specifying the state space is equivalent to specifying the dynamics of the state variable. When these dynamics are unobserved, the common practice of applying a finite-difference procedure—an inherently subjective choice—can substantially distort both the resulting AD price matrix and the recovered outcomes. In the equity risk premium bound setting, we first implement recovery to obtain a market-based state probability distribution where the aggregate stock return serves as the state variable. We then evaluate a sufficient condition for validating the equity risk premium bound using the recovered probability distribution.[1] Because the recovered distribution depends on the subjective specification input, so does the evaluation of the condition for the equity risk premium bound. Therefore, inconsistencies among the recovered probability distributions impair an objective validation of the equity risk premium bound's sufficient condition, even though the bound itself does not depend on subjective specifications.

Related literature: There is a long-standing interest in recovering market beliefs, risk preferences, and time preferences from asset prices. Early work by Breeden and Litzenberger (1978) derives the risk-neutral distribution under a fictitious null risk aversion using option prices. Ross (2015)'s Recovery Theorem provides sufficient conditions, i.e., time-separable preferences and time-homogeneous transition probabilities, to uniquely disentangle beliefs from preferences. Subsequent literature evaluates empirical merits of these assumptions. For instance, Borovička et al. (2016) and Hansen and Scheinkman (2017) link them to the dominance and recoverability of the transitory component in the SDF decomposition of Alvarez and Jermann (2005), while Bakshi et al. (2018), Qin et al. (2018), and Jackwerth and Menner (2020) document counterfactual asset pricing implications. Our paper contributes to this literature by showing that consistent recovery remains elusive even when the Recovery Theorem's assumptions are taken as given. Our tractable perturbative analysis uncovers the role for AD price matrix's entire (both left and

[1] This sufficient condition concerns the sign of a correlation parameter (involving the market-based stochastic discount factor and the state variable) under the physical probability distribution. Hence, the determination of this probability distribution and the associated correlation parameter is a relevant application of the recovery framework.

right) eigenspace in quantifying recovery inconsistencies, complementing literature's findings on the dominant (Perron–Frobenius) eigenspace (e.g., Borovička and Stachurski (2020)).

Another strand of the literature extends the Recovery Theorem by relaxing its assumptions or generalizing its setting. Carr and Yu (2012) derive recovery in a continuous setting with bounded state variables, Walden (2017) extends this to unbounded supports, Qin and Linetsky (2016) adapts recovery to continuous-time Markov processes, and Dillschneider and Maurer (2019) explore the role of Perron–Frobenius operator theory. Further contributions include Martin and Ross (2019) on a relationship between the recovered time preference and the unconditional expected return on long-maturity bonds, Jensen et al. (2019) on relaxing time homogeneity and accommodating growing state spaces, and Horvath (2025) on recovery in a dividend-related numeraire requiring asset prices associated with only a single tenor. We show how the consistency issue exists in these extended recovery settings and further illustrate how a subjective specification can also affect the evaluation of a sufficient condition for Martin (2017)'s lower bound on the equity risk premium.[2] Note that the recovery process addresses the physical probability measure. Its consistency issue does not concern the equity risk premium bounds derived from return moments in the risk-neutral probability measure, such as the bounds obtained by Chabi-Yo and Loudis (2020) and Chabi-Yo et al. (2023).

Empirically, we follow Audrino et al. (2021), who use a neural network approach à la Ludwig (2015) and regularization to construct stable implied volatility surfaces and AD matrices from sparse option data. Building on this, we implement separate recoveries under different specifications and compare respective recovery results while preserving no-arbitrage of observable price data via the law of one price. This allows us to isolate the effect of subjective specification choices and document systematic recovery inconsistencies. Overall, our findings underscore that survey data remain a more direct channel for learning about market beliefs and complex contingent decisions, as argued by Giglio et al. (2022). In a model-free, non-parametric setting, asset prices can only provide bounds on expectations, consistent with the results of Martin (2017) and Gormsen and Koijen (2020).

The current paper is organized as follows. Section 2 briefly reviews the basic recovery framework, introduces and illustrates the consistency requirement for the recovery results. Section 3 presents the main analysis. Section 3.1 establishes a necessary and sufficient condition for

[2] Martin (2017) demonstrates that a negative correlation condition (NCC) between market return and the product of the SDF and the market return implies a lower bound for the equity risk premium.

consistent recoveries (Proposition 1), Section 3.2 quantifies the recovery consistency issue and its persistence (Proposition 2) via a perturbative analysis, Section 3.3 discusses the robustness of the recovery consistency issue in extended versions of the recovery framework. Section 4 demonstrates the prevalence and significance of recovery inconsistencies in the data. Section 5 concludes. Online appendices present methodological details, simulation, calibration, further empirical evidence and technical derivations.

2 Recovery and Consistency Requirement

This section introduces the recovery consistency and discusses its quantitative and testable characteristics. We motivate the consistency notion in the original recovery theorem setup in Section 2.1 and introduce the recovery consistency requirement in Section 2.2.

2.1 Basic Recovery Framework

A brief summary of Ross (2015)'s original recovery framework and the recovery implementation is instructive to set the stage for our recovery consistency analysis.

Recovery setup and assumptions: The basic recovery framework in a discrete setting starts with a standard specification of the underlying (data-generating) finite state space $i \in \mathcal{S} \equiv \{1, \ldots, S\}$ and time $t \in \{0, \ldots, T\}$. Assume that the associated financial market is complete and free of arbitrage opportunities. As a result, a unique stochastic discount factor (SDF) process exists and can be identified with the marginal utility of the representative agent in the economy. To uniquely determine the representative agent's risk and time preferences, as well as the state probability distribution (in the physical measure) from asset prices, Ross (2015)'s recovery framework makes two important assumptions.

Assumption A1. *The preference is time-separable i.e., the SDF growth from the time state* (t,i) *to* $(t+1,j)$ *has the following functional form:* $M_{t,t+1}(i,j) = \delta \frac{M_j}{M_i}, \forall i,j \in \mathcal{S}, \forall t \in \{0,\ldots,T-1\}$*, where* δ *is a constant parameter and* M_k *depends only on the state* $k, \forall k \in \mathcal{S}$.

Assumption A2. *The state transition dynamics are time-homogeneous, i.e., the transition probabilities from the time state* (t,i) *to* $(t+1,j)$ *in the physical measure are time-independent:* $p_{t,t+1}(i,j) = p_{ij}, \forall i,j \in \mathcal{S}, \forall t \in \{0,\ldots,T-1\}$.

The first assumption associates the representative agent's discount factor (i.e., time prefer-

ence) with a constant δ, and marginal utility (i.e., risk preference) with the state-contingent M_i, for $i \in \mathcal{S}$, in the recovery process. The second assumption associates the underlying state transition with a Markovian recurrent dynamics, allowing for asset prices observed over various time horizons (i.e., tenors) to implicate this transition dynamics.

Recovery Theorem and implementation: Throughout, we employ the boldface notation to denote a vector or a matrix. Let the matrix $\mathbf{A}_{S\times S}$ denote the Arrow-Debreu (AD) price matrix, whose element A_{ij} is the price at the current time state (t,i) of the AD asset paying one unit of the numeraire at the next-period state $(t+1,j)$ and zero otherwise. Similarly, let the matrix $\mathbf{P}_{S\times S}$ denote the transition probability matrix containing the one-period transition probabilities p_{ij} in the physical measure. Given the two recovery assumptions above, the pricing of AD assets is $A_{ij} = \delta p_{ij}\frac{M_j}{M_i}$, or

$$(1) \qquad A_{ij}\frac{1}{M_j} = \delta p_{ij}\frac{1}{M_i}, \quad \forall i,j \in \mathcal{S} \quad \Longrightarrow \quad \sum_{j\in\mathcal{S}} A_{ij}\frac{1}{M_j} = \delta\frac{1}{M_i}, \quad \text{or} \quad \mathbf{A}\,\frac{\mathbf{1}}{\mathbf{M}} = \delta\,\frac{\mathbf{1}}{\mathbf{M}},$$

where $\frac{\mathbf{1}}{\mathbf{M}}$ denotes the $S\times 1$ vector of inverse marginal utilities. The above equation shows that this vector is an eigenvector of the AD price matrix $\mathbf{A}$ under the two recovery assumptions. Since $\mathbf{A}$ is a matrix of all positive (AD price) elements $\{A_{ij}\}$, it has a unique all-positive right eigenvector corresponding to its dominant and positive (largest) eigenvalue (Perron-Frobenius theory). This uniqueness of the Perron-Frobenius dominant eigenspace establishes Ross (2015)'s Recovery Theorem, in which the recovered characteristics $\{\delta, M_i, p_{ij}\}$ are associated with the unique dominant eigenvalue-eigenvector pair $\{\delta^{(1)}, \mathbf{x}^{(1,R)}\}$ (i.e., eigenspace) of the AD price matrix $\mathbf{A}$,

$$(2) \qquad \delta = \delta^{(1)}, \qquad \frac{1}{\mathbf{M}} = \mathbf{x}^{(1,R)}, \qquad p_{ij} = \frac{1}{\delta^{(1)}}A_{ij}\frac{x_j^{(1,R)}}{x_i^{(1,R)}}, \qquad \text{where} \quad \mathbf{A}\mathbf{x}^{(1,R)} = \delta^{(1)}\mathbf{x}^{(1,R)}.$$

While being central to the recovery framework, the AD price matrix $\mathbf{A}$ is not fully observed because at any current time state (t,i), AD contracts A_{kj} initiated in non-current states ($\{k\} \neq i$) are not available. Instead, $\mathbf{A}$ is implied from the prices of assets associated with different tenors given the time homogeneity (Assumption A2). Let $A_{\tau;ij}$ be the current price at (t,i) of the τ-period AD asset paying one unit of the numeraire in the future time state $(t+\tau,j)$ (and zero otherwise). Note that the pricing of $\tau+1$-period AD assets is recursive by rolling the τ-period

AD prices an additional period, $A_{\tau+1;ij} = \sum_{k=1}^{S} A_{\tau;ik} A_{kj}$, or in matrix notation,

$$\underbrace{\mathbf{A}_{\tau+1}}_{S\times S} = \underbrace{\mathbf{A}_{\tau}}_{S\times S}\,\underbrace{\mathbf{A}}_{S\times S} \qquad \Longrightarrow \qquad \mathbf{A} = \mathbf{A}_{\tau}^{-1}\,\mathbf{A}_{\tau+1}, \tag{3}$$

where S rows of $S\times S$ matrix $\mathbf{A}_{\tau}$ (resp., matrix $\mathbf{A}_{\tau+1}$) contain the current observable AD prices of S tenors in $\{1,\ldots,S\}$ (resp., S tenors in $\{2,\ldots,S+1\}$). That is, the information from a collection of observable (current) prices of $S+1$ different tenors are required to deduce the complete set of state-contingent prices involving S states.[3] The dominant eigenspace of matrix $\mathbf{A}$, which is implied from the observable price matrices $\mathbf{A}_{\tau}$ and $\mathbf{A}_{\tau+1}$ in recursive system (3), then delivers the recovery results.

Beyond the dominant eigenspace: A preliminary and important observation about the above recovery framework informs our subsequent analysis of the recovery consistency. Namely, the time separability and homogeneity assumptions of the recovery delineate an exact and separate correspondence for every pair of respective eigenspaces of AD price matrix $\mathbf{A}$ and transition probability matrix $\mathbf{P}$. For every k-th eigenspace, the right (column) eigenvectors $\mathbf{x}^{(k,R)}_{S\times 1}$ and $\mathbf{p}^{(k,R)}_{S\times 1}$, and separately, the left (row) eigenvectors $\mathbf{x}^{(k,L)}_{1\times S}$ and $\mathbf{p}^{(k,L)}_{1\times S}$, of these matrices are related by the marginal utilities in the same way,[4]

$$\mathbf{x}^{(k,R)} = \mathbf{Diag}\left(\frac{\mathbf{1}}{\mathbf{M}}\right)\mathbf{p}^{(k,R)}, \qquad \mathbf{x}^{(k,L)} = \mathbf{p}^{(k,L)}\mathbf{Diag}\left(\mathbf{M}\right), \quad \delta^{(k)} = \delta\,\delta_p^{(k)}, \qquad \forall k\in\mathcal{S}, \tag{4}$$

where $\mathbf{Diag}\left(\mathbf{M}\right)$ and $\mathbf{Diag}\left(\frac{\mathbf{1}}{\mathbf{M}}\right)$ respectively are $S\times S$ diagonal matrices of marginal and inverse marginal utilities and δ is the time discount factor. The dominant pair ($k=1$) characterizes key results of the recovery framework. When the the state space specification $\mathcal{S}$ is known or given, the right eigenspace $(1,R)$ in (4) indeed identifies the dominant right eigenvector of AD price matrix with the inverse marginal utilities, which delivers the Recovery Theorem.[5] The left eigenspace $(1,L)$ in (4) identifies the dominant left eigenvector of AD price matrix with the

[3] In principle, since one row of matrix $\mathbf{A}$ (the one containing the prices of AD assets initiated in the current state) is observed, we only need to collect AD prices for S different tenors. In practice, our empirical analysis (Section 4) employs options of all tenors in our sample and determines $\mathbf{A}$ from the system (3) via a least-squares approach. The employment of S, $S+1$, or more available tenors does not alter the nature of the recovery consistency issue because this issue stems from the specification employed in the recovery process (as we elaborate in Section 3.3.3).

[4] The eigenspace notation is $\mathbf{A}\,\mathbf{x}^{(k,R)} = \delta^{(k)}\,\mathbf{x}^{(k,R)}$, $\mathbf{x}^{(k,L)}\,\mathbf{A} = \delta^{(k)}\,\mathbf{x}^{(k,L)}$, and $\mathbf{P}\,\mathbf{p}^{(k,R)} = \delta_p^{(k)}\,\mathbf{p}^{(k,R)}$, $\mathbf{p}^{(k,L)}\,\mathbf{P} = \delta_p^{(k)}\,\mathbf{p}^{(k,L)}$, where $k\in\{1,\ldots,S\}$.

[5] Note that the dominant eigenvalue and eigenvector of the stochastic matrix $\mathbf{P}$ are respectively $\delta_p^{(1)} = 1$ and $\mathbf{p}^{(1,R)} = \mathbf{1}_{S\times 1}$. As a result, the equation in (4) concerning the right eigenspace at $k=1$ recovers the inverse marginal utilities, $\mathbf{x}^{(1,R)} = \mathbf{Diag}\left(\frac{1}{\mathbf{M}}\right)\mathbf{p}^{(1,R)} = \frac{1}{\mathbf{M}}$.

steady-state risk-neutral state probability distribution, which determines the asymptotic pricing of long-term bond yields (Martin and Ross (2019)).

Motivated by the fact that the underlying state space specification is not observed, the recovery consistency inquiry asks whether the results recovered using different specifications are reconcilable. The higher-order eigenspaces ($k > 1$) inform this inquiry via the property that the exact pairwise relationships in (4) break down for a general specification (i.e., other than the underlying specification, as quantified in Section 3). Intuitively, this breakdown reflects a loss of price information when price data is employed in the recoveries based on different state space specifications. The entire spectrum of the implied AD price matrix characterizes the recovery results obtained for a specification under consideration as well as their divergence from the underlying (true) characteristics. Going beyond the dominant eigenspaces of the AD price and transition probability matrices therefore extends the characterization of the recovery to the characterization of the recovery consistency, providing us with an analytical approach to quantify and relate the recovery consistency to the price information retention in the recovery process. In particular, Section 3.2.2 below demonstrates this spectral decomposition and employs it to quantify the recovery consistency issue.

2.2 Consistency Requirement

Consistency is an important requirement inherent to the recovery process. This is because the specification inputs needed in the recovery process, such as the number of states S of the underlying state space, are not observed prior to the recovery implementation. As a result, different recovery results obtained uniquely under different specification inputs are subject to a basic requirement of being mutually consistent as they all pertain to the same underlying market model. To illustrate, the transition probabilities recovered under two different specifications need to be reconcilable (i.e., identical) after we aggregate them in accordance with the mapping and consolidation of states in the two specifications. This section introduces the consistency requirement for recoveries, setting up an analytical framework for the recovery consistency analysis via examining impacts of the state space specification on the recovery results. This analysis helps to qualify consistent recoveries and explain their conceptual and empirical discrepancies when the consistency requirement fails.

Recovery consistency setup: It is instructive to illustrate the recovery consistency in a thought-

experiment setup, noting that the consistency issue is generic and exists regardless of the way the setup is constructed. Consider two different analysts recovering the same (objective and unobserved) underlying market model. We assume that the first analyst adopts $\mathcal{S} = \{1, \ldots, S\}$ and the second adopts $\overline{\mathcal{S}} = \{\overline{1}, \ldots, \overline{S}\}$ as their respective subjective specification input for the recovery process. Without loss of generality, let $\overline{S} < S$. We refer to $\mathcal{S}$ and $\overline{\mathcal{S}}$ as the original and consolidated specification, respectively, and employ an overbar to denote quantities associated with the consolidated specification.[6]

In the recovery framework, the state space specification is inherent to the information structure contained in (and revealed by) asset prices. To capture this information structure of the state space specification, let the partition of the consolidated specification $\overline{\mathcal{S}} = \{\overline{1}, \ldots, \overline{j}, \ldots, \overline{S}\}$ be nested within the original specification $\mathcal{S} = \{1, \ldots, j, k, \ldots, S\}$. That is, each consolidated state $\overline{j} \in \overline{\mathcal{S}}$ either (i) coincides with a single original state, $\overline{j} = j \in \mathcal{S}$, or (ii) contains (couples) several original states, $\overline{j} = \{j, k, \ldots\} \subset \mathcal{S}$. This nesting partition of state spaces, $\overline{\mathcal{S}} \subset \mathcal{S}$, signifies that the original (finer) specification $\mathcal{S}$ unambiguously contains more information about the state space structure than the consolidated (coarser) $\overline{\mathcal{S}}$.

The first analyst determines the implied AD price matrix $\mathbf{A}$ from Equation (3) and recovers the original market model of time and risk preferences and transition probability $\{\delta, \mathbf{M}_{S\times 1}, \mathbf{P}_{S\times S}\}$ characterized by the unique dominant eigenspace of $\mathbf{A}$ (1). Endowed with the consolidated specification $\overline{\mathcal{S}}$, the second analyst perceives and constructs the set of (consolidated) τ-period AD assets and their current prices $\{\overline{A}_{\tau;\overline{i}\,\overline{j}}\}$, each paying one unit of the numeraire in the respective consolidated state $\overline{j}$ in τ periods (and zero otherwise). For the analysts' current states to be reconcilable, note that $i \in \overline{i}$. Given an integrated and arbitrage-free financial market, the asset prices observed by the analysts are related by the law of one price (LoP), $\overline{A}_{\tau;\overline{i}\,\overline{j}} = \sum_{j\in\overline{j}} A_{\tau;i\,j}$, $\forall \overline{j} \in \overline{\mathcal{S}}$. Similar to (3), the second analyst determines the implied consolidated AD price matrix $\overline{\mathbf{A}}_{\overline{S}\times\overline{S}}$ from the recursive equation system associated with the consolidated specification, $\overline{\mathbf{A}} = \overline{\mathbf{A}}_{\tau}^{-1}\,\overline{\mathbf{A}}_{\tau+1}$,[7] and recovers the market model $\{\overline{\delta}, \overline{\mathbf{M}}_{\overline{S}\times 1}, \overline{\mathbf{P}}_{\overline{S}\times\overline{S}}\}$ characterized by the unique

[6] The demonstration of the recovery consistency issue just requires the two specifications to be different for a comparison of the recovery results associated with these specifications. That the first analyst's (original) specification coincides with the underlying $\mathcal{S}$ is just for convenience, helping to quantify the recovery inconsistency from the underlying (preferences and probabilities) characteristics in the thought-experiment setting. Importantly, the recovery consistency issue does not posit or rely on observing the underlying specification or characteristics. Our empirical analysis of recovery consistency (Section 4) does not assume the knowledge of the underlying (true) specification.

[7] Similar to $\mathbf{A}_{\tau}$ and $\mathbf{A}_{\tau+1}$ in (3), $\overline{\mathbf{A}}_{\tau}$ and $\overline{\mathbf{A}}_{\tau+1}$ are $\overline{S}\times\overline{S}$ matrices that stack observable current prices $\{\overline{A}_{\tau;\overline{i}\,\overline{j}}\}$ of tenors $\tau \in \{1, \ldots, \overline{S}\}$ and $\tau \in \{2, \ldots, \overline{S}+1\}$ in their rows. Given a finer specification $\mathcal{S}$, the first analyst therefore needs $(S - \overline{S})$ extra tenors compared to the second analyst (associated with the coarser $\overline{\mathcal{S}}$). An explicit illustration is in Equation (6) below.

dominant eigenspace of matrix $\overline{\mathbf{A}}$.

Consistent recoveries: Given that the same underlying market model drives observable asset prices, the recovery results obtained by different analysts are subject to the consistency requirement that these results pertain to the same underlying market model. When this requirement is not met, the two sets of recovered results are inconsistent with each other, indicating that at least one of them is also inconsistent with the underlying market model.[8]

As two analysts employ different subjective state space specifications, quantifying the consistency requirement first involves the formulation (and translation) of one analyst's recovery results in the other analyst's specification, before their recovery results can be compared. That is, the recovery consistency requirement centers on reconciling different (specification-specific) recovery results for a meaningful comparison and verification. Crucially, this consolidation step is where the information contained in asset prices can be misconstrued by analysts, giving rise to a loss of price information in the recovery process and the recovery consistency issue. While all our recovery consistency results and derivations hold for general setting, a simple (and same) example helps to illustrate aspects of these general results throughout.

Example 1. *Consider two (original and consolidated) state space specifications* $\mathcal{S} = \{1, 2, 3\}$ *and* $\overline{\mathcal{S}} = \{\overline{1}, \overline{2}\}$ *with nesting partitions* $\overline{\mathcal{S}} \subset \mathcal{S}$*, where* $\overline{1} = 1$ *(single state) and* $\overline{2} = \{2, 3\}$ *(coupled state). Assume that the current state is the single state* $\overline{1} = 1$.

We now describe the recovery processes, their consistency requirement and verification in this illustrating example, which informs our general analysis of the recovery consistency in the next section.

Recovery implementation and consistency requirement: Starting with the (underlying) market model $\{\delta, M_i, p_{ij}\}$ associated with the original specification $i, j \in \mathcal{S} = \{1, 2, 3\}$, current and observable asset prices $\{A_{\tau,1j}\}$ for all target states $j \in \mathcal{S}$ and tenors τ can be generated. Endowed with the original specification $\mathcal{S}$, the first analyst perceives and employs these observable prices (not the underlying market model) to obtain the 3×3 implied AD price matrix $\mathbf{A} = \mathbf{A}_\tau^{-1}\mathbf{A}_{\tau+1}$ (3), solves for its unique dominant eigenspace, and by construction, recovers the underlying model $\{\delta, M_i, p_{ij}\}$. Endowed with the consolidated specification $\overline{\mathcal{S}}$, the second analyst perceives and employs the current and observable τ-period consolidated AD asset prices

[8] Our analysis does not rule out (or rely on) the premise in which both analysts' specifications and their recovery results are inconsistent with the underlying.

$\{A_{\tau,1\bar{j}}\}$.[9] This consolidation step helps the second analyst to obtain the 2×2 implied AD price matrix $\overline{\mathbf{A}} = \overline{\mathbf{A}}_\tau^{-1}\overline{\mathbf{A}}_{\tau+1}$ (Footnote 7), solve for its unique dominant eigenspace and recover the model $\{\overline{\delta}, \overline{M}_{\bar{i}}, \overline{p}_{\bar{i}\bar{j}}\}$.

The recovery consistency concerns the compatibility of characteristics recovered by the two analysts as these characteristics pertain to the same underlying market model. Given the nesting partition of specifications in Example 1, the associated consistency requirement is intuitive and characterized by the following conditions

$$\overline{\delta} = \delta, \qquad \overline{M}_{\bar{1}} = M_1, \qquad \overline{p}_{\bar{1}\bar{1}} = p_{11}, \qquad \overline{p}_{\bar{1}\bar{2}} = p_{12}+p_{13}. \tag{5}$$

That is, the consistent recovered characteristics by different analysts are identical for single (identical) states, and consistently aggregatable for coupled (consolidated) states.

Consistency and information retention: The comparison of analysts' recovery results starts with the consolidation step. Recovering a market model of $S = 3$ states, the first analyst employs assets across 4 different tenors stacked in 3×3 observable τ-period matrices $\mathbf{A}_\tau = \{A_{\tau,ij}\}$ (concerning tenors $\tau \in \{1,2,3\}$) and $\mathbf{A}_{\tau+1} = \{A_{\tau+1,ij}\}$ (concerning tenors $\tau+1 \in \{2,3,4\}$) for the recursive equations (3). For the second analyst, recovering a market model of $\overline{S} = 2$ states requires 3 tenors in 2×2 matrices $\overline{\mathbf{A}}_\tau$ (concerning $\tau \in \{1,2\}$) and $\overline{\mathbf{A}}_{\tau+1}$ (concerning $\tau+1 \in \{2,3\}$). As the observable prices employed by analysts are related by the LoP (Footnote 9), $\overline{\mathbf{A}}_\tau$ is deduced from aggregating relevant columns of $\mathbf{A}_\tau$,

$$\underbrace{\begin{bmatrix} A_{1,11} & A_{1,12} & A_{1,13} \\ A_{2,11} & A_{2,12} & A_{2,13} \\ A_{3,31} & A_{3,32} & A_{3,33} \end{bmatrix}}_{\mathbf{A}_\tau} \to \begin{bmatrix} A_{1,11} & A_{1,12}+A_{1,13} \\ A_{2,11} & A_{2,12}+A_{2,13} \\ A_{3,11} & A_{3,12}+A_{3,13} \end{bmatrix} = \begin{bmatrix} \overline{A}_{1,\bar{1}\bar{1}} & \overline{A}_{1,\bar{1}\bar{2}} \\ \overline{A}_{2,\bar{1}\bar{1}} & \overline{A}_{2,\bar{1}\bar{2}} \\ \overline{A}_{3,\bar{1}\bar{1}} & \overline{A}_{3,\bar{1}\bar{2}} \end{bmatrix} \to \underbrace{\begin{bmatrix} \overline{A}_{1,\bar{1}\bar{1}} & \overline{A}_{1,\bar{1}\bar{2}} \\ \overline{A}_{2,\bar{1}\bar{1}} & \overline{A}_{2,\bar{1}\bar{2}} \end{bmatrix}}_{\overline{\mathbf{A}}_\tau}, \tag{6}$$

where that last operation removes the extra tenor not needed in the recovery associated with the coarser $\overline{S}$ (Footnote 7). This consolidation step clearly illustrates the difference in the price information utilized by the two recoveries, which is the source of the recovery consistency issue. As the second analyst's coarser specification $\overline{S}$ requires fewer tenors of asset price inputs, this step drops the last row of consolidated asset prices (last operation in (6)) in the deduction of

[9] For the current Example 1, in the consolidation step, the τ-period consolidated AD asset prices employed by the second analyst is deduced from those by the first analyst by the LoP, $\overline{A}_{\tau;\bar{1}\bar{1}} = A_{\tau;11}$ and $\overline{A}_{\tau;\bar{1}\bar{2}} = A_{\tau;12}+A_{\tau;13}$.

$\overline{\mathbf{A}}_\tau$. However, such an operation is not inconsequential because the eliminated row may carry non-redundant information, beyond what is in the retained rows of $\overline{\mathbf{A}}_\tau$. When this happens, intuitively, the information retained in the asset prices employed by the two analysts differ, leading to different and inconsistent recovery results.[10] Building on the insight of this simple example, Proposition 1 below formalizes an equivalent relationship between the recovery consistency and the information retention in general setting. An application of this proposition then explicitly demonstrates the consistency of the consolidation step (6) (as discussed below (11)).

3 Recovery Consistency Analysis

This section presents the current paper's main analysis and conceptual findings about the recovery consistency. We first adopt a qualitative approach to establish a necessary and sufficient condition for consistent recoveries from a price information perspective (Section 3.1). We then employ a quantitative approach to assess the robustness and magnitude of the recovery consistency issue (Section 3.2) and discuss its relevance in extended settings (Section 3.3).

3.1 Qualitative Aspects of Recovery Consistency

Recall that the recovery results are characterized by the dominant eigenspace of the AD price matrix (1). Hence, the most direct approach to compare different analysts' recovery results is to relate their respective AD price matrices. However, as these matrices can only be implied from observable prices of different tenors (3) in accordance with a state space specification input, we first need to relate the subjective specifications of different analysts. Consider a nesting partition of the two analysts' specifications, $\overline{\mathcal{S}} \subset \mathcal{S}$, in the recovery consistency setup (Section 2.2). These specifications can be quantified by a binary indicator $\mathbf{C}_{k\bar{j}}$,

$$\mathbf{C}_{k\bar{j}} = 1 \text{ if } k \in \bar{j}, \qquad \mathbf{C}_{k\bar{j}} = 0 \text{ if } k \notin \bar{j}, \qquad \forall k \in \mathcal{S}, \bar{j} \in \overline{\mathcal{S}}. \tag{7}$$

The values of this indicator together form a $S \times \overline{S}$ indicator matrix $\mathbf{C}$, which maps the two specifications and characterizes the state space information associated with these specifications. Employing the LoP to relate observable AD prices in different specifications (Footnote 9) and solving

[10] Note that the second analyst drops the last row of the middle 3×2 matrix in (6) to obtain $\overline{\mathbf{A}}_\tau$, and drops the first row to obtain $\overline{\mathbf{A}}_{\tau+1}$. Whereas, the first analyst needs further information (concerning the tenor $\tau = 4$, which is not in $\mathbf{A}_\tau$ (6)) for the recovery.

for the AD price matrices, the mapping $\mathbf{C}$ of two specifications implies the following relationship between these matrices

$$\mathbf{A}_{S\times S}\mathbf{C}_{S\times\overline{S}} = \mathbf{C}_{S\times\overline{S}}\overline{\mathbf{A}}_{\overline{S}\times\overline{S}}. \tag{8}$$

It is important to observe that Equation (8) quantifies and expresses the recovery consistency requirement in terms of analysts' specifications and their AD price matrices.[11] This feature allows us to identify the premise of the recovery consistency issue, which is inherent in the information structure and subjectivity of analysts' state space specifications. Recall that while these AD price matrices $\mathbf{A}$ and $\overline{\mathbf{A}}$ are implied from price data (3), indicator matrix $\mathbf{C}$ (7) arises exclusively from analysts' subjective (exogenous) specifications. Given a set of price data generated by an underlying (objective) market model, not every exogenous indicator matrix $\mathbf{C}$ satisfies the consistency condition (8). Equivalently, not every two subjective specifications of the state space are simultaneously consistent with the observed price data. Building on this insight of the recovery consistency condition (8), the following proposition presents the exact (i.e., necessary and sufficient) premise for consistent recoveries,

Proposition 1 (Recovery consistency issue)**.** *Let $\mathcal{S} \supset \overline{\mathcal{S}}$ denote two (subjective and nesting) state space specifications of the same underlying (but unobserved) market model. The recovery results obtained in the two specifications are mutually consistent if and only if all states $\{j\} \in \mathcal{S}$ that belong to a coupled state $\overline{j} \in \overline{\mathcal{S}}$ are associated with identical characteristics, i.e., marginal utilities and transition probabilities,*

$$M_i = M_k, \qquad p_{i\,\overline{h}} = p_{k\,\overline{h}}; \qquad \forall i,k \subset \overline{j}; \quad \overline{j},\overline{h} \in \overline{\mathcal{S}}. \tag{9}$$

Above, $p_{i,\overline{k}} \equiv \sum_{k\in\overline{k}} p_{ik}$ denotes the one-period aggregate transition probability. A proof of this proposition is relegated to Appendix C.1. Intuitively, Proposition 1 asserts that when the characteristics associated with the fine model $\mathcal{S}$ are indistinguishable to the coarse $\overline{\mathcal{S}}$, no information is lost or distorted between adopting a coarser $\overline{\mathcal{S}}$ and a finer $\mathcal{S}$, preserving the recovery consistency among the two specifications. Several observations are in order. First, the above intuitive relationship between information retention and consistency across different recoveries is

[11] While the the recovery consistency requirement (5) is intuitive and expressed in terms of various relationships between recovered characteristics (time and risk preferences, and transition probabilities), the consistency condition (8) is concise and expressed in terms of a matrix equation of AD prices and the state space mapping $\mathbf{C}$.

utmost (i.e., equivalent) and manifest in the fact that (9) is both a necessary and sufficient condition. Second, this condition is restrictive, indicating that the recovery results are almost surely inconsistent across state space specifications subjectively adopted by different analysts. That is, without observing the state space specification, the subjectively presumed $\overline{\mathcal{S}}$ and $\mathcal{S}$ satisfying the necessary and sufficient condition (9) for recovery consistency is practically a measure-zero premise. Third, Proposition 1 reveals an endogenous nature of the recovery consistency issue. Namely, apart from specifications, condition (9) also involves the characteristics (preferences and transition probabilities) that are to be recovered. Such an endogeneity motivates our approach to analyze and demonstrate the recovery consistency issue by employing various analysts of different subjective specifications, even when a set of recovery results is uniquely obtained for each specification. It is important to observe that the approach and two-analyst setup do not impose or restrict, but identify, the premise for consistent recoveries and the lack thereof. Appendix B presents a simulation analysis, in which the underlying market model is known by design, affirming a higher level of recovery inconsistencies when analysts' subjective specifications deviate more significantly from Proposition 1's recovery consistency condition. The appendix also provides a simple calibration analysis (calibrated to the U.S. aggregate consumption and stock market dynamics) illustrating the direction (i.e., overshooting or undershooting) of recovery inconsistencies in the presence of adverse economic states.

It is instructive to illustrate Proposition 1's connection between consistent recoveries and price information retention for the specific Example 1 (of single state $\overline{1} = 1$ and coupled states $\overline{2} = \{2,3\}$). When condition (9) holds, the one-period AD prices satisfy $\overline{A}_{\overline{1}\,\overline{1}} = A_{11}$, $\overline{A}_{\overline{2}\,\overline{1}} = A_{21} = A_{31}$, $\overline{A}_{\overline{1}\,\overline{2}} = A_{12} + A_{13}$, and $\overline{A}_{\overline{2}\,\overline{2}} = A_{22} + A_{23} = A_{32} + A_{33}$.[12] These price identities in turn assure a consistent (information-preserving) relationship between the implied one-period AD price matrices $\mathbf{A}_{3\times 3}$ and $\overline{\mathbf{A}}_{2\times 2}$. Namely, summing the coupled (i.e., 2nd and 3rd) columns of $\mathbf{A}$ creates an auxiliary 3×2 matrix $\mathbf{A}^{+}$ of identical (i.e., redundant) 2nd and 3rd rows (per the price identities above, $A_{21} = A_{31}$, $A_{22} + A_{23} = A_{32} + A_{33}$). Removing the extra 3rd row reproduces $\overline{\mathbf{A}}$

[12] First, substituting condition (9) into AD asset pricing equations $A_{ij} = \delta p_{ij} \frac{M_j}{M_i}$ implies price identities $A_{21} = A_{31}$, and $A_{22} + A_{23} = A_{32} + A_{33}$. Second, the LoP applied on Example 1's nesting specifications $\{\overline{1} = 1,\ \overline{2} = \{2,3\}\}$ implies $\overline{A}_{\overline{1}\,\overline{1}} = A_{11}$, $\overline{A}_{\overline{2}\,\overline{1}} = A_{21}$, $\overline{A}_{\overline{1}\,\overline{2}} = A_{12} + A_{13}$, and $\overline{A}_{\overline{2}\,\overline{2}} = A_{22} + A_{23}$.

without a loss of price information as this row is redundant,

$$(10)\qquad \underbrace{\begin{bmatrix} A_{11} & A_{12} & A_{13} \\ A_{21} & A_{22} & A_{23} \\ A_{31} & A_{32} & A_{33} \end{bmatrix}}_{\mathbf{A}} \longrightarrow \underbrace{\begin{bmatrix} A_{11} & A_{12}+A_{13} \\ A_{21} & A_{22}+A_{23} \\ A_{31} & A_{32}+A_{33} \end{bmatrix}}_{\mathbf{A}^{+}} \longrightarrow \underbrace{\begin{bmatrix} A_{11} & A_{12}+A_{13} \\ A_{21} & A_{22}+A_{23} \end{bmatrix}}_{\overline{\mathbf{A}}},$$

leading to information-preserving dominant eigenspaces of $\mathbf{A}$ and $\overline{\mathbf{A}}$,[13]

$$(11)\qquad \underbrace{\begin{bmatrix} A_{11} & A_{12} & A_{13} \\ A_{21} & A_{22} & A_{23} \\ A_{31} & A_{32} & A_{33} \end{bmatrix}}_{\mathbf{A}} \underbrace{\begin{bmatrix} x_1^{(1,R)} \\ x_2^{(1,R)} \\ x_2^{(1,R)} \end{bmatrix}}_{\mathbf{x}^{(1,R)}} = \delta \underbrace{\begin{bmatrix} x_1^{(1,R)} \\ x_2^{(1,R)} \\ x_2^{(1,R)} \end{bmatrix}}_{\mathbf{x}^{(1,R)}} \longrightarrow \underbrace{\begin{bmatrix} A_{11} & A_{12}+A_{13} \\ A_{21} & A_{22}+A_{23} \end{bmatrix}}_{\overline{\mathbf{A}}} \underbrace{\begin{bmatrix} x_1^{(1,R)} \\ x_2^{(1,R)} \end{bmatrix}}_{\overline{\mathbf{x}}^{(1,R)}} = \delta \underbrace{\begin{bmatrix} x_1^{(1,R)} \\ x_2^{(1,R)} \end{bmatrix}}_{\overline{\mathbf{x}}^{(1,R)}}.$$

That is, the dominant eigenvalues are identical, $\delta^{(1)} = \overline{\delta}^{(1)} = \delta$. and the non-redundant (first two) components of $\mathbf{x}^{(1,R)}$ coincide with components of $\overline{\mathbf{x}}^{(1,R)}$, preserving the consistency of the two analysts' recovery results characterized by the respective dominant eigenspaces. Note that the price identities (Footnote 12) underlying the consistent relationship (10) between the implied one-period AD price matrices also assure a consistent information retention across the observable τ-period price matrices $\mathbf{A}_\tau$ and $\overline{\mathbf{A}}_\tau$ employed by the two analysts. Summing the coupled (2nd and 3rd) columns and removing a (3rd) extra redundant row consistently transform $\mathbf{A}_\tau$ into $\overline{\mathbf{A}}_\tau$ as required for the recovery consistency (6).[14]

When condition (9) fails, the consolidation between the implied $\mathbf{A}$ and $\overline{\mathbf{A}}$, as well as between the observable $\mathbf{A}_\tau$ and $\overline{\mathbf{A}}_\tau$, is not consistent. In this premise, the extra rows resulting from the consolidation step are not redundant (not identical), implicating a loss of price information across the specifications that two analysts employ in their recovery processes. As a result, the dominant eigenspaces of $\mathbf{A}$ and $\overline{\mathbf{A}}$, while being unique for respective specifications $\mathcal{S}$ and $\overline{\mathcal{S}}$, characterize different sets of recovery results that do not satisfy the consistency requirement. Equipped with Proposition 1 and insights from the specific Example 1, we next analyze the

[13] The auxiliary matrix $\mathbf{A}^{+}$ (10) having identical last two rows implies that the last two components of $\mathbf{A}$'s dominant eigenvector are also identical $x_2^{(1,R)} = x_3^{(1,R)}$, delivering (11).

[14] In fact, thanks to the recursive equations, $\mathbf{A}_{\tau+1} = \mathbf{A}_\tau \mathbf{A}$ and $\overline{\mathbf{A}}_{\tau+1} = \overline{\mathbf{A}}_\tau \overline{\mathbf{A}}$ (3), the relationship goes both directions. A consistent consolidation (summing coupled columns and removing extra and redundant rows) between the implied one-period AD matrices $\mathbf{A}$ and $\overline{\mathbf{A}}$ leads to a consistent consolidation between the observable τ-period AD matrices $\mathbf{A}_\tau$ and $\overline{\mathbf{A}}_\tau$ for all τ, and vice versa.

severity and robustness of the recovery consistency issue in a general setting.

3.2 Quantitative Aspects of Recovery Consistency

Proposition 1's finding of a restrictive premise (9) for consistent recoveries across subjective specifications motivates a crucial inquiry about quantitative and relevant impacts of specifications on the recovered results. In particular, using a perturbative analysis, we examine whether a convergence of subjective specifications (i.e., $\overline{\mathcal{S}}$ becomes finer, approaching $\mathcal{S}$) leads to a convergence of the associated recovery results (Section 3.2.1). We relate the convergence properties to the consistent price information retention in different recovery specifications (Proposition 2 and Section 3.2.2). Technical derivations concerning in this section are relegated to Appendix C.2.

3.2.1 Perturbative Setup of Recoveries

A perturbative setup provides an analytical framework to quantify a persistent difference in the recovery results for converging specifications of generic numbers of states, indicating even more severe recovery inconsistencies when the specifications sufficiently (non-perturbatively and realistically) differ from each other. The perturbative setup therefore serves as a modeling convenience, not a limitation or presumption, to demonstrate a robust recovery consistency issue.

Perturbative setup: Consider two subjective (original and consolidated) nesting specifications $\mathcal{S} \supset \overline{\mathcal{S}}$ with respectively $S \geq \overline{S}$ states of the market model, in which the current state is a single state $1 = \bar{1}$. To deviate from Proposition 1's consistent but restrictive recovery premise, the perturbative setup features an unperturbed (zero-order) consistent component and a perturbative (first-order) inconsistent component. Throughout, subscript 0 denotes the unperturbed component in a generic decomposition $X(\varepsilon) = X_0 + \varepsilon\,\Delta X$, where ε is a common small perturbative parameter.[15] Equipped with this notation, the underlying market model's marginal utilities and time discount factor in the perturbative setup are decomposed as follows,

$$M_i(\varepsilon) = M_{0\bar{i}} + \varepsilon \underbrace{\Delta M_i}_{\equiv k_i} \quad \forall i \in \bar{i},\ \ \bar{i} \in \overline{\mathcal{S}}, \qquad \text{and} \qquad \delta(\varepsilon) = \delta_0 + \varepsilon\Delta\delta, \tag{12}$$

where the state-specific real parameters $\{k_i\}$ model the SDF perturbative component $\{\Delta M_i\}$

[15] We interchangeably employ the sign Δ and subscript 1 to denote the the perturbative component.

with $|\varepsilon\, k_i| \ll |M_{0\bar{i}}|$, and the state-independent parameter $\Delta\delta$ models the discount factor perturbative component with $|\varepsilon\Delta\delta| \ll |\delta_0|$. Other than ε being a small parameter, we do not impose any constraints on the perturbative component of the setup (12). That is, the perturbative component is independent of (i.e., exogenous to) the unperturbed component because the former is not limited a priori by consistency constraints in the perturbative setup. For simplicity, we adopt unperturbed (consistent) underlying transition probabilities $\{p_{ij}\}$ as in (9).[16] Note that the perturbative setup is not restrictive or peculiar because any general (non-perturbative) setup can always be decomposed into a consistent and an inconsistent (not necessarily small) component. In this regard, our tractable analysis and findings in the perturbative setup just present an indicator of a more significant recovery consistency issue of the general setup, in which retaining terms up to the linear order in ε is not enough to quantify the magnitude of inconsistencies. Several further observations concerning the perturbative setup are in order.

First, by construction, the unperturbed components being consistent mean that zero-order (unperturbed) characteristics $\{\delta_0, M_{0i}, p_{ij}\}$ associated with the original specification $\mathcal{S}$ satisfies the necessary and sufficient consistency condition (9). As a result, the recovery process employing price data generated by these zero-order characteristics, but adapted to the consolidated specification $\overline{\mathcal{S}}$, yields consistent zero-order (unperturbed) characteristics $\{\overline{\delta}_0, \overline{M}_{0\bar{i}}, \overline{p}_{\bar{i}\,\bar{j}}\}$.[17] The consistency of unperturbed components and Proposition 1 motivate the setup (12) in which the underlying unperturbed marginal utilities in all original states i of a coupled state $\bar{i}$ are equal. Second, full recovery results (not their unperturbed and perturbative components separately) under different specifications are our subject of interest because the underlying (true) market model is the full model. Due to the exogeneity (i.e., independence) between the constrained (consistent) unperturbed and unconstrained (generic) perturbative components discussed earlier, as desired, such a full market model (12) is not constrained by Proposition 1's restrictive premise. Third and importantly, fixing the underlying specification $\mathcal{S}$ and a (small, but strictly non-zero) parameter $\varepsilon \neq 0$, our analysis examines and demonstrates how the recovery results associated with another specification $\overline{\mathcal{S}}$ remain divergent from the underlying characteristics in the limit of $\overline{\mathcal{S}}$ approaching $\mathcal{S}$. It is the exogeneity between unperturbed and perturbative components that enables persistent recovery inconsistencies of the full model, starting from a loss

[16] While a perturbation to the probabilities can be formulated and added to the current perturbative setup (12), it does not change our finding that recovery inconsistencies persist even when analysts' subjective specifications diverge perturbatively, and is omitted to simplify the exposition.

[17] That is, as an application of Proposition 1, the second analyst's recovery results in that process satisfy $\{\overline{\delta}_0, \overline{M}_{0\bar{i}}, \overline{p}_{\bar{i}\,\bar{j}}\}$, where $\overline{\delta}_0 = \delta_0$, $\overline{M}_{0\bar{i}} = M_{0i}$, and $\overline{p}_{\bar{i}\,\bar{j}} = \sum_{j\in\bar{j}} p_{ij}$, $\forall i \in \bar{i}$, and $\bar{i}, \bar{j} \in \overline{\mathcal{S}}$.

of price information inherent to its perturbative component.[18]

Perturbative decomposition: Given a small perturbative parameter ε and for tractability, our perturbative analysis retains the two leading (zero- and first-) orders in ε. As a result, every quantity (e.g., marginal utility) X of interest in the full model under specification $\mathcal{S}$ has a decomposition into unperturbed and perturbative components, $X(\varepsilon) = X_0 + \varepsilon X_1$. In the full model under specification $\overline{\mathcal{S}}$, the corresponding quantity $\overline{X}$ has the decomposition $\overline{X}(\varepsilon) = \overline{X}_0 + \varepsilon \overline{X}_1$. By construction, the unperturbed components are consistent, namely X_0 and $\overline{X}_0$ are compatible after the consolidation of respective specifications $\mathcal{S}$ and $\overline{\mathcal{S}}$ (satisfying Proposition 1). Since the underlying (true) market model (12) is a full model (i.e. having both unperturbed and perturbative components), the recovery consistency analysis concerns the full quantities $X(\varepsilon)$ and $\overline{X}(\varepsilon)$ and their relationship (but not X_0 and $\overline{X}_0$ and their relationship).

Given the market model (12), the τ-period observable AD prices matrices associated with $\mathcal{S}$ and $\overline{\mathcal{S}}$ can be decomposed into unperturbed and perturbative matrix components,[19]

$$(13)\qquad \begin{cases} \mathbf{A}_\tau(\varepsilon) = \mathbf{A}_{0\tau} + \varepsilon\, \mathbf{B}_\tau, \\ \mathbf{A}_{\tau+1}(\varepsilon) = \mathbf{A}_{0\tau+1} + \varepsilon\, \mathbf{B}_{\tau+1}, \end{cases} \qquad \begin{cases} \overline{\mathbf{A}}_\tau(\varepsilon) = \overline{\mathbf{A}}_{0\tau} + \varepsilon\, \overline{\mathbf{B}}_\tau, \\ \overline{\mathbf{A}}_{\tau+1}(\varepsilon) = \overline{\mathbf{A}}_{0\tau+1} + \varepsilon\, \overline{\mathbf{B}}_{\tau+1}. \end{cases}$$

The analysts solve the respective recursive systems (3) and obtain the implied one-period AD price matrices,[20]

$$(14)\qquad \begin{aligned} \mathbf{A}(\varepsilon) &= \mathbf{A}_0 + \varepsilon\, \mathbf{B}, \quad \text{with} \quad \mathbf{A}_0 = \mathbf{A}_{0\tau}^{-1}\mathbf{A}_{0\tau+1}, \quad \mathbf{B} = \mathbf{A}_{0\tau}^{-1}\left(\mathbf{B}_{\tau+1} - \mathbf{B}_\tau \mathbf{A}_0\right), \\ \overline{\mathbf{A}}(\varepsilon) &= \overline{\mathbf{A}}_0 + \varepsilon\, \overline{\mathbf{B}}, \quad \text{with} \quad \overline{\mathbf{A}}_0 = \overline{\mathbf{A}}_{0\tau}^{-1}\overline{\mathbf{A}}_{0\tau+1}, \quad \overline{\mathbf{B}} = \overline{\mathbf{A}}_{0\tau}^{-1}\left(\overline{\mathbf{B}}_{\tau+1} - \overline{\mathbf{B}}_\tau \overline{\mathbf{A}}_0\right). \end{aligned}$$

Per Recovery Theorem, these implied AD price matrices $\mathbf{A}(\varepsilon)$, $\overline{\mathbf{A}}(\varepsilon)$, and their dominant eigenspaces quantify the respective recovery results of the two analysts. By construction, their unperturbed component matrices $\mathbf{A}_0$ and $\overline{\mathbf{A}}_0$ are consistent, i.e., the associated dominant eigenspaces char-

[18] In contrast, the vanishing limit of $\varepsilon \to 0$ while $\mathcal{S}$ and $\overline{\mathcal{S}}$ remain distinctive specifications is not the subject of interest because in this limit, the recovery concerns only the unperturbed component, which is consistent by construction (12).

[19] Substituting (12) into the τ-period AD price $A_{\tau;1j}(\varepsilon) = \delta(\varepsilon)^\tau p_{\tau;1j} \frac{M_j(\varepsilon)}{M_1(\varepsilon)}$ produces the linear expansion $A_{\tau;1j}(\varepsilon) = \delta^\tau p_{\tau;1j} \frac{M_{0\bar{j}}}{M_{0\bar{1}}} + \varepsilon\, \delta^\tau p_{\tau;1j} \frac{M_{0\bar{j}}}{M_{0\bar{1}}} \left(\tau \frac{\Delta\delta}{\delta} + \frac{k_j}{M_{0\bar{j}}} - \frac{k_1}{M_{0\bar{1}}}\right)$. Identifying these expansions with the matrix equation $\mathbf{A}_\tau(\varepsilon) = \mathbf{A}_{0\tau} + \varepsilon \mathbf{B}_\tau$ (13) yields explicit expressions for the components (tj) of the unperturbed and perturbative matrices: $[\mathbf{A}_{0\tau}]_{tj} = \delta^t p_{t;1j} \frac{M_{0\bar{j}}}{M_{0\bar{1}}}$ and $[\mathbf{B}_\tau]_{tj} = \delta^t p_{t;1j} \frac{M_{0\bar{j}}}{M_{0\bar{1}}} \left(t \frac{\Delta\delta}{\delta} + \frac{k_j}{M_{0\bar{j}}} - \frac{k_1}{M_{0\bar{1}}}\right)$. Expressions for $\overline{\mathbf{A}}_{0\tau}$ and $\overline{\mathbf{B}}_\tau$ follow similarly from the consolidated τ-period AD prices $\{\overline{A}_{\tau;\bar{1}\bar{j}}(\varepsilon)\}$.

[20] These recursive systems have solutions $\mathbf{A}(\varepsilon) = \mathbf{A}_\tau^{-1}(\varepsilon)\mathbf{A}_{\tau+1}(\varepsilon)$ and $\overline{\mathbf{A}}(\varepsilon) = \overline{\mathbf{A}}_\tau^{-1}(\varepsilon)\overline{\mathbf{A}}_{\tau+1}(\varepsilon)$ in the perturbative setup. Expanding, retaining, and matching the two leading (zero- and first-) orders in ε of these solutions deliver (14).

acterize consistent recovered results in the zero order. The solutions of the perturbative component matrices $\mathbf{B}$ and $\overline{\mathbf{B}}$, which couple the unperturbed ($\mathbf{A}_{0\tau}$, $\overline{\mathbf{A}}_{0\tau}$) with perturbative ($\mathbf{B}_\tau$, $\overline{\mathbf{B}}_\tau$) observable matrices in product forms, elucidate the compounded structure of the recovery consistency issue. Namely, while the consistency issue originates from different (inconsistent) price information retained in the observable perturbative component matrices $\mathbf{B}_\tau$ and $\overline{\mathbf{B}}_\tau$, its overall impacts on the recovery results are compounded further (multiplied) by the observable unperturbed component matrices $\mathbf{A}_{0\tau}$ and $\overline{\mathbf{A}}_{0\tau}$. The presence of free parameters $\{k_i\}$ (12) assures the exogeneity (between consistent unperturbed and inconsistent perturbative components) behind this compounded structure (Footnote 19), which we employ to quantify a persistent recovery consistency issue among converging specifications next.

3.2.2 Perturbative Analysis of Recoveries

AD price matrices, eigenspaces, and information retention: The analysis starts with relating the implied one-period AD matrices $\mathbf{A}(\varepsilon)$ and $\overline{\mathbf{A}}(\varepsilon)$ and their components (14), whose dominant eigenspaces characterize the recovery results under $\mathcal{S}$ and $\overline{\mathcal{S}}$. Since the unperturbed component is consistent by construction, the focus is on the price information retained in the perturbative component.

Generalizing the notation and operations underlying the consolidation and comparison of recovered characteristics in nesting specifications (10), let $\mathbf{X}^+$ denote the $S\times\overline{S}$ auxiliary (column-sum) matrix resulting from summing relevant columns $j \in \bar{j}$ of a generic $S \times S$ matrix $\mathbf{X}$ that correspond to a coupled state $\bar{j}$, separately for every $\bar{j} \in \overline{\mathcal{S}}$. Also, let $\mathbf{X}_-$ denote another $\overline{S} \times S$ auxiliary (row-removed) matrix resulting from removing $(S - \overline{S})$ extra rows of the $S \times S$ matrix $\mathbf{X}$ that are not needed for the recovery under the coarser specification $\overline{\mathcal{S}}$.[21] The LoP in the consolidation step (6) implies the following relationship between the price information retained in the perturbative component of analysts' one-period AD price matrices

$$\underbrace{\overline{\mathbf{A}}_{0\tau}}_{\overline{S}\times\overline{S}}\ \underbrace{\overline{\mathbf{B}}}_{\overline{S}\times\overline{S}} \;=\; \underbrace{\mathbf{A}_{0\tau-}}_{\overline{S}\times S}\ \underbrace{\mathbf{B}^+}_{S\times\overline{S}} \quad\Longrightarrow\quad \overline{\mathbf{B}} \;=\; \overline{\mathbf{A}}_{0\tau}^{-1}\ \mathbf{A}_{0\tau-}\,\mathbf{B}^+, \tag{15}$$

[21] The matrix notation $\mathbf{X}^+$ reflects its column construction from relevant columns of $\mathbf{X}$ in the consolidation step (6), $\mathbf{X}^+_{:,\bar{j}} \equiv \sum_{j\in\bar{j}} \mathbf{X}_{:,j}$, for all $\bar{j} \in \overline{\mathcal{S}}$ (where $\mathbf{X}_{:,j}$ denotes column j of matrix $\mathbf{X}$). The matrix notation $\mathbf{X}_-$ reflects the fact that the first analyst will need $S - \overline{S}$ extra tenors of observable asset prices compared to the second analyst in the recovery process (Footnote 7), i.e., removing $(S - \overline{S})$ extra rows in $\mathbf{X}$ (associated with $\mathcal{S}$) to obtain $\mathbf{X}_-$ (associated with $\overline{\mathcal{S}}$) helps to compare the recovery results across specifications.

where $\mathbf{A}_{0\tau-}$ is the row-removed version of the τ-period observable unperturbed price matrix component $\mathbf{A}_{0\tau}$, and $\mathbf{B}^+$ the column-sum version of the one-period implied perturbative AD price matrix component $\mathbf{B}$. Two observations are in order. First, the price information retained in $\overline{\mathbf{B}}$ and $\mathbf{B}$ differs almost surely. Indeed, the price information employed by the first analyst (stored in columns of $\mathbf{B}$) is aggregated and hence lost in the column-sum formation of $\mathbf{B}^+$. The removing of extra asset tenors that are employed by the first analyst (rows of $\mathbf{A}_{0\tau}$) further curtails price information input (rows of $\mathbf{A}_{0\tau-}$) used by the second analyst. These two sources of information loss are coupled in $\overline{\mathbf{B}}$ (15) via the product $\mathbf{A}_{0\tau-}\mathbf{B}^+$. The exogeneity (independence) between unperturbed (inherent in $\mathbf{A}_{0\tau-}$) and perturbative (inherent in $\mathbf{B}^+$) components then rules out a consistent price information retention in their coupling, leading to inconsistent information contained in $\mathbf{B}$ and $\overline{\mathbf{B}}$. Second, such a consistent retention of the price information takes place only in a special and restrictive premise of measure zero, enforcing the first observation. Indeed, only when the $S \times \overline{S}$ matrix $\mathbf{B}^+$ is such that its extra $(S - \overline{S})$ rows are identical, (15) reduces to the identity $\overline{\mathbf{B}} = (\mathbf{B}^+)_-$, in which the latter matrix's expression follows the above (Footnote 21) notation.[22] That is, $\overline{\mathbf{B}}$ can be effectively obtained from $\mathbf{B}$ by first summing relevant columns and then removing extra rows. Since these extra rows are identical (i.e., redundant) in this special premise, their removal does not affect the information retention, and hence, preserves the recovery consistency for the full (unperturbed and perturbative) model. However, such an effective operation only holds in the current special premise because, in general, we cannot directly aggregate (sum) columns of an implied one-period AD price matrix to obtain another (both need to be solved separately from recursive equation systems). As the perturbative component is not subject to the consistency constraints (i.e., the exogeneity between $\mathbf{B}$ and $\overline{\mathbf{B}}$) in the setup (12), this special premise is unlikely (i.e., restrictive).

We next relate eigenspaces of the implied AD price matrices $\mathbf{A}(\varepsilon)$ and $\overline{\mathbf{A}}(\varepsilon)$. The dominant eigenproblem of these matrices, $\mathbf{A}(\varepsilon)\mathbf{x}^{(1,R)}(\varepsilon) = \delta^{(1)}(\varepsilon)\mathbf{x}^{(1,R)}(\varepsilon)$ and $\overline{\mathbf{A}}(\varepsilon)\overline{\mathbf{x}}^{(1,R)}(\varepsilon) = \overline{\delta}^{(1)}(\varepsilon)\overline{\mathbf{x}}^{(1,R)}(\varepsilon)$,

[22] In this special premise, the coupling $\mathbf{A}_{0\tau-}\mathbf{B}^+$ reduces to $\overline{\mathbf{A}}_{0\tau}(\mathbf{B}^+)_-$, where in our notation, the $\overline{S} \times \overline{S}$ matrix $(\mathbf{B}^+)_-$ is obtained by removing extra rows of the $S \times \overline{S}$ matrix $\mathbf{B}^+$ (while $\mathbf{B}^+$ is obtained by summing relevant columns of the $S \times S$ matrix $\mathbf{B}^+$). Substituting this reduction into (15) yields $\overline{\mathbf{B}} = (\mathbf{B}^+)_-$.

has the following respective solution,[23]

$$\delta^{(1)}(\varepsilon) = \delta_0^{(1)} + \varepsilon\, \mathbf{x}_0^{(1,L)}\, \mathbf{B}\, \mathbf{x}_0^{(1,R)}, \qquad \mathbf{x}^{(1,R)}(\varepsilon) = \mathbf{x}_0^{(1,R)} + \varepsilon \sum_{k=2}^{S} \frac{\mathbf{x}_0^{(k,L)}\, \mathbf{B}\, \mathbf{x}_0^{(1,R)}}{\delta_0^{(1)} - \delta_0^{(k)}}\, \mathbf{x}_0^{(k,R)}, \tag{16}$$

$$\overline{\delta}^{(1)}(\varepsilon) = \overline{\delta}_0^{(1)} + \varepsilon\, \overline{\mathbf{x}}_0^{(1,L)}\, \overline{\mathbf{B}}\, \overline{\mathbf{x}}_0^{(1,R)}, \qquad \overline{\mathbf{x}}^{(1,R)}(\varepsilon) = \overline{\mathbf{x}}_0^{(1,R)} + \varepsilon \sum_{k=2}^{\overline{S}} \frac{\overline{\mathbf{x}}_0^{(k,L)}\, \overline{\mathbf{B}}\, \overline{\mathbf{x}}_0^{(1,R)}}{\overline{\delta}_0^{(1)} - \overline{\delta}_0^{(k)}}\, \overline{\mathbf{x}}_0^{(k,R)}, \tag{17}$$

where $\delta_0^{(k)}$, $\mathbf{x}_0^{(k,R)}$ and $\mathbf{x}_0^{(k,L)}$ are the k-th eigenvalue and right (column) and left (row) eigenvectors of the unperturbed matrix component $\mathbf{A}_0$, and similar notation (with a bar) denotes corresponding quantities of $\overline{\mathbf{A}}_0$ (14). Consistent unperturbed component implies $\delta_0^{(1)} = \overline{\delta}_0^{(1)} = \delta_0$. Therefore, we substitute the unperturbed consistent dominant eigenvalues $\delta_0^{(1)}$ and $\overline{\delta}_0^{(1)}$ by δ_0 hereafter.

The two analysts' recovered preferences, $\delta(\varepsilon) = \delta^{(1)}(\varepsilon)$, $M(\varepsilon) = \frac{1}{\mathbf{x}^{(1,R)}(\varepsilon)}$ (16) and $\overline{\delta}(\varepsilon) = \overline{\delta}^{(1)}(\varepsilon)$, $\overline{M}(\varepsilon) = \frac{1}{\overline{\mathbf{x}}^{(1,R)}(\varepsilon)}$ (17), clearly decompose the coupling of unperturbed and perturbative components (14) into the acting of the perturbative component ($\mathbf{B}$ and $\overline{\mathbf{B}}$) on the eigenspaces of all orders (i.e., spectrum) of the unperturbed component ($\mathbf{A}_0$ and $\overline{\mathbf{A}}_0$). Given the consistent unperturbed component by construction, their eigenspaces of corresponding order can be consistently related across the two specifications by the exact pairwise relationship (4). As a result, the above spectral decomposition provides a tractable framework to compare full recovery results and demonstrate their persistent inconsistencies in terms of the unperturbed spectrum $\{\overline{\delta}_0^{(k)}\}$ when the subjective specifications $\mathcal{S}$ and $\overline{\mathcal{S}}$ converge. We quantify and analyze this consistency issue in the recovered preferences next.

Inconsistency in the recovered time preferences: To the first perturbative order (i.e., up to the multiplicative factor ε), the divergence in recovered time preferences (16) and (17) can be decom-

[23] The the dominant eigenspace (16) follows from the corresponding eigenequation in explicit perturbative expansions, $(\mathbf{A}_0 + \varepsilon\, \mathbf{B}) \left(\mathbf{x}_0^{(1,R)} + \varepsilon\, \Delta\mathbf{x}^{(1,R)}\right) = (\delta_0^{(1)} + \varepsilon\, \Delta\delta^{(1)}) \left(\mathbf{x}_0^{(1,R)} + \varepsilon\, \Delta\mathbf{x}^{(1,R)}\right)$. We then match terms of same order of ε, multiply to the left of the eigenequation by the left unperturbed eigenvectors $\mathbf{x}_0^{(k,L)}$, $k \in \{2, \ldots, S\}$ of matrix $\mathbf{A}_0$, and employ the orthonormality between these left and right eigenvectors, $\mathbf{X}_0^L \mathbf{X}_0^R = \mathbb{1}_{S\times S}$ to solve for perturbative components $\Delta\delta^{(1)}$ and $\Delta\mathbf{x}^{(1,R)}$.

posed as,[24]

$$(18) \qquad \overline{\delta}^{(1)}(\varepsilon) - \delta^{(1)}(\varepsilon) \;\sim\; \underbrace{\left[\overline{\mathbf{x}}_0^{(1,L)}\, \overline{\mathbf{A}}_{0\tau}^{-1} \mathbf{A}_{0\tau-} \;-\; \mathbf{x}_0^{(1,L)}\right]}_{(1\times S)-\text{ consistent unperturbed factor}} \cdot \underbrace{\mathbf{B}^{+}\, \overline{\mathbf{x}}_0^{(1,R)}}_{(S\times 1)-\text{ perturbative factor}} .$$

As a scalar product of a row and a column vectors, the decomposition (18) represents the covariation (across states) of unperturbed and perturbative factors. As a result, the inconsistency in recovered time preferences depends on not only the magnitude of these factors but also on their alignment (i.e., cross-state correlation) in the state space. As the perturbative component $\mathbf{B}^{+}$ is unconstrained by the consistency condition, this alignment can have any degree, giving rise to almost surely inconsistent recovered discount factors, $\overline{\delta}^{(1)}(\varepsilon) \neq \delta^{(1)}(\varepsilon)$. Only in the special premise mentioned earlier, in which the auxiliary matrix $\mathbf{B}^{+}$'s extra rows are redundant, their removal does not have an impact on the information retention. As a result, $\overline{\delta}^{(1)}(\varepsilon) = \delta^{(1)}(\varepsilon)$, i.e., the recovered time preferences are consistent only in this special and restrictive premise.[25]

Given the likelihood of the recovery consistency issue and per the discussion below (12), the key question of interest is whether a finer subjective specification $\overline{\mathcal{S}}$ (with a larger number $\overline{S}$ of states) delivers a smaller recovery inconsistency for the time preference. To address this inquiry, recall that the exogeneity between the two factors of the scalar product (18) makes their alignment ambiguous. For a fixed underlying model and original specification $\mathcal{S}$, a finer subjective specification $\overline{\mathcal{S}}$ corresponds to a larger number $\overline{S}$ of coupled states, i.e., fewer original states are combined into coupled states in the aggregate. As a result, $\mathbf{B}^{+}$ is constructed by consolidating (i.e., summing) fewer columns of the original $\mathbf{B}$. This procedure does not necessarily produce a more consistent $\mathbf{B}^{+}$ (characterized by identical relevant rows $j \in \overline{j}$ within each coupled state $\overline{j} \in \overline{\mathcal{S}}$) because $\mathbf{B}$ is a priori unconstrained (arbitrary). In contrary, it is possible that the resulting $\mathbf{B}^{+}$ can boost the product (18) when $\overline{S}$ increases. That is, when fewer columns of $\mathbf{B}$ are consolidated, extra rows of the resulting $\mathbf{B}^{+}$ can become more dissimilar, moving further away from the special premise of recovery consistency mentioned earlier (i.e., the price information retention differs more across two specifications). In such cases, the recovery inconsistencies increase with a finer subjective specification $\overline{\mathcal{S}}$.

[24] To arrive at the divergence (18), we employ the identity $\overline{\mathbf{B}} = \overline{\mathbf{A}}_{0\tau}^{-1} \mathbf{A}_{0\tau-} \mathbf{B}^{+}$ (15) and the consistency property of the unperturbed right eigenvectors $\mathbf{x}_0^{(1,R)}$ and $\overline{\mathbf{x}}_0^{(1,R)}$ (i.e. these vectors share identical relevant components) to reduce $\mathbf{B}\,\mathbf{x}_0^{(1,R)}$ to $\mathbf{B}^{+}\,\overline{\mathbf{x}}_0^{(1,R)}$, as in (11).

[25] When $\mathbf{B}$ and $\overline{\mathbf{B}}$ are consistent, these matrices satisfy $\mathbf{B}^{+}_{j,:} = \overline{\mathbf{B}}_{\overline{j},:}$, $\forall j \in \overline{j}$, $\overline{j} \in \overline{\mathcal{S}}$, which then imply $\mathbf{A}_{0\tau-}\mathbf{B}^{+} = \overline{\mathbf{A}}_{0\tau}\overline{\mathbf{B}}$, and $\mathbf{x}_0^{(1,L)}\mathbf{B}^{+} = \overline{\mathbf{x}}_0^{(1,L)}\overline{\mathbf{B}}$, nullifying the RHS of (18).

A counting argument offers a deeper insight into this non-convergence property of the recovery results. Namely, a finer subjective specification involves a more complex recovery process, and hence, is subject to larger errors and inconsistencies. A finer subjective specification $\overline{\mathcal{S}}$ (i.e., a larger number $\overline{S}$ of states) requires a larger number of observed tenors, and hence, a larger recursive equation system to determine the implied one-period AD price matrix $\overline{\mathbf{A}}(\varepsilon) = \overline{\mathbf{A}}_{\tau}^{-1}(\varepsilon)\,\overline{\mathbf{A}}_{\tau+1}(\varepsilon)$ (3). In this inversion of the τ-period $\overline{\mathbf{A}}_{\tau}(\varepsilon)$ of a larger dimension $\overline{S}\times\overline{S}$, even a small difference between specifications $\mathcal{S}$ and $\overline{\mathcal{S}}$ (and the associated asset prices) construed and employed by analysts can result in significant inconsistencies among their recovery results. That is, this dimensionality problem and the non-convergent recovery consistency issue reflect the endogenous nature of the implied AD price matrix's determination that is central but not directly observed in the recovery.

To explicitly demonstrate this counting argument, we observe that price matrices belong to the class of Vandermonde matrices, whose known analytical inverse gives rise to the following expression for the divergence (18) of the recovered time preferences (Appendix C.2)

(19)
$$\overline{\delta}^{(1)}(\varepsilon) - \delta^{(1)}(\varepsilon) \;\sim\; \left[\overline{\mathbf{x}}_0^{(1,L)}\,\overline{\mathbf{X}}^{R}\,\mathbf{Diag}\left(\frac{1}{\overline{X}_{01}^{(R)}}\right)\overline{\mathbf{D}}_{\overline{S}}^{-1}\,\mathbf{D}_{S-}\,\mathbf{Diag}\left(X_{01}^{(R)}\right)\mathbf{X}^{L} \;-\; \mathbf{x}_0^{(1,L)}\right]\mathbf{B}^{+}\,\overline{\mathbf{x}}_0^{(1,R)},$$

where matrices $\mathbf{X}^L$ and $\mathbf{X}^R$ contain left (row) and right (column) eigenvectors of the unperturbed AD price matrix $\mathbf{A}_0$, or $\mathbf{X}^L\mathbf{A}_0\mathbf{X}^R = \mathbf{Diag}\left(\delta_0^{(1)},\ldots,\delta_0^{(S)}\right)$, and diagonal matrix $\mathbf{Diag}\left(X_{01}^{(R)}\right)$ contains elements of the dominant right eigenvector $x_0^{(1,R)}$ on the diagonal. Vandermonde matrices $\mathbf{D}_S$ and $\overline{\mathbf{D}}_{\overline{S}}$ are associated with the recovery recursive equation systems in $\mathcal{S}$ and $\overline{\mathcal{S}}$. Specifically, the tractable inverse matrix $\overline{\mathbf{D}}_{\overline{S}}^{-1}$ is given by its elements

$$\left[\overline{\mathbf{D}}_{\overline{S}}^{-1}\right]_{1i} = \frac{\left(\delta_0^{(1)}\right)^{\overline{S}-i} + a_1\left(\delta_0^{(1)}\right)^{\overline{S}-i-1} + \ldots + a_{\overline{S}-i-1}\left(\delta_0^{(1)}\right) + a_{\overline{S}-i}}{\delta_0^{(1)}\prod_{j\neq 1}^{\overline{S}}(\delta_0^{(1)} - \delta_0^{(j)})}, \quad i\in\{1,\ldots,\overline{S}\}, \tag{20}$$

where coefficients a's are given in (C.18). The substitution of (20) into (19) shows that the divergence of the recovered time preferences is a rational function of $\overline{S}$ eigenvalues $\{\delta_0^{(j)}\}_{j=1}^{\overline{S}}$ of the unperturbed one-period AD price matrix. When the subjective specification becomes finer, the divergence of the recovered time preferences features a larger degree of singularities (larger number of poles for the underlying rational function (20), as detailed in (C.21)-(C.22)). As a result, a larger $\overline{S}$ does not mitigate the inconsistency in the recovered time preference when

AD price matrix $\mathbf{A}_0$ has sufficiently dense spectrum (small eigenvalue gaps $|\delta_0^{(1)} - \delta_0^{(j)}|$). In this case, intuitively, a more elaborate subjective specification $\overline{S}$ increases recovery inconsistencies because the (non-linear) recursive determination of the implied AD price matrix amplifies the impact of price information retention on the recovery results.

Inconsistency in the recovered risk preferences: To the first perturbative order (i.e., up to the multiplicative factor ε), the divergence in the recovered risk preferences concerns a comparison of two vectors of dimensions S (16) and $\overline{S}$ (17),[26]

$$(21) \qquad \sum_{k=2}^{\overline{S}} \underbrace{\frac{\overline{\mathbf{x}}_0^{(k,L)}\,\overline{\mathbf{B}}\,\overline{\mathbf{x}}_0^{(1,R)}}{\delta_0 - \overline{\delta}_0^{(k)}}}_{\text{loadings } \overline{l}_M^{(k)}} \cdot \overline{\mathbf{x}}_0^{(k,R)} \quad \text{vs.} \quad \sum_{k=2}^{S} \underbrace{\frac{\mathbf{x}_0^{(k,L)}\,\mathbf{B}\,\mathbf{x}_0^{(1,R)}}{\delta_0 - \delta_0^{(k)}}}_{\text{loadings } l_M^{(k)}} \cdot \mathbf{x}_0^{(k,R)},$$

where $l_M^{(k)}$ and $\overline{l}_M^{(k)}$ are the loadings of the recovered risk preferences $\mathbf{x}^{(1,R)}(\varepsilon)$ (16) and $\overline{\mathbf{x}}^{(1,R)}(\varepsilon)$ (17) respectively on the k-th (unperturbed) eigenvectors $\mathbf{x}_0^{(k,R)}$ and $\overline{\mathbf{x}}_0^{(k,R)}$. In the difference with the divergence in the recovered time preferences (18), the divergence in the recovered risk preferences (21) involves the entire spectrum of the unperturbed AD price matrices A_0 and $\overline{A}_0$. The loadings $\overline{l}_M^{(k)}$ and $l_M^{(k)}$ are larger when the associated (unperturbed) eigenvalues are closer to the dominant (unperturbed) eigenvalues (i.e., smaller gaps $|\overline{\delta}_0^{(k)} - \delta_0|$ and $|\delta_0^{(k)} - \delta_0|$). This impact pattern reflects the spectral distribution. Namely, the lower k-th eigenvectors $\overline{\mathbf{x}}_0^{(k,R)}$ and $\mathbf{x}_0^{(k,R)}$ (those associated with k-th smallest eigenvalues) have a stronger influence on the recovery results $\overline{\mathbf{x}}^{(1,R)}(\varepsilon)$ and $\mathbf{x}^{(1,R)}(\varepsilon)$ of the full model (16), (17), because they are closer to the dominant eigenvectors in the spectrum.[27] This finding uncovers an important role of AD price matrices' spectrum (i.e., eigenvalue distribution) on the recovery inconsistencies.

Similar to the dominant eigenvectors, the respective non-redundant elements of the k-th eigenvectors $\mathbf{x}_0^{(k,R)}$ and $\overline{\mathbf{x}}_0^{(k,R)}$ also coincide, for $k \in \{2, \ldots, \overline{S}\}$ (Footnote 26). As a result, the divergence of corresponding terms in the spectral decomposition of the recovered risk preferences

[26] Note that by construction of consistent unperturbed component (12), the non-redundant unperturbed elements coincide, $\mathbf{x}_{0i}^{(1,R)} = \overline{\mathbf{x}}_{0\,\overline{i}}^{(1,R)}$, $\forall i \in \overline{i} \in \overline{\mathcal{S}}$, and cancel out in (16) and (17).

[27] To illustrate this spectral gap impact, consider the (degenerate) limit $|\delta_0^{(k)} - \delta_0| \to 0$. In this limit, the recovery solution is degenerate and can be chosen as a linear combination of the 1st (dominant) and the k-th eigenvectors, i.e., both have similar influence of the recovery outcome.

(21) is driven by the divergence of the associated loadings,

(22)
$$\bar{l}_M^{(k)} - l_M^{(k)} = \underbrace{\frac{1}{\delta_0 - \delta_0^{(k)}}}_{\text{spectrum gap factor}} \underbrace{\left[\overline{\mathbf{x}}_0^{(k,L)} \; \overline{\mathbf{A}}_{0\tau}^{-1} \mathbf{A}_{0\tau-} \; - \; \mathbf{x}_0^{(k,L)}\right]}_{(1\times S)-\text{unperturbed consistent factor}} \cdot \underbrace{\mathbf{B}^+ \, \overline{\mathbf{x}}_0^{(1,R)}}_{(S\times 1)-\text{perturbative factor}}, \quad k \in \{2, \ldots, \overline{S}\}.$$

This decomposition mirrors the divergence of recovered time preferences (18). Specifically, the divergence of the k-th corresponding loadings (22) features a scalar product of an unperturbed consistent and a perturbative vector-valued factors, but it is further scaled by a spectral gap factor (i.e., the spectral impact discussed bellow (21)), resulting in an almost surely divergent loadings $\bar{l}_M^{(k)} \neq l_M^{(k)}$. Crucially, when the unperturbed AD price matrix have a dense spectrum (large factors $\frac{1}{\left|\delta_0^{(k)} - \delta_0\right|}$, $k \in \{2, \ldots, \overline{S}\}$), the impact of the different price information retentions is multiplied and aggregated into a significant inconsistency of the recovered risk preferences (21).

A finer subjective specification $\overline{\mathcal{S}}$ does not warrant a more consistent price information retention, and therefore, the inconsistency of recovered risk preferences persists when $\overline{S}$ increases.[28] Quantitatively, a counting argument using expressions (19)-(20) of the matrix inverse $\overline{\mathbf{A}}_{0\tau}^{-1}$ shows that the divergence of the recovered risk preferences is a rational function of a higher degree of irregularities when the subjective specification $\overline{\mathcal{S}}$ becomes finer. That is, a small difference between the price information retained in $\overline{\mathcal{S}}$ and $\mathcal{S}$ is exacerbated due to the recovery process's increasing complexity as $\overline{S}$ increases. We summarize these quantitative findings on the persistent recovery consistency issue in the following proposition.

Proposition 2 (Persistent recovery consistency issue)**.** *Let $\mathcal{S} \supset \overline{\mathcal{S}}$ denote two (subjective and nesting) state space specifications of the same underlying market model. The recovered characteristics under the two specifications remain mutually inconsistent when the specification $\overline{\mathcal{S}}$ becomes finer (but remains strictly distinct from $\mathcal{S}$) when (i) the spectrum of the AD price matrix $\mathbf{A}_0$ (14) is sufficiently dense, and (ii) extra rows of the column-sum matrix $\mathbf{B}^+$ (15) are non-redundant.*

A derivation of this proposition is relegated to Appendix C.2. As elaborated earlier, condition (i) addresses the quantitative aspect, assuring that the inconsistencies (18)-(20) and (21) are

[28] When $\overline{S}$ increases, fewer columns of $\mathbf{B}$ are consolidated, extra rows of the resulting $\mathbf{B}^+$ can become more dissimilar because this perturbative component is arbitrary (unconstrained) in general, as we observed below (18) for the divergence $\overline{\delta}^{(1)}(\varepsilon) - \delta^{(1)}(\varepsilon)$. Furthermore, note that the inconsistency quantified by (22) is conservative because it concerns only the paired loadings, i.e., those $\{l_M^{(k)}\}$ indexed by $k \in \{1, \ldots, \overline{S}\}$. The unpaired loadings, i.e., the extra loadings $\{l_M^{(k)}\}$ indexed by $k \in \{\overline{S}+1, \ldots, S\}$ in the recovery under $\mathcal{S}$ that have no counterpart $\bar{l}_M^{(k)}$ under $\overline{\mathcal{S}}$, when included, enable a larger and more robust divergence between the recovered risk preferences under these specifications.

significant, and condition (ii) addresses the qualitative aspect, assuring that the inconsistencies do not vanish as $\overline{S}$ increases. In particular, condition (ii) holds only in a special and restrictive premise because the perturbative component is unconstrained a priori. Next, we discuss the relevance and robustness of the recovery consistency issue in connection with the related literature.

3.3 Application and Generalizations

This section presents an application of the recovery consistency analysis in an estimation process of the equity premium's lower bound (Section 3.3.1), before discussing aspects of the recovery consistency in a continuous setting (Section 3.3.2), a best-fist approach (Section 3.3.3), and a generalized and no-arbitrage framework (Section 3.3.4).

3.3.1 On Determining the Equity Premium's Lower Bound

As an application of the recovery consistency analysis, we consider the setting of Martin (2017)'s prominent lower bound on the equity market risk premium. This bound is derived given a negative correlation condition (NCC) in the physical measure between the market return and the product of the SDF and market return. In a market-based (recovery) framework in which neither the SDF nor the physical measure is directly observed, the determination of this NCC provides an illustration for the recovery process and its consistency analysis. Specifically, let M_t,R_t and R_{ft} denote respectively the SDF, market return and risk-free rate at a generic time t, and Q the risk-neutral measure. Martin (2017) derives an identity for the equity premium, $E_t[R_T] - R_{ft} = \frac{1}{R_{ft}} Var_t^Q[R_T] - Cov_t\left[M_T R_T, R_T\right]$. Under the NCC, i.e., $Cov_t\left[M_T R_T, R_T\right] < 0$, the market risk premium is bounded from below by the discounted conditional variance of future market return in the risk-neutral measure $\frac{1}{R_{ft}} Var_t^Q[R_T]$, which can be determined using price data of traded options on the stock market.

Our analysis concerns the market-based determination (i.e., the recovery) of the covariance underlying the NCC by two analysts with nesting (original and consolidated) state specifications $\mathcal{S} \supset \overline{\mathcal{S}}$, in which the future state-contingent payoffs (cum-dividend stock index prices) $\{Y_j\}$ quantifies the future uncertain return R_T. As such, the analysis does not affect the Martin (2017)'s bound (which is determined consistently in the risk-neutral measure) but the evaluation of the underlying NCC covariance (in the physical measure to be recovered) qualifying the

bound. Different recovered characteristics lead to different subjective evaluations of the NCC, and potentially, different conclusions concerning the equity premium bound by different analysts. Let the initial state be a single state 1. The two NCC covariances relevant to the two analysts are,[29]

$$(23) \qquad \begin{cases} C_{\mathcal{S}} \equiv Cov_{\mathcal{S}}\left(MY,Y\right) = \sum_j p_{1j}\left(M_jY_j - E_{\mathcal{S}}\left[MY\right]\right)\left(Y_j - E_{\mathcal{S}}\left[Y\right]\right), \\ \overline{C}_{\overline{\mathcal{S}}} \equiv Cov_{\overline{\mathcal{S}}}\left(\overline{M}\,\overline{Y},\overline{Y}\right) = \sum_{\overline{j}} \overline{p}_{1\,\overline{j}}\left(\overline{M}_{\overline{j}}\overline{Y}_{\overline{j}} - E_{\overline{\mathcal{S}}}\left[\,\overline{M}\,\overline{Y}\,\right]\right)\left(\overline{Y}_{\overline{j}} - E_{\overline{\mathcal{S}}}\left[\,\overline{Y}\,\right]\right), \end{cases}$$

For a tractable comparative analysis, we employ the perturbative setup (12) in which a generic quantity X has a (consistent) unperturbed component and a (unconstrained) perturbative component in both specifications, i.e., $X_j(\varepsilon) = X_{j0} + \varepsilon\Delta X_j$ and $\overline{X}_{\overline{j}}(\varepsilon) = \overline{X}_{\overline{j}\,0} + \varepsilon\Delta\overline{X}_{\overline{j}}$, with the unperturbed component satisfying Proposition 1's consistency condition, $X_{j0} = \overline{X}_{\overline{j}\,0}$, $\forall j \in \overline{j}$, $\forall\overline{j} \in \overline{\mathcal{S}}$. To compare the covariances (23), we use the LoP to relate and decompose the consolidated payoff $\overline{Y}_{\overline{j}}$ in terms of its original counterparts,[30]

$$\overline{Y}_{\overline{j}}(\varepsilon) = \sum_{j\in\overline{j}} \frac{\delta(\varepsilon)}{\overline{\delta}(\varepsilon)}\,\frac{p_{1j}}{\overline{p}_{1\,\overline{j}}}\,\frac{M_j(\varepsilon)/M_1(\varepsilon)}{\overline{M}_{\overline{j}}(\varepsilon)/M_1(\varepsilon)}\,Y_j(\varepsilon) = \overline{Y}_{0\overline{j}} + \varepsilon\Delta\overline{Y}_{\overline{j}}, \quad \forall\overline{j} \in \overline{\mathcal{S}}, \quad \text{where}$$

$$(24) \quad \overline{Y}_{0\,\overline{j}} = Y_{0j}, \qquad \Delta\overline{Y}_{\overline{j}} = E_{\overline{j}}\left[\Delta Y_j\right] + \left(\frac{\Delta\delta}{\delta_0^{(1)}} - \frac{\Delta\overline{\delta}}{\overline{\delta}_0^{(1)}}\right)Y_{0j} + \left(E_{\overline{j}}\left[\frac{\Delta M_j/M_1}{M_{0j}/M_{01}}\right] - \frac{\Delta\overline{M}_{\overline{j}}/\overline{M}_{\overline{1}}}{\overline{M}_{0\overline{j}}/\overline{M}_{0\overline{1}}}\right)Y_{0j}.$$

This no-arbitrage perturbative decomposition of the consolidated market future payoffs in terms of analysts' recovered characteristics is intuitive. An overestimation in the second analyst's recovered time or risk discount factors, $\frac{\Delta\overline{\delta}}{\overline{\delta}_0^{(1)}} > \frac{\Delta\delta}{\delta_0^{(1)}}$ or $\frac{\Delta\overline{M}_{\overline{j}}/\overline{M}_{\overline{1}}}{\overline{M}_{0\overline{j}}/\overline{M}_{0\overline{1}}} > E_{\overline{j}}\left[\frac{\Delta M_j/M_1}{M_{0j}/M_{01}}\right]$, is accompanied by an offsetting underestimation in the analyst's future payoffs, $\Delta\overline{Y}_{\overline{j}} < E_{\overline{j}}\left[\Delta Y_j\right]$, or vice versa. Such changes (and their directions) stem from the absence of arbitrage opportunities, in which case the observable current (expected discounted) prices of these state-contingent payoffs satisfy the LoP (Footnote 30).

Next, substituting the perturbative decomposition (24) into (23) delineates the deviation be-

[29] The realized return R_T equals the realized cum-dividend payoff Y_j at T divided by the current price at t, which does not affect the conditional covariance at t.

[30] Given a complete market, the LoP relates the state-contingent asset prices across different specifications as $\sum_{j\in\overline{j}}\delta(\varepsilon)p_{1j}\frac{M_j(\varepsilon)}{M_1}Y_j(\varepsilon) = \overline{\delta}(\varepsilon)\,\overline{p}_{1\,\overline{j}}\,\frac{\overline{M}_{\overline{j}}(\varepsilon)}{M_1}\,\overline{Y}_{\overline{j}}(\varepsilon)$, which derives the first expression of $\overline{Y}_{\overline{j}}(\varepsilon)$ in (24). Its unperturbed and perturbative components then follow from matching terms of same powers of ε and that the consistent unperturbed component in the setup (12) satisfies Proposition 1.

tween analysts' NCC covariances into a product of perturbative and unperturbed components

$$\overline{C}_{\overline{\mathcal{S}}} - C_{\mathcal{S}} \sim Cov_{\overline{\mathcal{S}}}\left\{\overline{M}_{0\bar{j}}\,\overline{Y}_{0\bar{j}}\ ,\ \Delta\overline{Y}_{\bar{j}} - E_{\bar{j}}\left[\Delta Y_j\right]\right\} \ +\ Cov_{\overline{\mathcal{S}}}\left\{\Delta\left(\overline{M}_{\bar{j}}\,\overline{Y}_{\bar{j}}\right) - E_{\bar{j}}\left[\Delta\left(M_j\,Y_j\right)\right]\ ,\ \overline{Y}_{0\bar{j}}\right\}$$

$$= \left\{2\left(\frac{\Delta\delta}{\delta_0^{(1)}} - \frac{\Delta\overline{\delta}}{\overline{\delta}_0^{(1)}}\right) + \left(E_{\bar{j}}\left[\frac{\Delta M_j/M_1}{M_{0j}/M_{01}}\right] - \frac{\Delta\overline{M}_{\bar{j}}/\overline{M}_{\bar{1}}}{\overline{M}_{0\bar{j}}/\overline{M}_{0\bar{1}}}\right)\right\} \underbrace{Cov_{\overline{\mathcal{S}}}\left\{\overline{M}_{0\bar{j}}\,\overline{Y}_{0\bar{j}}\ ,\ \overline{Y}_{0\bar{j}}\right\}}_{<0 \quad \text{(unperturbed NCC)}}, \tag{25}$$

where the unperturbed component is consistent across specifications, i.e., we have $Cov_{\overline{\mathcal{S}}}\left\{\overline{M}_{0\bar{j}}\,\overline{Y}_{0\bar{j}}\ ,\ \overline{Y}_{0\bar{j}}\right\} = Cov_{\mathcal{S}}\left\{M_{0\,j}\,Y_{0\,j}\ ,\ Y_{0\,j}\right\}$. Equation (25) signifies the fact that, because recovery results directly concern the quantities (SDF and payoffs) in the NCC covariances, a divergence in analysts' recovered time or risk preferences results in a divergence in their NCC covariances.

For the sake of specificity, we assume that this unperturbed covariance (the last factor in (25)) is negative, i.e., the unperturbed component conforms with Martin (2017)'s NCC premise. Since the perturbative component is unconstrained (and exogenous to the unperturbed component) in general, their product in the divergence decomposition (25) can take any sign, giving rise to different NCC evaluations across analysts. Qualitatively, an overestimation of the second analyst's recovered time or risk discount factors (i.e., $\frac{\Delta\overline{\delta}}{\overline{\delta}_0^{(1)}} > \frac{\Delta\delta}{\delta_0^{(1)}}$, as discussed below (24)) weakens the NCC under the second analyst's perspective compared to the first analyst's (i.e., the first analyst's NCC $C_{\mathcal{S}} < 0$ implies the second analyst's NCC $\overline{C}_{\overline{\mathcal{S}}} < 0$ because the divergence (25) is negative in this case). In contrast, an underestimation toughens the NCC under the second analyst (i.e., $C_{\mathcal{S}} < 0$ does not assure $\overline{C}_{\overline{\mathcal{S}}} < 0$ because the divergence (25) is positive in this case). Quantitatively, the divergence in the recovered time preferences $\left(\frac{\Delta\delta}{\delta_0^{(1)}} - \frac{\Delta\overline{\delta}}{\overline{\delta}_0^{(1)}}\right)$ is quantified by (18)-(19), and in the recovered risk preferences $\left(E_{\bar{j}}\left[\frac{\Delta M_j/M_1}{M_{0j}/M_{01}}\right] - \frac{\Delta\overline{M}_{\bar{j}}/\overline{M}_{\bar{1}}}{\overline{M}_{0\bar{j}}/\overline{M}_{0\bar{1}}}\right)$ quantified by (16)-(17) and (21)-(22), both of which are large when Proposition 1's recovery consistency condition is violated.[31] As a result, the recovery consistency issue has a direct impact on divergent evaluations of the NCC by different analysts.

[31] Note that as $\delta(\varepsilon) = \delta_0^{(1)} + \varepsilon\Delta\delta$, $\overline{\delta}(\varepsilon) = \overline{\delta}_0^{(1)} + \varepsilon\Delta\overline{\delta}$, and consistent unperturbed component $\delta_0^{(1)} = \overline{\delta}_0^{(1)}$, we have $\frac{\Delta\delta}{\delta_0^{(1)}} - \frac{\Delta\overline{\delta}}{\overline{\delta}_0^{(1)}} = \frac{\delta(\varepsilon)-\overline{\delta}(\varepsilon)}{\delta_0^{(1)}}$, which is (19). Similarly, with the recovered risk preferences $M(\varepsilon) = \frac{1}{\mathbf{x}^{(1,R)}(\varepsilon)}$ (16), $\overline{M}(\varepsilon) = \frac{1}{\overline{\mathbf{x}}^{(1,R)}(\varepsilon)}$ (17), and consistent unperturbed component $\mathbf{x}_0^{(1,R)} = \overline{\mathbf{x}}_0^{(1,R)}$, the divergence $E_{\bar{j}}\left[\frac{\Delta M_j/M_1}{M_{0j}/M_{01}}\right] - \frac{\Delta\overline{M}_{\bar{j}}/\overline{M}_{\bar{1}}}{\overline{M}_{0\bar{j}}/\overline{M}_{0\bar{1}}}$ can be reduced (up to a proportional coefficient) to the divergence of two terms in (21).

3.3.2 Continuous Setting

A discussion of the recovery in a parallel continuous setting offers an alternative perspective and further insight into Proposition 2's finding that a finer subjective specification does not improve the recovery consistency issue. To this end, consider a continuous setting whose underlying state variable y_t is characterized by the following stochastic process

$$\frac{dy_t}{y_t} = \mu_y^Q dt + \sigma_y dB_t^Q, \tag{26}$$

where μ_y^Q and σ_y are processes adapted to the natural filtration generated by a standard Brownian motion B_t^Q in the risk-neutral measure. Let $V(y_t)$ denote the state-contingent price process of a generic traded asset. The risk-neutral pricing of this asset, $V(y_t) = E_t^Q\left[e^{-r_t dt} V(y_{t+dt})\right]$, together with an application of the Itô's lemma on the state dynamics (26) implies that

$$V(y_t) = V(y_t) + E_t^Q\left[e^{-r_t dt} V(y_{t+dt}) - V(y_t)\right] = \left[\mathbb{1} + dt(-r_t + \mathcal{D}^Q)\right] V(y_t), \tag{27}$$

with the infinitesimal generator $\mathcal{D}^Q = \mu_y^Q\, y_t \frac{\partial}{\partial y_t} + \frac{1}{2}\,\sigma_y^2\, y_t^2 \frac{\partial^2}{\partial y_t^2}$. A comparison of the pricing equation using (i) state prices, $V_i = \sum_k A_{ik} V_k$, with (ii) the risk-neutral pricing (27) identifies a mapping between the dt-period AD price matrix $\mathbf{A}$ in the discrete setting and the infinitesimal generator $\mathcal{D}^Q$ in the continuous setting. Namely, $\mathbf{A} \longleftrightarrow \mathbb{1} + dt(-r_t + \mathcal{D}^Q)$, or

$$\sum_{y_k} A(y_i, y_k) V(y_k) = V(y_i) + dt\left[-r_i + \mu_y^Q\, y_i \frac{\partial}{\partial y_i} + \frac{1}{2}\,\sigma_y^2\, y_i^2 \frac{\partial^2}{\partial y_i^2}\right] V(y_i). \tag{28}$$

While an explicit construction for $A_{ik} \equiv A(y_i, y_k)$ can be obtained by applying a simple finite-difference scheme on the right-hand side of the mapping (28), not all finite-difference schemes deliver a consistent construction for the AD price matrix.[32] It is important to observe that this inconsistency originates from the underlying state distribution's inputs on the determination of the infinitesimal operator. Indeed, the infinitesimal operator $\mathcal{D}^Q$ arises from the conditional

[32] To illustrate, consider the simple finite-difference scheme $\frac{\partial}{\partial y_i} V(y_i) = \frac{V(y_{i+1}) - V(y_{i-1})}{2dy}$ and $\frac{\partial^2}{\partial y_i^2} V(y_i) = \frac{V(y_{i+1}) + V(y_{i-1}) - 2V(y_i)}{(dy)^2}$ for the mapping (28). This scheme delivers $A_{ii-1} \equiv A(y_i, y_i - dy) = dt\left[-\frac{1}{2dy}\,\mu_y^Q\, y_i + \frac{1}{2(dy)^2}\,\sigma_y^2\, y_i^2\right]$ and $A_{ii} \equiv A(y_i, y_i) = 1 - dt\left[r_i + \frac{1}{(dy)^2}\,\sigma_y^2\, y_i^2\right]$. When the finite-difference scheme is such that $dy > \frac{\sigma_y^2\, y_i}{\mu_y^Q} > 0$, the AD price A_{ii-1} is negative (hence, violates the no-arbitrage assumption and is inconsistent). Similarly, when $0 < dy < \sigma_y\, y_i$, the AD price A_{ii} is negative (hence, inconsistent).

expectation of the infinitesimal expansion

$$(29)\qquad \underbrace{\frac{1}{dt}E_t^Q\left[V(y_{t+dt})-V(y_t)\right]}_{=\mathcal{D}^Q V(y_t)} = \frac{\partial V(y_t)}{\partial y_t}\underbrace{\frac{1}{dt}E_t^Q\left[dy_t\right]}_{=\mu_y^Q\, y_t} + \frac{1}{2}\frac{\partial^2 V(y_t)}{\partial y_t^2}\underbrace{\frac{1}{dt}E_t^Q\left[(dy_t)^2\right]}_{=\sigma_y^2\, y_t^2},$$

where the equality is a convergence in the probability limit in accordance with the normally distributed of the state variable $\frac{dy_t}{y_t} \in \mathcal{N}\left(\mu_y^Q dt, \sigma_y^2 dt\right)$ (26). As a result, an ad-hoc finite-difference scheme of the differentials $\frac{\partial}{\partial y_t}V(y_t)$ and $\frac{\partial^2}{\partial y_t^2}V(y_t)$ that does not take into account the underlying state variable distribution may entail an inconsistent construction of the AD price matrix and inconsistent associated recovery results. In particular, a finer finite-difference scheme (i.e., a smaller step size dy of the state space grid) may generate negative (and hence, inconsistent) AD prices (see Footnote 32). This feature of the continuous setting mirrors Proposition 2's persistent recovery consistency issue in the discrete setting, in which a finer subjective specification does not mitigate the divergence between the analysts' recovery results in general.

3.3.3 Best-fit Recovery

Given a specification of S states, the basic recovery recursive system employs just enough observable τ-period AD price data (i.e., $S+1$ tenors τ) to solve for the $S \times S$ one-period AD price matrix $\mathbf{A}$ from $\mathbf{A}_{\tau+1} = \mathbf{A}_\tau\,\mathbf{A}$ (3). Similarly, a second analyst perceiving another specification $\overline{S}$ of $\overline{S} < S$ states needs less price data (of $\overline{S}+1$ tenors) to solve for the respective $\overline{S} \times \overline{S}$ AD price matrix $\overline{\mathbf{A}}$ from $\overline{\mathbf{A}}_{\tau+1} = \overline{\mathbf{A}}_\tau\,\overline{\mathbf{A}}$. While the price information retained and employed differs almost surely across these recovery processes (Proposition 1) and the difference persists even when the two specifications become closer (Proposition 2), a natural question is whether employing more than just enough (e.g., all available) price data improves the recovery consistency issue.

To address this question, consider a least-squares approach that utilizes more price data than needed to obtain best-fit recovery results. Specifically, the best-fit recovery approach interprets the recovery systems obtaining $\mathbf{A}$ from $\mathbf{A}_{\tau+1} = \mathbf{A}_\tau\,\mathbf{A}$ and $\overline{\mathbf{A}}$ from $\overline{\mathbf{A}}_{\tau+1} = \overline{\mathbf{A}}_\tau\,\overline{\mathbf{A}}$ as regression equation systems. This approach employs flexibly all T available tenors in price data (possibly $T > S, \overline{S}$) to uniquely obtain a set of least-squares characteristics (also implemented in Section

4). These regressions produce the respective one-period AD asset price matrices

$$\begin{aligned} \text{Original system:} \quad & \mathbf{A} = [\mathbf{A}_T' \, \mathbf{A}_T]^{-1} \, \mathbf{A}_T' \, \mathbf{A}_{T+1}, \\ \text{Consolidated system:} \quad & \overline{\mathbf{A}} = \left[\overline{\mathbf{A}}_T' \, \overline{\mathbf{A}}_T\right]^{-1} \, \overline{\mathbf{A}}_T' \, \overline{\mathbf{A}}_{T+1}, \end{aligned} \tag{30}$$

where observable $T \times S$ matrix $\mathbf{A}_T$ and $T \times \overline{S}$ matrix $\overline{\mathbf{A}}_T$ contain all available original and consolidated τ-period AD asset prices associated respectively with $\mathcal{S}$ and $\overline{\mathcal{S}}$.

First, we recall a basic issue in the recovery approach that employs just enough price data (3). Namely, even when τ-period observable prices (in $\mathbf{A}_\tau$ and $\overline{\mathbf{A}}_\tau$) employed by different analysts are related by the LoP, different information are retained and utilized in their implied one-period AD price matrices ($\mathbf{A}$ and $\overline{\mathbf{A}}$). Second, when we employ redundant price data, note that the LoP still applies and relates observable prices (in $\mathbf{A}_T$ and $\overline{\mathbf{A}}_T$) separately for each individual tenor τ in the data set.[33] This rigidity (i.e., only observable asset prices of the same tenor are related) of the LoP implies that including more tenors in the price data does not resolve the basic issue above. Intuitively, the difference in the information retention arises from the difference in the state space specifications, but not from the amount of price data employed. Quantitatively, to see this problem explicitly in the perturbative setup, consider the perturbative expansions $\mathbf{A}_T(\varepsilon) = \mathbf{A}_{T0} + \varepsilon \, \mathbf{B}_T$ and $\overline{\mathbf{A}}_T(\varepsilon) = \overline{\mathbf{A}}_{T0} + \varepsilon \, \overline{\mathbf{B}}_T$. Substituting these expansions into the best-fit solutions (30) yields the perturbative expressions for the one-period AD price matrices (using all available price data). These implied matrices have the same features and issues analyzed in Section 3.2. That is, as long as specifications $\mathcal{S}$ and $\overline{\mathcal{S}}$ differ, the perturbative components of these one-period AD price matrices (using all available price data) are inconsistent in general, leading to almost surely inconsistent recovery results. In other words, the relative loss of information between two subjective recovery implementations persists regardless of employing just enough or redundant price data.

3.3.4 Generalized and Arbitrage-based Recoveries

Recall that the basic recovery approach aims to recover the entire transition probability matrix $\mathbf{P}_{S\times S}$ by solving for the entire implied AD price matrix $\mathbf{A}_{S\times S}$. It is the determination of this entire matrix, while subjectively prescribing a dimension S to $\mathbf{A}$, that gives rise to the recovery

[33] Specifically, given the same initial current state i, the current AD asset prices observed by the two analysts are related by the LoP $\overline{A}_{\tau;i\,\overline{j}} = \sum_{j\in\overline{j}} A_{\tau;ij}$, for every tenor $\tau \in \{1,\ldots,T\}$.

consistency issue. Therefore, it is important to know whether alternative approaches, those aiming to recover only the transition probabilities starting from the actual current state, are subject to inconsistencies. We consider two prominent alternative approaches, namely the generalized recovery by Jensen et al. (2019) and the arbitrage-based recovery by Horvath (2025).

Generalized recovery: The generalized recovery is tasked with recovering the transition probabilities from the current state using all available tenors of price data, requiring only the time-separable preference Assumption A1. Without loss of generality, let 1 denote the state at the current time $t = 0$. The pricing of the τ-period observable AD asset prices concerns the corresponding τ-period transition probabilities and risk and time preferences, $A_{\tau;1i}\frac{M_1}{M_i} = \delta^\tau p_{0,\tau}(1,i)$. Aggregating these pricing equations across all target states $\forall i \in \mathcal{S}$ for each tenor τ yields

$$\sum_{i\in\mathcal{S}} A_{\tau;1i}\frac{M_1}{M_i} \;=\; \delta^\tau, \qquad \tau \in \{1,\dots,T\}, \tag{31}$$

where T is the longest available tenor. Together, these T non-linear equations constitute a generalized recovery system that solves for S unknown time and risk preferences $\left\{\delta, \frac{M_1}{M_2}, \dots, \frac{M_1}{M_S}\right\}$.[34] When $S \geq T$, there are multiple solutions to this non-linear equation system in general, ruling out an unambiguous (unique) recovery. When $S < T$, the system does not have a solution in general, also ruling out a successful recovery. Importantly, Jensen et al. (2019) observe that when the observable AD prices $\{A_{\tau;1i}\}$ employed in the recovery process are generated by (and construed consistently with) an underlying model satisfying the time-separable preference assumption, equation system (31) has a unique solution, enabling the generalized recovery. The consistency issue in the generalized recovery arises when the analyst's subjective specification $\mathcal{S}$ deviates from (i.e., being inconsistent with) the underlying. Specifically, along the thought-experiment construction and analysis of Section 3.2 on the recovery consistency issue, a second analyst perceiving an another subjective specification $\overline{\mathcal{S}}$ obtains a different recovery system $\sum_{i\in\overline{\mathcal{S}}} \overline{A}_{\tau;1\,\bar{i}}\frac{\overline{M}_1}{\overline{M}_{\bar{i}}} = \overline{\delta}^\tau$, $\tau \in \{1,\dots,T\}$, whose solution $\left\{\overline{\delta}, \frac{\overline{M}_1}{\overline{M}_{\bar{2}}}, \dots, \frac{\overline{M}_1}{\overline{M}_{\bar{S}}}\right\}$ cannot be reconciled with that obtained by the first analyst in general. Quantitatively, the non-linearity of the recovery system (31) enhances the deviation between the recovery results obtained by different analysts when they employ (subjective and inconsistent) specifications.

Arbitrage-based recovery: The arbitrage-based recovery is tasked with recovering the transition

[34] The non-linearity of the generalized recovery system (31) reflects in various powers δ^τ of the time discount factor unknown.

probabilities from the current state to any target state for a single tenor (e.g., $\tau = 1$) using asset prices associated only with that tenor. This is achieved by formulating the basic recovery in an alternative numeraire other than the standard (dollar) numeraire. The arbitrage-based recovery (i) assumes observable (and foreseeable) dividends $\{D_{ti}\}$ and ex-dividend aggregate stock (market) prices $\{Y_{ti}\}$ at time states $\{(t,i)\}$ in a complete financial market setting, (ii) defines the dividend account numeraire $\mathfrak{D}$, (iii) adopts the time separability Assumption A1 for the risk preference $M^{\mathfrak{D}}_{t,t+\tau}(1,i)$ associated with this numeraire, and (iv) adopts the time homogeneity Assumption A2 to designate the ex-dividend stock price as the state variable in all periods, $Y_{ti} = Y_i$, $\forall t$. These defining properties are quantified via a change of numeraire in the pricing of the stock market (Horvath (2025)),

$$(32)\quad Y_{ti} = E_t\left[M_{t,t+1}(i,j)\left(Y_{t+1\,j} + D_{t+1\,j}\right)\right] = E_t\left[M^{\mathfrak{D}}_{t,t+1}(i,j)Y_{t+1\,j}\right], \quad \text{with} \quad M^{\mathfrak{D}}_{t,t+1}(i,j) = \frac{M^{\mathfrak{D}}_j}{M^{\mathfrak{D}}_i},$$

where $M_{t,t+1}(i,j)$ is the SDF growth associated with the dollar numeraire. Note that a change of numeraire does not entail a change in the transition probability distributions (i.e., measures) $\{p_{ij}\}$. Hence, the arbitrage-based recovery is first implemented in the numeraire $\mathfrak{D}$ (in which the time separability is assumed), before translating these results into the dollar numeraire. Specifically, let $\mathbf{A}^{\mathfrak{D}}$ denote the one-period AD price matrix associated with numeraire $\mathfrak{D}$, and $\mathbf{Y}$ the column vector stacked with stock prices $\{Y_i\}$. Equation (32) implies that stock prices constitute the unique dominant eigenvector of this positive matrix, $\mathbf{A}^{\mathfrak{D}}\mathbf{Y} = \mathbf{Y}$ (with unit eigenvalue), while the basic recovery (2) implemented in $\mathfrak{D}$ implies that the $\mathfrak{D}$-inverse marginal utilities also constitute the unique dominant eigenvector, $\mathbf{A}^{\mathfrak{D}}\frac{1}{\mathbf{M}^{\mathfrak{D}}} = \frac{1}{\mathbf{M}^{\mathfrak{D}}}$. From these follow $\frac{1}{\mathbf{M}^{\mathfrak{D}}} = \mathbf{Y}$ and the arbitrage-based recovery results in the dollar measure,[35]

$$(33)\qquad \delta = 1, \qquad M_{t,t+1}(i,j) = \frac{Y_i}{Y_j + D_j}, \qquad p_{ij} = A_{ij}\frac{Y_j + D_j}{Y_i}.$$

Given a state space specification $\mathcal{S}$ of the arbitrage-based recovery setup and by restricting to

[35] On one hand, starting with the stock pricing Equation (32) $Y_i = \sum_j p_{ij}\delta\frac{M^{\mathfrak{D}}_j}{M^{\mathfrak{D}}_i}Y_j = \sum_j A^{\mathfrak{D}}_{ij}Y_j$, or $\mathbf{A}^{\mathfrak{D}}\mathbf{Y} = \mathbf{Y}$. On the other hand, starting with the AD assets paying in numeraire $\mathfrak{D}$, $A^{\mathfrak{D}}_{ij} = p_{ij}\delta\frac{M^{\mathfrak{D}}_j}{M^{\mathfrak{D}}_i}$, or $A^{\mathfrak{D}}_{ij}\frac{1}{M^{\mathfrak{D}}_j} = p_{ij}\delta\frac{1}{M^{\mathfrak{D}}_i}$, summing over j yields $\mathbf{A}^{\mathfrak{D}}\frac{1}{\mathbf{M}^{\mathfrak{D}}} = \delta\frac{1}{\mathbf{M}^{\mathfrak{D}}}$. These two results identify uniquely $\delta = 1$ and $Y_i = \frac{1}{M^{\mathfrak{D}}_i}$, $\forall i$, (as positive matrix $\mathbf{A}^{\mathfrak{D}}$ has a unique dominant Perron-Frobenius eigenvector). Next, given the complete market setting, pricing equation (32) implies that $M_{t,t+1}(i,j) = \frac{M^{\mathfrak{D}}_j}{M^{\mathfrak{D}}_i}\frac{Y_j}{Y_j+D_j} = \frac{Y_i}{Y_j}\frac{Y_j}{Y_j+D_j} = \frac{Y_i}{Y_j+D_j}$, $\forall i,j$, delivering the recovered risk preferences in (33). Finally, substituting this $M_{t,t+1}(i,j)$ into the pricing equation of AD assets paying in the dollar numeraire $A_{ij} = p_{ij}M_{t,t+1}(i,j)$ yields $p_{ij} = A_{ij}\frac{1}{M_{t,t+1}(i,j)} = A_{ij}\frac{Y_j+D_j}{Y_i}$, delivering the recovered transition probabilities in (33).

the initial current state, $i = 1$, the recovered characteristics in (33) are readily obtained (without solving for the entire implied AD price matrix $\mathbf{A}$, as $\{A_{1j}\}$ are observable for actual current state $i = 1$). Since the specification is an input into the arbitrage-based recovery, consider a second analyst perceiving a different partition $\overline{\mathcal{S}}$ and recovering $\{\overline{\delta}, \overline{M}_{t,t+1}(1,\overline{j}), \overline{p}_{1\,\overline{j}}\}$. These recovery results cannot be reconciled with those obtained by the first analyst in general, e.g., $\sum_{j\in\overline{j}} p_{ij} \neq \overline{p}_{1\,\overline{j}}$, signifying the consistency issue due to an unknown and subjective state space specification in the recovery process.[36]

4 Empirical Analysis

This section presents an empirical analysis of the recovery consistency issue. Section 4.1 describes sources and properties of data. Section 4.2 describes the neural network and regularization methodologies of a recent literature that we employ in the recovery implementation step. Section 4.3 formulates various theory-implied recovery consistency measures, presents the time series of recovery results under different specifications, and demonstrates their inconsistencies using these consistency measures. Appendix A reports the robustness of these empirical results and analysis for alternative sample periods and specifications.

Altogether, employing the related literature's advanced methodologies addressing large but sparse and noisy option price data, our empirical analysis demonstrates a significant and robust recovery consistency issue in different sample periods and across different specifications (i.e., models). While we quantify inconsistencies as irreconcilable differences between the recovery results of two models, it is important to emphasize that our empirical analysis does not assume either specification to be the data-generating (true but unobserved) model.

[36] Intuitively, the time separability assumption is formulated conceptually for the underlying specification in the arbitrage-based recovery while it is not observed prior to the recovery process, giving rise to necessary subjective specification inputs by analysts. Quantitatively, by the LoP, $\overline{A}^{\mathfrak{D}}_{1\,\overline{j}} = \sum_{j\in\overline{j}} A^{\mathfrak{D}}_{1j}$ where $A^{\mathfrak{D}}_{1j} = p_{1j}\delta\frac{M^{\mathfrak{D}}_j}{M^{\mathfrak{D}}_1}$ and $\overline{A}^{\mathfrak{D}}_{1\,\overline{j}} = \overline{p}_{1\,\overline{j}}\delta\frac{\overline{M}^{\mathfrak{D}}_{\overline{j}}}{M^{\mathfrak{D}}_1}$. As a result, the consistency of recovered probabilities $\overline{p}_{1\,\overline{j}} = \sum_{j\in\overline{j}} p_{1j}$ holds only when $M^{\mathfrak{D}}_j = \overline{M}^{\mathfrak{D}}_{\overline{j}}$, or equivalently, $Y_j = \overline{Y}_{\overline{j}}, \forall j \in \overline{j}, \forall \overline{j} \in \overline{\mathcal{S}}$ (because $\mathbf{M}^{\mathfrak{D}} = \frac{1}{\mathbf{Y}}$ and $\overline{\mathbf{M}}^{\mathfrak{D}} = \frac{1}{\overline{\mathbf{Y}}}$ in the arbitrage-based recovery, Footnote 35). That is, analysts obtain consistent recovered probabilities only in a zero-measure premise where the observable state variable (stock price) is identical in all original states j's that pertain to a state $\overline{j}$, for all $\overline{j} \in \overline{\mathcal{S}}$.

4.1 Data

For our subsequent recovery consistency analysis, we first closely follow the empirical methodology of Ludwig (2015) and Audrino et al. (2021) who employ neural network techniques to obtain a robust estimate of the implied volatility surface and state prices. To validate our replication of this methodology, we repeat our data collection and entire analysis in Appendix A to conform with their data and original sample periods (referred to as the benchmarks hereafter).

We employ out-of-the-money (OTM) call and put options on S&P 500 for each Wednesday between January 5, 2000 and August 30, 2023 for the analysis in the main text, and use the data up to December 26, 2012 in Appendix A for validation.[37] We obtain daily closing option and spot prices, interest rates, and index dividend yields from OptionMetrics. We keep the options with the average of the (best) bid and ask prices above \$0.50. We employ the convention in which moneyness $m \equiv \frac{K}{X}$ is the ratio of strike (K) to spot price (X) and tenor τ indicates days to maturity. We restrict the moneyness m's and tenor τ's domains to $m \in [0.4, 1.6]$ and $\tau \in [20, 730]$.

In general, OptionMetrics does not provide interest rates (r) for all tenors for a given date. Therefore, for each date, we linearly interpolate and extrapolate the data so that we obtain the full term structure of interest rates. Following Aït-Sahalia and Lo (1998), for each date and tenor in the data, we compute the implied forward prices (F) from close to at-the-money (ATM) call and put pairs, i.e., $m \in [0.99, 1.01]$, using the put-call parity. We then derive the implied dividend yield (d) from the spot-forward parity $F = Xe^{(r-d)\tau}$. However, the ATM option pairs might not be available for all combinations of dates and tenors in the data. In such a case, we supplement our data by using the S&P 500 dividend yield from OptionMetrics, and we apply the same interpolation and extrapolation procedure for the dividend yield data. Given the dividend yield, we are able to transform the OTM put options into in-the-money (ITM) calls. Hence, our empirical implementation will focus solely on the call options.

Lastly, following literature, we require that the options satisfy the general price bounds,

$$Xe^{-d\tau} \geq C \geq \max\{0, (F-K)e^{-r\tau}\}, \tag{34}$$

[37] We use the previous trading day if there was no trading on a Wednesday.

and the restrictions on vertical and butterfly spreads

$$-e^{-r\tau} \leq \frac{\partial C}{\partial K} \leq 0 \text{ and } \frac{\partial^2 C}{\partial K^2} \geq 0, \tag{35}$$

where C denotes call option price. We exclude options that violate these conditions. Our final sample consists of 1,326,696 call options, and the summary statistics of average implied volatilities and prices for different moneyness and tenors is given in Table 1.

Table 1: Summary statistics of call options

m	DITM < 0.90	ITM $[0.90, 0.99]$	ATM $(0.99, 1.01)$	OTM $[1.02, 1.10]$	DOTM > 1.10
Panel A: Maturity < 180 days					
IV (%)	33.22	20.17	15.60	14.26	18.64
Price	634.08	189.42	72.67	30.35	8.86
N	279,836	245,371	70,162	215,747	54,798
Panel B: Maturity 180 — 365 days					
IV (%)	31.29	21.14	18.95	16.90	16.08
Price	920.65	301.12	192.05	112.56	23.85
N	143,439	39,841	8,984	39,797	62,007
Panel C: Maturity > 365 days					
IV (%)	28.54	20.88	19.31	17.84	15.86
Price	920.15	344.86	245.54	170.05	44.50
N	81,511	20,421	4,574	20,050	40,158

Notes: This table reports the average implied volatilities (IV) and prices of the call options on S&P 500 in our sample for different categories of moneyness m and maturities. Moneyness is defined as the ratio of strike to spot price. Our sample contains option data for every Wednesday from January 5, 2000 to August 30, 2023.

Table 1 broadly reproduces the features of the benchmark data employed by Audrino et al. (2021) for the extended sample period to August 2023 (also see Table A.1 in Appendix A for the sample period matching theirs). The implied volatilities, which are key to our subsequent empirical analysis, are also in line with the summary statistics in Ludwig (2015), whose use of the neural network methodology in obtaining the IV surface estimate is adopted by both Audrino et al. (2021) and the current paper. These findings provide a necessary validation for the data processing step before we implement the recovery.

4.2 Recovery Implementation: Outline and Methodologies

The empirical procedure for the recovery consistency analysis is outlined below. First, for each date in our sample, we obtain an implied volatility (IV) surface that is smooth, arbitrage-free, and parametrized by a fine grid of 601 moneyness states. We refer to this fine grid as the original specification $\mathcal{S}$ or the full model, which is associated with the first analyst in the thought experiment (Step 1). Next, we implement a recovery process to obtain the time and risk preferences and probability distribution under the physical measure associated with the fine grid of the IV surface (Step 2). Finally, we use the law of one price to construct observable state prices associated with a consolidated grid of 150 moneyness states (referred to as the consolidated specification $\overline{\mathcal{S}}$, or the consolidated model associated with the second analyst) and implement another recovery process for this consolidated model (Step 3). A comparative analysis of recovery results under $\mathcal{S}$ and $\overline{\mathcal{S}}$ is key to our paper's demonstration of recovery inconsistencies (Section 4.3). Our empirical results are robust to the choices of $\mathcal{S}$ and $\overline{\mathcal{S}}$.[38]

Step 1: Implied Volatility Surface and State Prices

To determine the τ-period AD price matrix (also referred to as the state prices hereafter) $\mathbf{A}_\tau$ (3) via Breeden and Litzenberger (1978)'s methodology, we adopt the neural network approach of the literature to generate the implied volatility (IV) surface for moneyness $m \in [0.4, 1.6]$ and tenor $\tau \in [20, 730]$. This approach is flexible and robust and also results in a smooth, arbitrage-free IV surface.

The key idea behind this approach is to model the implied total variance $\nu(m,\tau)$ using a two-layer neural network

$$\nu(m,\tau) \equiv \sigma^2(m,\tau)\tau = \beta_0 + \sum_{i=1}^{N} \beta_i f(\alpha_{0i} + \alpha_{1i} m + \alpha_{2i}\sqrt{\tau}), \tag{36}$$

where $\sigma(m,\tau)$ is the implied volatility, $f(x) = \frac{1}{1+e^{-x}}$ is the sigmoid activation function, and N is the number of neurons (or neural nodes) in the hidden layers.[39]

Once we obtain 15 no-arbitrage solutions of IV surface, we take the average of the 5 solutions

[38] For robustness check, Appendix A.3 presents the recovery inconsistency results associated with 150- and 1201-state specifications employed in the literature.

[39] For each neuron i, α_{0i} and $(\alpha_{1i}, \alpha_{2i})$ represent the bias and weights of input data, respectively, and β_i denotes the weight of the output. β_0 is the bias in the neural network.

with lowest residual sum of squares. Finally, we compute the $T \times S$ matrix of state prices $\mathbf{A}_\tau$ using numerical differentiation, where T is the number of tenors of the observable AD prices. We provide further details of this approach in Appendix A.2.

Step 2: Recovery of the Full Model

We start with recovering the full one-period (monthly) AD transition matrix $\mathbf{A}$ of $S = 601$ states (also referred to as the underlying model in our thought experiment's terminology). As pointed out in the literature, directly computing $\mathbf{A}$ via (3) can lead to unstable solutions because $\mathbf{A}_\tau$ is often ill-conditioned. Therefore, we solve $\mathbf{A}$ using ridge regression with an endogenous L^2 penalty parameter determined by minimizing the generalized Kullback-Leibler divergence between the state prices $\mathbf{A}_\tau$ implied from the data and those generated by the Markov transition model (3) (see details in Appendix A.2). After obtaining the state price transition matrix (i.e., one-period AD price matrix) $\mathbf{A}$, we solve and identify its dominant eigenspace $(\delta^{(1)}, \mathbf{x}^{(1,R)})$ with the recovered time and risk preferences and subsequently determine the recovered transition probabilities under the physical measure (2).[40]

Step 3: Recovery of the Consolidated Model

To empirically assess the impact of state space specification on recovery results, we consider a second (and separate) recovery implementation based on the specification $\overline{\mathcal{S}}$ (referred to as the consolidated model in our thought experiment's terminology). For clarity of the empirical analysis and exposition, we consider a nesting structure $\overline{\mathcal{S}} \subset \mathcal{S}$ of the two specifications. This aims to model the feature that some underlying states of $\mathcal{S}$ associated with the first analyst are inadvertently combined (consolidated) into a state of the second analyst's subjective coarser specification $\overline{\mathcal{S}}$. While the AD assets initiated in the current state and employed in the recovery process are perceived by analysts in accordance with their subjective specifications, these assets are traded. Therefore, their prices are necessarily related by the law of one price (i.e., the consolidation process) to prevent arbitrage opportunities. From the original $S = 601$ states and the observable current asset prices in the full model, we employ this consolidation process to obtain the observable current asset prices in the consolidated model $\overline{\mathcal{S}}$ of $\overline{S} = 150$ states. We then

[40] The τ-period physical and risk-neutral transition probabilities from state i to state j respectively are $p_{t,t+\tau}(i,j) = \delta^{-1} A_{\tau;ij} x_i^{(1,R)}$ and $q_{t,t+\tau}(i,j) = e^{r\tau} A_{\tau;ij}$, where $x_i^{(1,R)}$ denotes the i-th entry of vector $\mathbf{x}^{(1,R)}$, and $A_{\tau;ij}$ denotes the (i,j) entry of matrix $\mathbf{A}_\tau$.

estimate the one-period (monthly) associated AD transition matrix $\overline{\mathbf{A}}$ of 150 consolidated states (using the ridge regression with an endogenous L^2 regularization as in Step 2 above). Finally, we recover the probability transition matrix $\overline{\mathbf{P}}$ and marginal utilities $\overline{\mathbf{M}}$ in the consolidated model $\overline{\mathcal{S}}$.

4.3 Empirical Results

We first report the summary statistics for the recovered full, 601-state model. We then demonstrate recovery inconsistencies by comparing the full model's recovered marginal utilities and transition probabilities with those of the consolidated model. We further analyze how recovery inconsistencies vary with theory-implied measures quantifying the violation of the recovery consistency condition in the data. The empirical analysis in the main text concerns the sample period from January 5, 2000 to August 30, 2023. Appendix A.3 presents robustness results using data up to December 26, 2012 (the benchmark sample period) for a validation of the our recovery implementation.

Recovery Results

Following procedures detailed in the previous section to estimate the implied volatility surface and implement the recovery, we obtain the risk-neutral and physical (recovered) probability distributions for one-month ahead transitions. For each date in our sample, we compute the one-month ahead moments (mean, volatility, skewness, and kurtosis) of returns based on the values of S&P 500 in all states, using their associated (risk-neutral and physical) probabilities just obtained. This produces a time series for each of these four cross-sectional return moments under the risk-neutral and physical measures. Based on these time series, Table 2 reports the summary statistics of the first four moments of the risk-neutral and recovered 30-day-to-maturity cross-sectional returns. Both risk-neutral and recovered return distributions feature negative skewness and excess kurtosis, signifying the presence of tail events in the stock index returns. The median of the mean return under the risk-neutral measure is negative, which is driven by the fact that the risk-free rate is lower than the dividend yield during periods of the low interest rate regime (Audrino et al. (2021)).

Table 2: Summary statistics of risk-neutral and recovered moments

	Median	Std dev	Min	25th	75th	Max
Panel A: Risk-neutral moments						
Mean (%)	−2.02	4.04	−41.95	−3.71	−0.01	5.07
Volatility (%)	19.34	8.36	9.65	15.26	24.55	79.99
Skewness	−1.60	0.75	−5.16	−2.20	−1.17	−0.01
Kurtosis	10.12	7.94	2.97	6.75	15.52	56.10
Panel B: Recovered moments						
Mean (%)	10.63	5.08	−26.28	7.62	14.24	37.44
Volatility (%)	14.88	7.14	6.39	11.89	19.63	66.99
Skewness	−1.11	0.52	−5.76	−1.47	−0.85	0.00
Kurtosis	6.70	3.74	3.00	5.23	8.97	55.60

Notes: This table reports the summary statistics of the risk-neutral and recovered moments of 30-day-to-maturity cross-sectional returns on S&P 500 for the 601-state full model. Returns are computed by considering all possible values of S&P 500 on the grid in the next period. Mean and volatility are annualized and reported as percentages. All moments are unconditional over the period of January 5, 2000 to August 30, 2023.

Recovery Inconsistencies in Risk Preferences

Motivated and guided by our previous conceptual analysis of the recovery consistency issue, we empirically identify the premises where the recovery consistency condition is more likely to be violated. We then document and verify that recovery results are indeed inconsistent in these premises. One such premise is where the marginal utility attains its extrema (lowest or highest values). For each date in our sample, we identify and record the value of the minimum recovered marginal utility $\overline{M}_{\bar{j}_{\min}}$ of the consolidated model, with $\bar{j}_{\min}$ denoting the associated consolidated state in which the minimum recovered marginal utility takes place. Then, among the original states of the full model that correspond (i.e., belong) to this consolidated state, we identify and record the values of the minimum, maximum and median marginal utilities ($M_{j_{\min}}, M_{j_{\max}}$ and $M_{j_{\text{med}}}$, respectively), where $j_{\min}, j_{\max}, j_{\text{med}} \in \bar{j}_{\min}$.[41]

Panel A of Figure 1 plots the time series of the recovered marginal utility $\overline{M}_{\bar{j}_{\min}}$ (green line) of the consolidated model and the corresponding recovered marginal utilities $M_{j_{\min}}$ (red line) and $M_{j_{\max}}$ (blue line) of the full model. The plot shows a difference between $M_{j_{\min}}$ and $M_{j_{\max}}$ that persists in most dates of the sample period (from January 2000 to August 2023). This difference becomes significantly more pronounced in the recent period (from 2014 onward), coinciding

[41] Note that $M_{j_{\min}}, M_{j_{\max}}$ or $M_{j_{\text{med}}}$ do not necessarily represent the global minimum, maximum or median marginal utilities across all states of the full model. Furthermore, these marginal utilities will likely differ for different consolidated states.

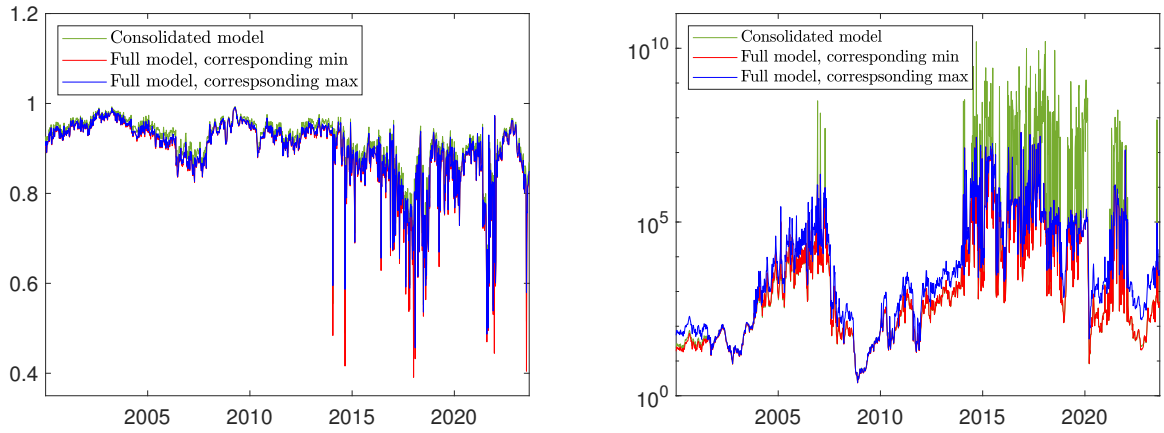

(a) Minimum marginal utilities of the consolidated model

(b) Maximum marginal utilities of the consolidated model

Figure 1: Comparison of marginal utilities of the consolidated and full models

Notes: This figure plots the time series of the recovered minimum ($\overline{M}_{\bar{j}_{\min}}$) and maximum ($\overline{M}_{\bar{j}_{\max}}$) marginal utilities of the (150-state) consolidated model, along with the minimum ($M_{j_{\min}}$) and maximum ($M_{j_{\min}}$) marginal utilities among the original states of the (601-state) full model that correspond to the minimum ($j_{\min} \in \bar{j}_{\min}$) and maximum ($j_{\max} \in \bar{j}_{\max}$) marginal utilities states respectively in the consolidated model. Current state's marginal utility is normalized to one. The sample period is every Wednesday from January 5, 2000 to August 30, 2023.

with the period when $\overline{M}_{\bar{j}_{\min}}$ also differs more significantly from $M_{j_{\min}}$ and $M_{j_{\max}}$.[42] Contrasting this empirical pattern with Proposition 1's necessary and sufficient condition for consistent recoveries, which posits on equal marginal utilities M_j for all original states j belonging to a consolidated state $\bar{j}$, indicates that this condition is violated for states around the minimum recovered marginal utility in the consolidated model (and more significantly violated for the period from 2014 onward). We verify this indication by comparing this recovered marginal utility $\overline{M}_{\bar{j}_{\min}}$ of the consolidated model with all corresponding recovered marginal utilities $\{M_j\}$, $j \in \bar{j}_{\min}$ of the full model. Not only $\overline{M}_{\bar{j}_{\min}}$ do not coincide with either of the minimum $M_{j_{\min}}$ and maximum $M_{j_{\max}}$ (and median $M_{j_{\text{med}}}$, Figure A.2 in Appendix A.3) of the corresponding marginal utilities in the full model, but also $\overline{M}_{\bar{j}_{\min}}$ is outside of the range $[M_{j_{\min}}, M_{j_{\max}}]$ for most of the dates in the sample. That is, the second analyst recovering $\overline{M}_{\bar{j}_{\min}}$ for the consolidated state $\bar{j}_{\min}$ cannot reconcile the result with the marginal utility range $[M_{j_{\min}}, M_{j_{\max}}]$ recovered by the first analyst for all original states j belonging to the consolidated state $\bar{j}_{\min}$, i.e., inconsistent recovered risk preferences.

[42] This observation informs, and is supported by, a more formal statistical correlation analysis of the level of recovery inconsistencies and measures quantifying the violation of the recovery consistent condition in the data (Tables 3 and A.3).

We repeat this empirical analysis of recovery inconsistencies for the premise of the maximum recovered marginal utility $\overline{M}_{\bar{j}_{\max}}$ of the consolidated model. Panel B of Figure 1 plots the time series of the recovered marginal utility $\overline{M}_{\bar{j}_{\max}}$ of the consolidated model and the corresponding range of the recovered marginal utilities of the full model. This plot exhibits similar patterns, but with significantly larger magnitudes, than those observed in Panel A. These results indicate significant and persistent inconsistencies between the recovered $\overline{M}_{\bar{j}_{\max}}$ and the recovered marginal utilities at the corresponding original states. They also indicate that recovery inconsistencies are significantly larger around consolidated states of highest marginal utilities (i.e., adverse states) than around those of lowest marginal utilities (i.e., good states). Intuitively, given that adverse states of the underlying market tend to be rarer, they plausibly are more elusive to the recovery process than other states. Further empirical evidence for inconsistencies in the recovered risk preferences for the benchmark period is presented in Figure A.3 (Appendix A.3).

Recovery Inconsistencies in Transition Probabilities

For each date in the sample, we record the recovered one-period transition probabilities $\{\overline{p}_{\bar{i}\,\bar{j}}\}$ between states $\bar{i}$ and $\bar{j}$ in the consolidated model and $\{p_{ij}\}$ between states i and j in the full model.[43] We compute the aggregate one-period transition probability $p_{i\,\bar{j}}$ from an original state i to a consolidated state $\bar{j}$ in the full model by summing over corresponding transitions. Below, we define the one-period relative probability differences associated with the transitions to a consolidated state $\bar{j}$ from the current state in the two models

$$dp_{\bar{1}\,\bar{j}} \equiv \frac{\overline{p}_{\bar{1}\,\bar{j}} - \sum_{j\in\bar{j}} p_{1j}}{\sum_{j\in\bar{j}} p_{1j}}, \qquad \bar{j} \in \overline{\mathcal{S}}. \tag{37}$$

The consistency condition (9) posits that these relative probability differences vanish for consistent recoveries of the full and consolidated models. The magnitude of $dp_{\bar{1}\,\bar{j}}$ therefore proxies for the inconsistencies in the recovered probabilities across the two models.

Panel A of Figure 2 plots the time series of the mean of the absolute values of relative probability difference, $|dp_{\bar{1}\,\bar{j}}|$, across all consolidated states $\bar{j} \in \overline{\mathcal{S}}$ for each date in our sample. This time series quantifies the unsigned average deviation from the consistent baseline of the recovered transition probabilities from the current state. Panel B plots the median of $dp_{\bar{1}\,\bar{j}}$ across

[43] Recall that the Recovery Theorem recovers the entire transition matrix $\mathbf{P}$ under the physical measure, including transitions from a non-current state i (2).

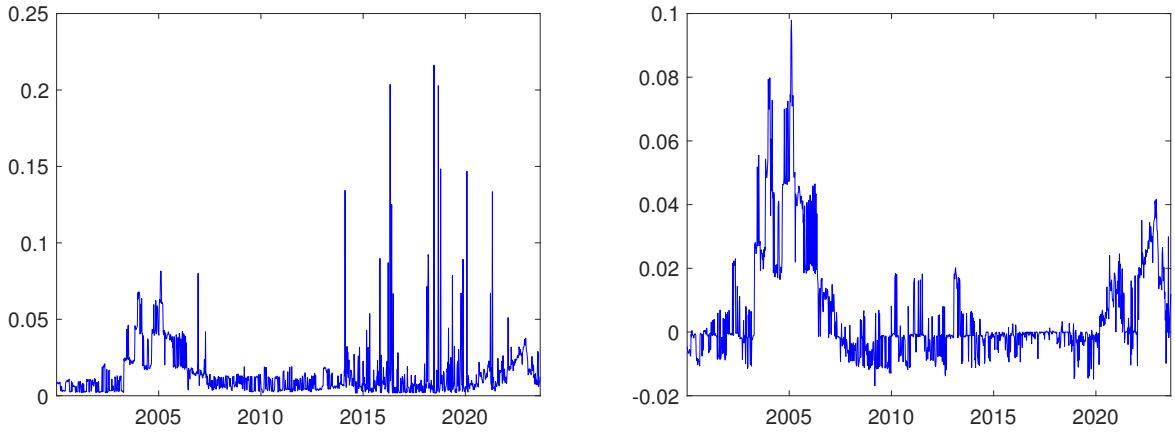

(a) Mean of absolute value of relative probability difference

(b) Median of relative probability difference

Figure 2: Relative probability difference between the consolidated and full models

Notes: This figure plots the mean and median of the relative differences of the one-month recovered transition probabilities between the (150-state) consolidated and (601-state) full models, starting from the current state to states in the consolidated model. Panel A plots the mean of the absolute values of the relative difference, and Panel B plots the median of the relative difference. The relative probability difference is defined as $\frac{\overline{p}_{\overline{1}\overline{j}} - \sum_{j\in\overline{j}} p_{1j}}{\sum_{j\in\overline{j}} p_{ij}}$, where $\overline{j} \in \overline{\mathcal{S}}$ and $j \in \mathcal{S}$, and $\overline{p}_{\overline{1}\overline{j}}$ and p_{1j} denote the recovered one-month transition probabilities from the current state of the consolidated and full models, respectively. The sample period is every Wednesday from January 5, 2000 to August 30, 2023.

$\overline{j} \in \overline{\mathcal{S}}$ for each date, which quantifies the signed average deviation of the recovered transition probabilities. Both panels show a non-vanishing relative probability difference for many dates of the sample period from January 2000 to August 2023, indicating persistent inconsistencies of the recovered transition probabilities. In terms of magnitude, the median value of the relative difference is large around 2005 and during the recent periods after 2020, while the mean value is larger between 2015 and 2020, indicating a skewed distribution of the inconsistencies in these periods. We further present two time-series examples of $dp_{\overline{1}\overline{j}}$ for the states $\overline{j}_{\min}$ and $\overline{j}_{\max}$ of the consolidated model's minimum and maximum recovered marginal utilities in Figure A.1 (Appendix A.3). The figure exhibits persistent inconsistencies in the recovered transition probabilities, with larger inconsistencies associated with the adverse state $\overline{j}_{\max}$, similar to the pattern observed in Figure 1.

Variations in Recovery Inconsistencies

In this section, we consider the variations in the inconsistencies of recovered marginal utilities and recovered transition probabilities.

Variable inconsistencies in recovered marginal utilities: To analyze the variations of recovery inconsistencies in marginal utilities with how well the condition for recovery consistency is met in the data, we introduce two empirical measures quantifying the recovery consistency associated with marginal utilities. The first consistency measure $\mathcal{C}_{\overline{j}}$ is a local measure, defined for a consolidated state $\overline{j} \in \overline{\mathcal{S}}$ as the difference between the maximum and minimum marginal utilities associated with original states j belonging to $\overline{j}$. Below, we consider two specific choices for the consolidated state $\overline{j}$, namely, $\overline{j}_{\min}$ and $\overline{j}_{\max}$. The second measure $\mathcal{C}_g$ is a global measure, defined as the standard deviation of marginal utilities across all $S = 601$ states in the full model,

$$\mathcal{C}_{\overline{j}} \equiv \max_{j \in \overline{j}} M_j - \min_{j \in \overline{j}} M_j, \qquad \overline{j} \in \{\overline{j}_{\max}, \overline{j}_{\min}\} \subset \overline{\mathcal{S}}, \qquad\qquad \mathcal{C}_g \equiv \sqrt{Var\left(M_j\right)}\Big|_{j \in \mathcal{S}}. \tag{38}$$

The condition for recovery consistency (9) posits identical M_j for all $j \in \overline{j}$, implying that $\mathcal{C}_{\overline{j}_{\max}} = 0$ and $\mathcal{C}_{\overline{j}_{\min}} = 0$.[44] As a result, the (non-vanishing) magnitudes of $\mathcal{C}_{\overline{j}_{\max}}$ and $\mathcal{C}_{\overline{j}_{\min}}$ indicate the presence and severity of inconsistencies in the recovered risk preferences locally at $\overline{j}_{\max}$ and $\overline{j}_{\min}$. Similarly, when the underlying market model features a significant state-dependent dynamics (i.e., highly variable $\{M_j\}$), the consolidation of $\mathcal{S}$ into a coarser $\overline{\mathcal{S}}$ needs to account for this variability to preserve the consistency (discussed below Equation (29)). As a result, a sizable magnitude of $\mathcal{C}_g$ exposes the simplicity of consolidation (grouping every four of the original 601 states in $\mathcal{S}$ into one of the 150 consolidated states in $\overline{\mathcal{S}}$) against data, entailing sizable recovery inconsistencies (globally across the state space).

To examine these relationships, Panel A of Table 3 reports the point estimates and the statistical significance of the time-series correlations between the consistency measures (38) and the degrees of recovered marginal utility inconsistencies. The latter are quantified by the deviations of the minimum and maximum recovered marginal utilities (in the consolidated model) from the median recovered marginal utilities (in the full model) among those associated with corresponding original states, $|\overline{M}_{\overline{j}_{\min}} - M_{j_{\text{med}}}|$, $j_{\text{med}} \in \overline{j}_{\min}$, and $|\overline{M}_{\overline{j}_{\max}} - M_{j_{\text{med}}}|$, $j_{\text{med}} \in \overline{j}_{\max}$, for each date in our sample. The global measure $\mathcal{C}_g$ positively and statistically significantly (p-value < 0.01) correlates with both inconsistency proxies, and the local measure $\mathcal{C}_{\overline{j}}$ positively and statistically significantly (p-value < 0.01) correlates with the deviation concerning $\overline{M}_{\overline{j}_{\min}}$.[45] These empirical results provide supporting evidence to the relationships discussed earlier that

[44] In fact, consistent recovery implies that $\mathcal{C}_{\overline{j}} = 0, \forall \overline{j} \in \overline{\mathcal{S}}$.

[45] The local measure $\mathcal{C}_{\overline{j}_{\max}}$ correlates slightly negatively with the deviation concerning $\overline{M}_{\overline{j}_{\max}}$, but the point estimate is statistically insignificant.

larger inconsistencies in the recovered risk preferences tend to take place when the consistency condition is violated more significantly.

Table 3: Variations in recovery inconsistencies

Panel A: Recovered marginal utilities				
	$\lvert\overline{M}_{\overline{j}_{\min}} - M_{j_{\text{med}}}\rvert$		$\lvert\overline{M}_{\overline{j}_{\max}} - M_{j_{\text{med}}}\rvert$	
$\mathcal{C}_{\overline{j}_{\min}}$	0.27^{***}			
	(9.75)			
$\mathcal{C}_{\overline{j}_{\max}}$			-0.01	
			(-0.49)	
$\mathcal{C}_g$	0.24^{***}		0.20^{***}	
	(8.70)		(7.13)	
Panel B: Recovered transition probabilities, one-month and one-year ahead				
	$\lvert\overline{p}_{1;\,\overline{1}\,\overline{j}_{\min}} - p_{1;\,1\overline{j}_{\min}}\rvert$	$\lvert\overline{p}_{1;\,\overline{1}\,\overline{j}_{\max}} - p_{1;\,1\overline{j}_{\max}}\rvert$	$\lvert\overline{p}_{12;\,\overline{1}\,\overline{j}_{\min}} - p_{12;\,1\overline{j}_{\min}}\rvert$	$\lvert\overline{p}_{12;\,\overline{1}\,\overline{j}_{\max}} - p_{12;\,1\overline{j}_{\max}}\rvert$
$\mathcal{C}^P_{1\,;\overline{1}\,\overline{j}_{\min}}$	0.48^{***}			
	(18.97)			
$\mathcal{C}^P_{1\,;\overline{1}\,\overline{j}_{\max}}$		0.32^{***}		
		(11.73)		
$\mathcal{C}^P_{12\,;\overline{1}\,\overline{j}_{\min}}$			0.33^{***}	
			(12.33)	
$\mathcal{C}^P_{12\,;\overline{1}\,\overline{j}_{\max}}$				0.69^{***}
				(33.73)

Notes: This table reports the time-series correlations between the consistency measures and degrees of recovery inconsistencies for every Wednesday from January 5, 2000 to August 30, 2023. The local consistency measure $\mathcal{C}_{\overline{j}}$ for marginal utilities is the difference between the maximum and minimum marginal utilities associated with original states j that belong to $\overline{j}_{\max}$ or $\overline{j}_{\min}$. The global inconsistency measure $\mathcal{C}_g$ is the standard deviation of marginal utilities across all $S = 601$ states in the full model. The local consistency measure $\mathcal{C}^P_{\tau\,;\overline{1}\,\overline{j}}$ for transition probabilities of one-month ($\tau = 1$) and one-year ($\tau = 12$) horizons is the difference between the maximum and minimum transition probabilities of corresponding horizons starting from an original state belonging to the current consolidated state $\overline{1}$ to $\overline{j}_{\max}$ or $\overline{j}_{\min}$. t-statistics are reported in parentheses. * indicates significance at the 10% level; **, at the 5% level; and ***, at the 1% level.

Variable inconsistencies in recovered transition probabilities: Similarly, we analyze the variations of recovery inconsistencies in transition probabilities with how well the recovery consistency condition (9) is met in the data. This consistency condition posits identical transition probabilities starting from any original states i, k belonging to a consolidated state $\overline{j}$ to another consolidated state $\overline{h}$, or, $p_{i\overline{h}} = p_{k\overline{h}}$, $\forall i, k \in \overline{j}$ and $\overline{j}, \overline{h} \in \overline{\mathcal{S}}$, for consistent recoveries. Accordingly, we employ the empirical deviation from these identities to construct a local consistency measure based on one-month and one-year transition probabilities from the current state to the consol-

idated state $\overline{j} \in \{\overline{j}_{\max}, \overline{j}_{\min}\}$ as follows

$$(39)\quad \mathcal{C}^{P}_{1;\overline{1}\,\overline{j}} \equiv \max_{h\in\overline{1}} p_{1;\,h\overline{j}} - \min_{h\in\overline{1}} p_{1;\,h\overline{j}}, \qquad \mathcal{C}^{P}_{12;\,\overline{1}\,\overline{j}} \equiv \max_{h\in\overline{1}} p_{12;\,h\overline{j}} - \min_{h\in\overline{1}} p_{12;\,h\overline{j}}, \qquad \overline{j} \in \{\overline{j}_{\max}, \overline{j}_{\min}\} \subset \overline{\mathcal{S}},$$

where $\overline{1}$ denotes the current state in the consolidated model, $p_{1;\,h\overline{j}} = \sum_{j\in\overline{j}} p_{1;\,hj}$, $p_{12;\,h\overline{j}} = \sum_{j\in\overline{j}} p_{12;\,hj}$, and $\{p_{1;\,hj}\}$ and $\{p_{12;\,hj}\}$ are respectively the one-month and one-year recovered transition probabilities between original states $h, j \in \mathcal{S}$ of the full model.[46] The (non-vanishing) magnitude of measures (39) indicates the presence and severity of recovery inconsistencies for these time horizons (and at the target state $\overline{j} \in \{\overline{j}_{\min}, \overline{j}_{\max}\}$). Panel B of Table 3 reports the point estimates and the statistical significance of the time-series correlations between the consistency measures (39) and the degrees of recovered probability inconsistencies of commensurate horizons. The latter are quantified by the difference between the probabilities (in the consolidated and full models) of the transitions from the current state to the states $\overline{j}_{\min}$ and $\overline{j}_{\max}$, namely, $|\overline{p}_{1;\,\overline{1}\,\overline{j}_{\min}} - \sum_{j\in\overline{j}_{\min}} p_{1;\,1\,j}|$, and $|\overline{p}_{1;\,\overline{1}\,\overline{j}_{\max}} - \sum_{j\in\overline{j}_{\max}} p_{1;\,1\,j}|$ (and similar expressions for the difference of probabilities for one-year transitions). The point estimates of all correlations are positive and statistically significant (p-value < 0.01), indicating that larger inconsistencies in recovered transition probabilities tend to take place when the violation of consistency condition is more significant. These empirical results hold for both one-month and one-year horizons, lending supporting evidence to inconsistencies in the recovered probabilities and their model-implied relationships. Further empirical evidence for variations of recovery inconsistencies with measures of consistency condition's violation for the benchmark period is presented in Table A.3 (Appendix A.3).

5 Conclusion

This paper examines the consistency problem in recovering market beliefs, time preferences, and risk preferences from asset prices, and provides a fundamental insight into the recovery framework. Because the required state space specification is unobserved prior to the recovery implementation, different subjective specifications can easily produce mutually inconsistent recovery results unless a strong necessary and sufficient condition is satisfied. This condition requires that no information about the underlying market be lost when moving across specifi-

[46] Note that $\{p_{1;\,hj}\}$ (and $\{p_{12;\,hj}\}$) is the (h, j) element of the recovered one-month (and one-year) transition probability matrix $\mathbf{P}$ (and $\mathbf{P}^{12}$) of the full model.

cations.

We further show that a finer specification does not necessarily imply greater consistency. Our analytical results are established through a tractable perturbation framework, and our empirical analysis employing option price data for alternative specifications and sample periods documents robust recovery inconsistencies whose magnitude increases with violations of the consistency condition.

These findings demonstrate that, although recovery is economically important, achieving an unambiguous and consistent identification of market fundamentals from asset prices remains a significant challenge.

References

Aït-Sahalia, Yacine, and Andrew W Lo, 1998, Nonparametric estimation of state-price densities implicit in financial asset prices, *The Journal of Finance* 53, 499–547.

Alvarez, Fernando, and Urban Jermann, 2005, Using asset prices to measure the persistence of the marginal utility of wealth, *Econometrica* 73, 1977–2016.

Audrino, Francesco, Robert Huitema, and Markus Ludwig, 2021, An empirical implementation of the Ross recovery theorem as a prediction device, *Journal of Financial Econometrics* 19, 291–312.

Bakshi, Gurdip, Fousseni Chabi-Yo, and Xiaohui Gao, 2018, A recovery that we can trust? Deducing and testing the restrictions of the recovery theorem, *The Review of Financial Studies* 31, 532–555.

Borovička, Jaroslav, Lars Peter Hansen, and José A Scheinkman, 2016, Misspecified Recovery, *The Journal of Finance* 71, 2493–2544.

Borovička, Jaroslav, and John Stachurski, 2020, Necessary and sufficient conditions for existence and uniqueness of recursive utilities, *Journal of Finance* 75, 1457–1493.

Breeden, Douglas T., and Robert H. Litzenberger, 1978, Prices of state-contingent claims implicit in option prices, *The Journal of Business* 51, 621–651.

Carr, Peter, and Jiming Yu, 2012, Risk, return, and Ross recovery, *The Journal of Derivatives* 20, 38–59.

Chabi-Yo, Fousseni, Chukwuma Dim, and Grigory Vilkov, 2023, Generalized Bounds on the Conditional Expected Excess Return on Individual Stocks, *Management Science* 69, 922–939.

Chabi-Yo, Fousseni, and Johnathan Loudis, 2020, The Conditional Expected Market Return, *Journal of Financial Economics* 137, 752–786.

Dillschneider, Yannick, and Raimond Maurer, 2019, Functional Ross recovery: Theoretical results and empirical tests, *Journal of Economic Dynamics and Control* 108, 103750.

Foresee, F Dan, and Martin T Hagan, 1997, Gauss-newton approximation to bayesian learning, in *Proceedings of international conference on neural networks (ICNN'97)*, volume 3, 1930–1935, IEEE.

Giglio, Stefano, Matteo Maggiori, Johannes Stroebel, and Stephen Utkus, 2022, Five Facts about Beliefs and Portfolios, *American Economic Review* 111, 1481–1522.

Gormsen, Niels Joachim, and Ralph S J Koijen, 2020, Coronavirus: Impact on Stock Prices and Growth Expectations, *Review of Asset Pricing Studies* 10, 574–597.

Hansen, Lars Peter, and José A Scheinkman, 2017, *Stochastic Compounding and Uncertain Valuation*, 21–50 (University of Chicago Press).

Horvath, Ferenc, 2025, Arbitrage-based Recovery, *Journal of Financial Economics* 163, 1–20.

Jackwerth, Jens Carsten, and Marco Menner, 2020, Does the Ross recovery theorem work empirically?, *Journal of Financial Economics* 137, 723–739.

Jensen, Christian Skov, David Lando, and Lasse Heje Pedersen, 2019, Generalized Recovery, *Journal of Financial Economics* 133, 154–174.

Ludwig, Markus, 2015, Robust estimation of shape-constrained state price density surfaces, *The Journal of Derivatives* 22, 56–72.

Man, Yiu-Kwong, 2017, On computing the vandermonde matrix inverse, *Proceedings of the World Congress on Engineering, WCE 2017 London, U.K.* 1.

Martin, Ian, 2017, What is the expected return on the market?, *The Quarterly Journal of Economics* 132, 367–433.

Martin, Ian, and Stephen Ross, 2019, Notes on the yield curve, *Journal of Financial Economics* 134, 689–702.

Nguyen, Derrick, and Bernard Widrow, 1990, Improving the learning speed of 2-layer neural networks by choosing initial values of the adaptive weights, in *1990 IJCNN international joint conference on neural networks*, 21–26, IEEE.

Qin, Likuan, and Vadim Linetsky, 2016, Positive eigenfunctions of Markovian pricing operators: Hansen-Scheinkman factorization, Ross recovery, and long-term pricing, *Operations Research* 64, 99–117.

Qin, Likuan, Vadim Linetsky, and Yutian Nie, 2018, Long forward probabilities, recovery, and the term structure of bond risk premiums, *The Review of Financial Studies* 31, 4863–4883.

Ross, Steve, 2015, The Recovery Theorem, *The Journal of Finance* 70, 615–648.

Walden, Johan, 2017, Recovery with unbounded diffusion processes, *Review of Finance* 21, 1403–1444.

Online Appendices
to the manuscript **Recovery, Specification, and Consistency.**

These appendices provide supporting materials for the paper. Appendix A describes data sources, empirical methodologies and further empirical results. Appendix B presents a simulation and a calibration analysis illustrating the severity and direction of recovery inconsistencies under various underlying state space configurations (uneven state distribution and adverse states). Appendix C provides technical derivations of Propositions 1 and 2.

A Data, Empirical Methodology and Further Results

We present details concerning option and interest rate data and their processing in Appendix A.1, empirical methodologies in Appendix A.2, further empirical results and analyses in Appendix A.3.

A.1 Data

Our data source is OptionMetrics IvyDB US database, which contains historical data on US listed index, ETF, and equity options. It also contains other relevant information such as interest rates and index dividend yields. In particular, we focus on options on S&P 500 (SPX) because they are among the most liquid and actively traded options.

Option Price Data: The sample period in our main empirical analysis is from January 5, 2000 to August 30, 2023, and we obtain call and put option prices for each Wednesday. If price data is unavailable for a particular Wednesday, potentially due to a holiday, we substitute it with the price from the previous trading day. We define moneyness to be the ratio of strike to spot price and keep only OTM options. We exclude options with the average best bid and best offer price less than \$0.50 or with missing price data. We also limit the options in our sample to a fixed moneyness domain of $m \in [0.4, 1.6]$ and days-to-maturity domain of $\tau \in [20, 730]$.

Interest Rate and Dividend Yield Data: We obtain both interest rate data and S&P 500 dividend yield data from OptionMetrics.[1] However, neither the interest rate nor the dividend yield data

[1] In 2024, OptionMetrics started to provide expiration/maturity dates for dividend yield data.

offers a comprehensive coverage of all combinations of dates and maturities (tenors), which is essential to compute the implied volatilities (IV) for options in our sample and the Black-Scholes prices for each point on the estimated IV surface.

For each date, we linearly interpolate the interest rates and dividend yields between quoted tenors. Since the available tenors in the data may fall within the interval of $[20, 730]$, we linearly extrapolate the data so that we obtain a full coverage of date and tenor pairs. It may be possible that the extrapolated data turn out to be negative. In such a case, we impose a lower bound of zero. We locally smooth interest rates and dividend yields so that the term structures do not contain kinks.

Data Processing: In order to apply the put-call parity to translate traded OTM puts into the corresponding ITM calls (which may not be traded), we would need to compute the implied forward prices for the date and tenor pairs of OTM puts. We first apply the method proposed by Aït-Sahalia and Lo (1998) and then supplement the data using the processed dividend yield data from OptionMetrics.

In Aït-Sahalia and Lo (1998), the forward prices are backed out from the put-call parity using the close to ATM option pairs. To do so, for each combination of date and tenor in our sample, we find pairs of call and put options that have the same strike price and have moneyness between 0.99 and 1.01. We then compute the forward price F via the put-call parity

$$C + Ke^{-r\tau} = P + Fe^{-r\tau}. \tag{A.1}$$

There could be multiple implied forward prices for a given pair of date and tenor as we consider a range of moneyness, albeit a small range. In such a case, we take the average of the implied forward prices. The dividend yields are then derived from the spot-forward parity.

However, due to data availability, this method does not guarantee that forward prices and dividend yields exist for all date and tenor pairs. Since dividend yield is crucial for deriving implied volatilities, we address this issue by incorporating the dividend yield data provided by OptionMetrics, as mentioned above. After this step, we are able to translate all OTM puts in our sample into ITM calls using the put-call parity.

To finalize the data for further analyses, such as estimating IV surface, we have to ensure that the options in our sample do not violate the no-arbitrage restrictions. In particular, call option prices C must satisfy the price bounds (34) as well as constraints on vertical and butterfly spreads (35). Finally, we back out the implied volatilities using Black-Scholes formula for each option in our sample.

A.2 Empirical Methodology

Below, we first describe the neural network approach to generate implied volatility surfaces, before discussing the associated recovery implementation.

Neural Network: We follow Ludwig (2015)'s approach of employing neural networks to estimate a stable implied volatility surface from the option data. Prior to estimating the model parameters in (36), we need to ensure the stability of the resulting surface at the tenor boundaries and prevent calendar arbitrage. Therefore, for each date, we augment our sample as follows. To prevent calendar arbitrage, we use the average IV of ATM calls (those with moneyness between 0.99 and 1.01) to create artificial option data for each grid point of moneyness between 1.2 and 1.6 and tenors between 10 and 20 days. To stabilize the results at the tenor boundaries, we keep the first string of options with $\tau > 730$ when processing the raw data, and extract the first string of options with $\tau \geq 20$ and repeat it for each grid point of $m \in [0.9, 1.1]$ at the tenor of 10 days.

Next, we compute the implied total variance for each option on a given date in our augmented data and estimate (36) to obtain the parameters for the implied volatility surface. We obtain the initial parameter values $\boldsymbol{\theta}_0$ of the neural network by following Nguyen and Widrow (1990) and set the number of neurons (i.e., non-linear basis expansions) to be $N = \max\{10, 10 + \lfloor Z \rfloor\}$ with $Z \sim \mathcal{N}(0, 2)$. We map the option prices in our sample to implied volatilities using the Black-Scholes formula and follow Foresee and Hagan (1997) to find the set of model parameters $\boldsymbol{\theta} = \{\beta_0\} \cup \{\alpha_{0i}, \alpha_{1i}, \alpha_{2i}, \beta_i\}_{i=1}^{N}$ that minimizes the residual sum of squares

$$\min_{\boldsymbol{\theta}} \; RSS(\boldsymbol{\theta}) = \min_{\boldsymbol{\theta}} \sum \omega(m)(\widehat{\nu}(m, \tau; \boldsymbol{\theta}) - \nu(m, \tau))^2, \tag{A.2}$$

where $\widehat{\nu}(m, \tau; \boldsymbol{\theta})$ is the fitted implied total variance (36) given $\boldsymbol{\theta}$ and $\nu(m, \tau)$ is from the data. The

weights $\omega(m)$ are given by $\phi(m|1,0.2)+\phi(m|1,0.1)$, where $\phi(\cdot|\mu,\sigma)$ is the normal density function with mean μ and standard deviation σ.

We plug $\boldsymbol{\theta}_0$ into the objective function $RSS(\boldsymbol{\theta})$. After initialization, solve (A.2) for the optimal parameters via Foresee and Hagan (1997) in the following steps:

1. Calculate the Jacobian matrix $\mathbf{J} = \frac{\partial RRS(\boldsymbol{\theta})}{\partial \boldsymbol{\theta}}$ and the Hessian matrix $\mathbf{H} = \mathbf{J}'\mathbf{J}$;
2. Calculate the residual vector $\mathbf{e} \equiv [\sqrt{\omega(m)_i}(\widehat{\nu}_i(m,\tau;\boldsymbol{\theta}) - \nu_i(m,\tau)))]$, where i denotes the ith observation;
3. Compute the gradient vector $\mathbf{g} = 2\mathbf{e}'\mathbf{J}$;
4. Update the parameters $\boldsymbol{\theta}_{new} = \boldsymbol{\theta} - (\mathbf{H} + \lambda\mathbf{I})^{-1}\mathbf{g}$, where $\mathbf{I}$ is the identity matrix and λ is the damping parameter;
5. Evaluate the objective function at $\boldsymbol{\theta}_{new}$;
6. If $RSS(\boldsymbol{\theta}_{new}) < RSS(\boldsymbol{\theta})$, update the damping parameter to $\lambda_{new} = \lambda/v_1$; otherwise, update it to $\lambda_{new} = \lambda v_2$, where $v_1, v_2 > 1$;
7. Repeat the previous steps until convergence or the maximum number of iterations is reached.

We train each network for 100 iterations and obtain an IV surface for $m \in [0.4, 1.6]$ and $\tau \in [20, 730]$, where the grid size of m is chosen to be 0.002, i.e., a total of 601 states. After obtaining a solution $\boldsymbol{\theta}^*$, we produce the associated implied total variance $\widehat{\nu}(m,\tau;\boldsymbol{\theta}^*)$ and back out the call option prices using the Black-Scholes formula for all grid points on the surface. Then, we check whether the conditions (34), (35), as well as the restriction on calendar spread

$$\widehat{\nu}(m,\tau_1;\boldsymbol{\theta}^*) > \widehat{\nu}(m,\tau_2;\boldsymbol{\theta}^*) \text{ if } \tau_1 > \tau_2. \tag{A.3}$$

are satisfied for each of these call prices. If so, we call $\boldsymbol{\theta}^*$ a valid solution to the problem (A.2). We choose the 5 solutions with lowest residual sum of squares (A.2) out of the 15 valid solutions and take the average as our estimated IV surface.

Recovery Implementation: We now detail the procedure to implement separate recoveries for different subjective specifications. For each specification, we follow Audrino et al. (2021)'s bench-

mark approach in employing a regularization procedure (ridge regression) to solve for a stable one-period AD price matrix and its inverse. We relate (i.e., consolidate) observable option price data under different specifications by the LoP and use them as inputs to separate recovery implementations and obtain recovery results for respective specifications. In the difference with the benchmark approach, we do not construct or relate recovery results across different specifications by interpolations.

We consider a model with $S = 601$ states of moneyness and $T = 711$ tenors (days), i.e., $m \in [0.4, 1.6]$ with tick size of 0.002 and $\tau \in [20, 730]$. We name this as the full model. As a baseline, we estimate the monthly AD price matrix $\mathbf{A}$ for each date. Recall that the state price transition (i.e., one-period AD price) matrices satisfy (3) under the assumptions in Ross (2015).

To estimate $\mathbf{A}$, we would solve the following S least squares problems

$$\min_{\mathbf{A}_{:i} \geq \mathbf{0}} (\mathbf{A}_{\tau+1;:i} - \mathbf{A}_\tau \mathbf{A}_{:i})'(\mathbf{A}_{\tau+1;:i} - \mathbf{A}_\tau \mathbf{A}_{:i}),\ i = 1, \ldots, S, \tag{A.4}$$

where $\mathbf{A}_{:i}$ and $\mathbf{A}_{\tau+1;:i}$ denote the i-th column of $\mathbf{A}$ and $\mathbf{A}_{\tau+1}$, respectively. However, $\mathbf{A}_\tau$ is often ill-conditioned, which leads to unstable solutions even with small perturbations in $\mathbf{A}_\tau$. Hence, we include L^2 regularization via the ridge regression

$$\min_{\mathbf{A}_{:i} \geq \mathbf{0}} (\mathbf{A}_{\tau+1;:i} - \mathbf{A}_\tau \mathbf{A}_{:i})'(\mathbf{A}_{\tau+1;:i} - \mathbf{A}_\tau \mathbf{A}_{:i}) + \zeta \mathbf{A}'_{:i}\mathbf{A}_{:i},\ i = 1, \ldots, S. \tag{A.5}$$

The key to solving (A.5) is to find the ridge parameter ζ. To do so, we choose $\zeta > 0$ to minimize the generalized Kullback-Leibler divergence $D_{KL}(\mathbf{A}_\tau \| \widehat{\mathbf{A}}_\tau)$ between the state prices $\mathbf{A}_\tau$ implied from the data and $\widehat{\mathbf{A}}_\tau$ generated by the Markov transition model (3),

$$D_{KL}(\mathbf{A}_\tau \| \widehat{\mathbf{A}}_\tau) = \sum_{j,\tau} \left[\mathbf{A}_{\tau;ij} \log \left(\frac{\mathbf{A}_{\tau;ij}}{\widehat{\mathbf{A}}_{\tau;ij}} \right) - (\mathbf{A}_{\tau;ij} - \widehat{\mathbf{A}}_{\tau;ij}) \right], \tag{A.6}$$

where $\mathbf{A}_{\tau;ij}$ and $\widehat{\mathbf{A}}_{\tau;ij}$ represent state prices paying off in state j with tenor τ, from the perspective of the current state i.

Specifically, we consider a grid of $\zeta \in (0, 0.3]$ and for each ζ on the grid, we solve (A.5) and obtain a transition matrix $\mathbf{A}(\zeta)$, which depends on ζ. We then compute the corresponding gen-

eralized Kullback-Leibler divergence $D_{KL}(\mathbf{A}_\tau \| \widehat{\mathbf{A}}_\tau; \zeta)$ defined in (A.6), which is minimized at the optimal ridge parameter ζ^*.[2] The AD transition matrix is therefore $\mathbf{A}(\zeta^*)$, which we then use to identify its dominant eigenspace $(\delta^{(1)}, \mathbf{x}^{(1,R)})$ and recover the physical transition probabilities and marginal utilities as follows

$$\delta = \delta^{(1)}, \qquad M_i = \frac{1}{x_i^{(1,R)}}, \qquad \mathbf{P} = \delta^{-1}\, \mathbf{Diag}(\mathbf{x}^{(1,R)})^{-1}\, \mathbf{A}(\zeta^*)\, \mathbf{Diag}(\mathbf{x}^{(1,R)}). \tag{A.7}$$

For the recovery of the consolidated model, we first sum up individual state prices within a consolidated state for a given tenor, using the LoP. As an example, we choose the number of states to be 150 for the consolidated model, and sum up every 4 states in the full model. For each consolidated state $\bar{j}$, we set the moneyness $\overline{m}_{\bar{j}}$ to be the median moneyness of all individual states $j \in \bar{j}$. Then, we solve for the optimal ridge parameter $\bar{\zeta}^*$ and the corresponding 150×150 transition matrix $\overline{\mathbf{A}}(\bar{\zeta}^*)$ and subsequently recover the 150-state transition probability matrix $\overline{\mathbf{P}}$ and marginal utilities $\overline{\mathbf{M}}$.

As it may require considerable computing power to solve the non-negative ridge regression (A.5) for a large number of states, Audrino et al. (2021) propose an alternative method of recovering 1201-state probabilities and marginal utilities. Specifically, instead of estimating a full 1201×1201 matrix $\mathbf{A}$, they reduce the number of states to 150 and estimate a 150×150 matrix $\widetilde{\mathbf{A}}$ via (A.5) and the associated 150×1 dominant eigenvector $\widetilde{\mathbf{x}}^{(1,R)}$ is obtained. After finding out the optimal ridge parameter $\widetilde{\zeta}^*$, they obtain the 150-state dominant right eigenvector $\widetilde{\mathbf{x}}^{(1,R)}$ of the matrix $\widetilde{\mathbf{A}}(\widetilde{\zeta}^*)$. Subsequently, a cubic spline interpolation to $\widetilde{\mathbf{x}}^{(1,R)}$ is used to restore to 1201 states. Finally, the recovered 1201-state probabilities $\widetilde{\mathbf{P}}$ and marginal utilities $\widetilde{\mathbf{M}}$ are obtained via (A.7).

A.3 Further Empirical Results

This appendix presents the robustness, replication and validation of the empirical methodology. We first present the recovery inconsistency results concerning 601-state versus 150-state specifications, before discussing the recovery implementation under the 1201-state (benchmark) spec-

[2] Following Audrino et al. (2021), we add 10^{-20} to $\mathbf{A}$ and $\widehat{\mathbf{A}}$ in (A.6) to avoid dividing by zero.

ification.

Concerning 601-state and 150-state specifications: We consider the 601-state (full model) versus 150-state (consolidated model) specifications as in the main text.

Robustness check (using median marginal utility): In Figure A.2 repeats the empirical exercise underlying Figure 1, but instead focuses on the median marginal utilities of the original states of the full model that correspond to either $\overline{M}_{\bar{j}_{\min}}$ (Panel A) or $\overline{M}_{\bar{j}_{\max}}$ (Panel B) of the consolidated model. Similar to Figure 1, we observe that there is a persistent difference between the marginal utilities of the two models, indicating inconsistencies in the recovered marginal utilities that are significant for the adverse state $\bar{j}_{\max}$ (of maximum recovered marginal utility in the consolidated model, Panel B) and for the recent period (from 2014 onward).

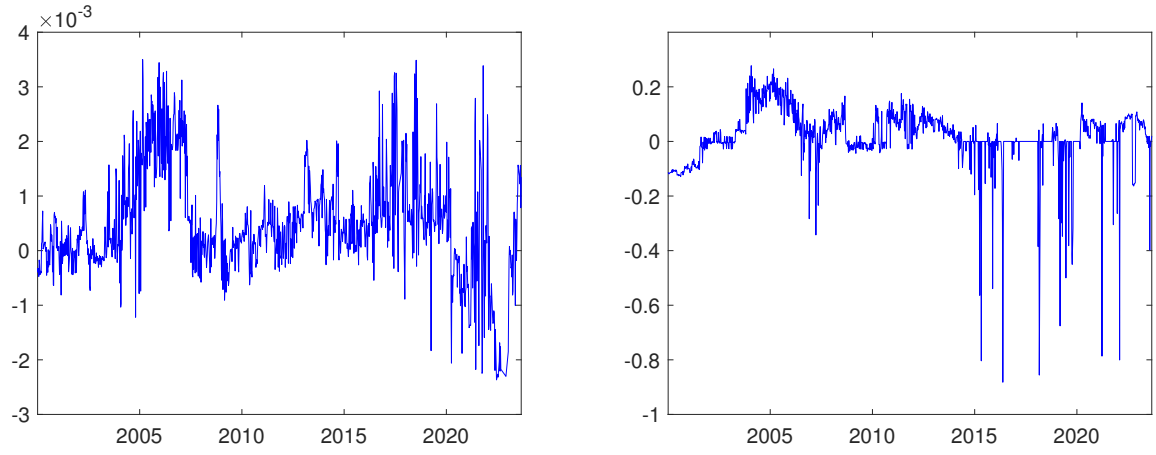

(a) Relative probability difference for minimum marginal utility state

(b) Relative probability difference for maximum marginal utility state

Figure A.1: Relative probability difference between the consolidated and full models

Notes: This figure plots the time series of relative differences of the one-month recovered transition probabilities between the (150-state) consolidated and (601-state) full models, starting from the current state to the minimum (Panel A) and the maximum (Panel B) marginal utility states in the consolidated model. The relative probability difference is defined as $\frac{\overline{p}_{\bar{1}\bar{j}}-\sum_{j\in\bar{j}}p_{1j}}{\sum_{j\in\bar{j}}p_{ij}}$, where $\bar{j}\in\overline{\mathcal{S}}$ and $j\in\mathcal{S}$, and $\overline{p}_{\bar{1}\bar{j}}$ and p_{1j} denote the recovered one-month transition probabilities from the current state of the consolidated and full models, respectively. The sample period is every Wednesday from January 5, 2000 to August 30, 2023.

Two time-series examples of relative probability differences (37): Panel A of Figure A.1 plots the time series of the relative probability difference $dp_{\bar{1}\bar{j}_{\min}}$ associated with the state $\bar{j}_{\min}$ (of minimum recovered marginal utility), and Panel B plots $dp_{\bar{1}\bar{j}_{\max}}$ associated with $\bar{j}_{\max}$ (of maximum recovered marginal utility). Both panels show a non-vanishing relative probability difference

for many dates of the sample period from January 2000 to August 2023, indicating persistent inconsistencies of the recovered transition probabilities. In terms of magnitude, the relative probability difference associated with the transition to the adverse state $\overline{j}_{\max}$ in Panel B is significantly larger than that to the good state $\overline{j}_{\min}$ in Panel A. This pattern is also observed earlier in Figure 1 for the inconsistencies in recovered marginal utilities. Intuitively, it is consistent with the fact that adverse states of the underlying market tend to be rarer, they are more elusive to the recovery process. Further empirical evidence for inconsistencies in the recovered probabilities for the benchmark period is presented in Figures A.4 and A.5.

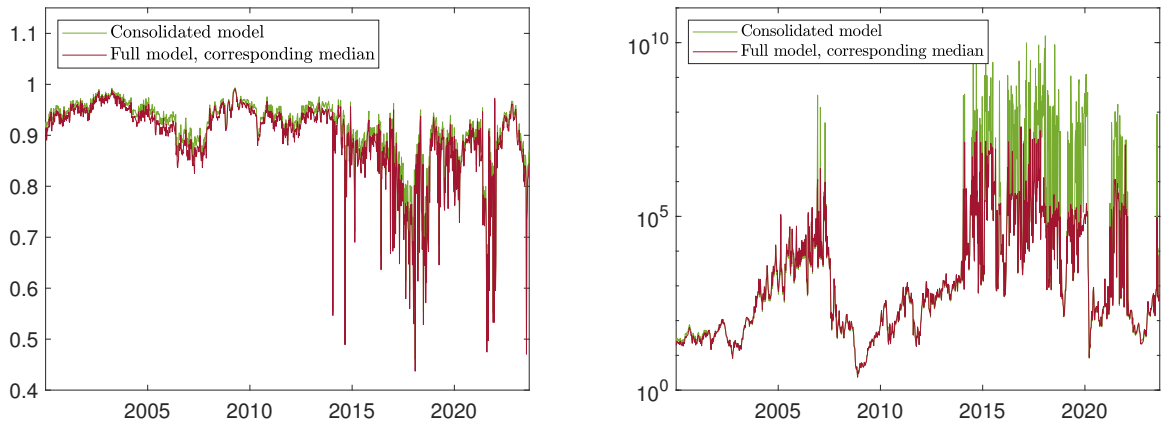

(a) Minimum marginal utilities of the consolidated model

(b) Maximum marginal utilities of the consolidated model

Figure A.2: Comparison of marginal utilities of the consolidated and full models

Notes: This figure plots the time series of the recovered minimum and maximum marginal utilities of the (150-state) consolidated model, along with the median marginal utilities among the original states of the (601-state) full model that correspond to the minimum and maximum marginal utilities states respectively in the consolidated model. Current state's marginal utility is normalized to one. The sample period is every Wednesday from January 5, 2000 to August 30, 2023.

Validation of methodology (January 5, 2000 – December 26, 2012): Now, we limit our sample period to the benchmark sample period from January 5, 2000 to December 26, 2012, which consists of 197,771 call options, to validate our recovery implementations with the benchmark literature. Table A.1 shows the summary statistics of implied volatilities for various moneyness and tenors. The summary statistics are in line with those reported in Ludwig (2015). For completeness, we also report the risk-neutral and recovered moments of cross-sectional returns in Table A.2.[3]

[3]The results in this table are broadly comparable with the corresponding moments reported in Audrino et al. (2021), who employ 1201-state specification in place of our 601-state specification in Table A.2.

Table A.1: Summary statistics of call options

m	DITM < 0.90	ITM $[0.90, 0.99]$	ATM $(0.99, 1.01)$	OTM $[1.02, 1.10]$	DOTM > 1.10
Panel A: Maturity < 180 days					
IV (%)	34.92	22.28	18.72	17.33	21.06
Price	273.79	86.68	39.08	16.66	4.49
N	35,136	23,999	6,423	24,758	13,845
Panel B: Maturity 180 — 365 days					
IV (%)	30.94	22.27	20.67	19.16	18.55
Price	353.17	130.38	86.65	54.80	13.57
N	22,563	7,975	1,884	8,007	15,464
Panel C: Maturity > 365 days					
IV (%)	28.60	21.78	20.57	19.80	18.14
Price	390.73	164.85	123.99	92.80	28.88
N	15,277	4,939	1,158	4,723	11,620

Notes: This table reports the average implied volatilities (IV) and prices of the call options on S&P 500 in our sample for different categories of moneyness m and maturities. Our sample contains option data for every Wednesday from January 5, 2000 to December 26, 2012. Moneyness is defined as the ratio of strike to spot price.

Table A.2: Summary statistics of risk-neutral and recovered moments

	Median	Std dev	Min	25th	75th	Max
Panel A: Risk-neutral moments						
Mean (%)	-1.70	4.70	-29.69	-4.31	1.80	5.07
Volatility (%)	21.32	8.87	10.44	16.85	26.54	73.88
Skewness	-1.22	0.40	-2.71	-1.55	-0.97	-0.47
Kurtosis	7.24	3.32	3.85	5.63	9.61	23.60
Panel B: Recovered moments						
Mean (%)	9.80	4.63	-3.82	7.24	13.38	26.87
Volatility (%)	17.60	7.60	9.04	13.63	21.74	66.99
Skewness	-0.90	0.24	-1.89	-1.09	-0.75	-0.37
Kurtosis	5.41	1.46	3.74	4.72	6.58	12.46

Notes: This table reports the summary statistics of the risk-neutral and recovered moments of 30-day-to-maturity cross-sectional returns on S&P 500 for the (601-state) full model. Returns are computed by considering all possible values of S&P 500 on the grid in the next period. Mean and volatility are annualized and reported as percentages. All moments are unconditional over the period of January 5, 2000 to December 26, 2012.

Recovery inconsistencies (January 5, 2000 – December 26, 2012): We examine the recovery consistencies between the 601-state (full model) and 150-state (consolidated model) specifications for the benchmark sample period (January 5, 2000 – December 26, 2012). To this end, Figure A.3's

Panel A (resp., Panel B) plots the time series of minimum (resp., maximum) recovered marginal utilities of the consolidated model at consolidated states $\bar{j}_{\min}$ (resp., $\bar{j}_{\max}$) against the corresponding minimum and maximum recovered marginal utilities of the full model among original states belonging to $\bar{j}_{\min}$ (resp., $\bar{j}_{\max}$). Figure A.4 further plots the mean and median of the relative probability difference (37), and Panels A and B of Figure A.5 provide two time-series examples of probabilities going to the minimum and maximum marginal utilities states of the consolidated model. Altogether, these plots (Figures A.3, A.4 and A.5) show persistent inconsistencies in both recovered marginal utilities and recovered transition probabilities. These patterns are similar to Figures 1 and 2 in the main text (which employ data of the entire sample period from January 5, 2000 – August 30, 2023), indicating the robustness of recovery inconsistencies.

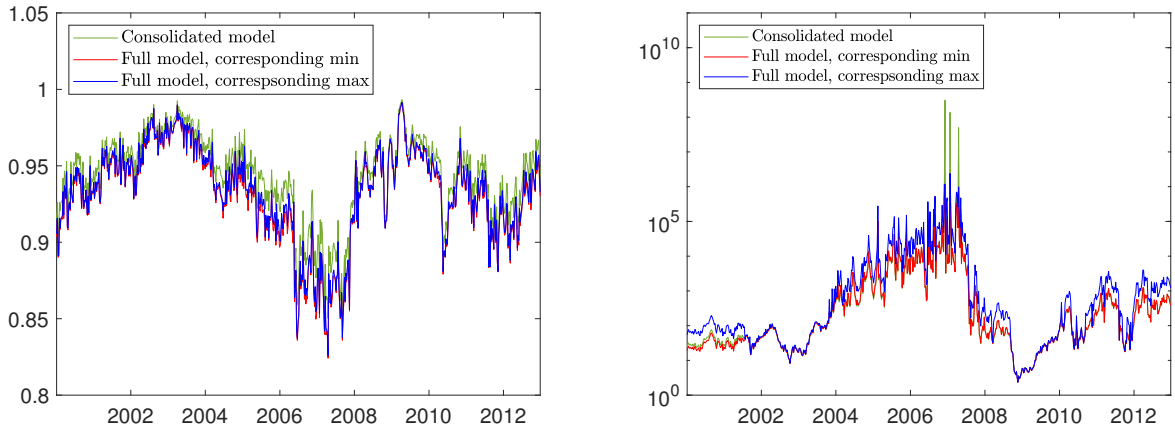

(a) Minimum marginal utilities of the consolidated model

(b) Maximum marginal utilities of the consolidated model

Figure A.3: Comparison of marginal utilities of the consolidated and full models

Notes: This figure plots the time series of the recovered minimum ($\overline{M}_{\bar{j}_{\min}}$) and maximum ($\overline{M}_{\bar{j}_{\max}}$) marginal utilities of the (150-state) consolidated model, along with the minimum ($M_{j_{\min}}$) and maximum ($M_{j_{\max}}$) marginal utilities among the original states of the (601-state) full model that correspond to the minimum ($j_{\min} \in \bar{j}_{\min}$) and maximum ($j_{\max} \in \bar{j}_{\max}$) marginal utilities states respectively in the consolidated model. Current state's marginal utility is normalized to one. The sample period is every Wednesday from January 5, 2000 to December 26, 2012.

Variations of recovery inconsistencies (January 5, 2000 – December 26, 2012): We examine the variation of recovery inconsistencies with measures quantifying violation of the recovery consistency condition for the benchmark sample period. Panel A (resp., Panel B) of Table A.3 reports the point estimates and the statistical significance of the time-series correlations between the local and global consistency measures $\mathcal{C}_{\bar{j}}$, $\mathcal{C}_g$ (38) (resp., the one-month and one-year consistency

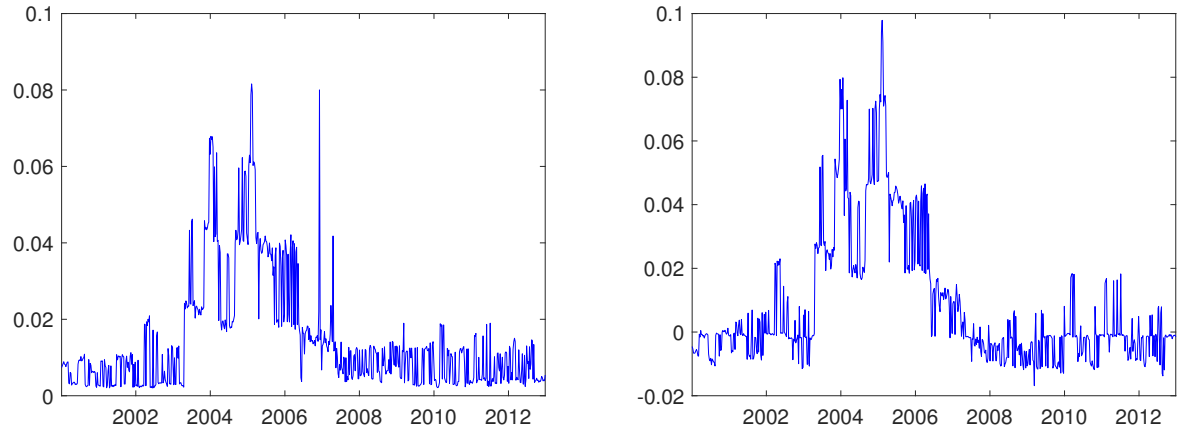

(a) Mean of absolute value of relative probability difference

(b) Median of relative probability difference

Figure A.4: Relative probability difference between the consolidated and full models

Notes: This figure plots the mean and median of the relative differences of the one-month recovered transition probabilities between the (150-state) consolidated and (601-state) full models, starting from the current state to states in the consolidated model. Panel A plots the mean of the absolute values of the relative difference, and Panel B plots the median of the relative difference. The relative probability difference is defined as $\frac{\overline{p}_{\overline{1}\,\overline{j}}-\sum_{j\in\overline{j}}p_{1j}}{\sum_{j\in\overline{j}}p_{ij}}$, where $\overline{j}\in\overline{\mathcal{S}}$ and $j\in\mathcal{S}$, and $\overline{p}_{\overline{1}\,\overline{j}}$ and p_{1j} denote the recovered one-month transition probabilities from the current state of the consolidated and full models, respectively. The sample period is every Wednesday from January 5, 2000 to December 26, 2012.

measures $\mathcal{C}^{P}_{1;\overline{1}\,\overline{j}}$, $\mathcal{C}^{P}_{12;\overline{1}\,\overline{j}}$ (39)) and the inconsistency level of recovered marginal utilities (resp., the inconsistency level of recovered transition probabilities of commensurate horizons). All but one of these correlation estimates are positive and statistically significant (p-value < 0.01), indicating that larger inconsistencies of recovered marginal utilities and transition probabilities tend to take place when the violation of consistency condition is more significant.[4] These findings for the benchmark sample period are similar to those for the entire sample period reported in Table 3 in the main text, signifying the robustness of these theory-implied variations of recovery inconsistencies in different sample periods.

Concerning 1201-state and 150-state specifications: For completeness and robustness, we now consider the 1201-state (full model) versus 150-state (consolidated model) specifications of the benchmark literature, and for the entire sample period January 5, 2000 to August 30, 2023. Unlike the literature, we examine and demonstrate recovery inconsistencies by implementing two separate recoveries for these two models, while relating (consolidating) observable price inputs

[4]The only statistically insignificant point estimate is positive.

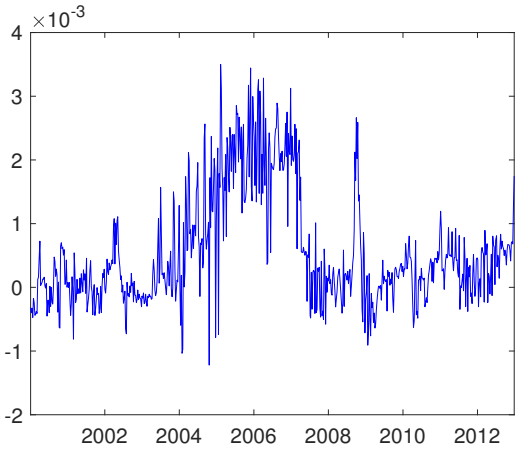

(a) Relative probability difference for minimum marginal utility state

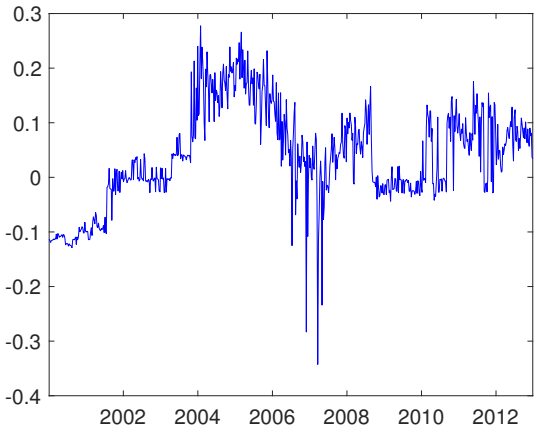

(b) Relative probability difference for maximum marginal utility state

Figure A.5: Relative probability difference between the consolidated and full models

Notes: This figure plots the time series of relative differences of the one-month recovered transition probabilities between the (150-state) consolidated and (601-state) full models, starting from the current state to the minimum (Panel A) and the maximum (Panel B) marginal utility states in the consolidated model. The relative probability difference is defined as $\frac{\overline{p}_{\overline{1}\overline{j}} - \sum_{j\in\overline{j}} p_{1j}}{\sum_{j\in\overline{j}} p_{ij}}$, where $\overline{j} \in \overline{\mathcal{S}}$ and $j \in \mathcal{S}$, and $\overline{p}_{\overline{1}\overline{j}}$ and p_{1j} denote the recovered one-month transition probabilities from the current state of the consolidated and full models, respectively. The sample period is every Wednesday from January 5, 2000 to December 26, 2012.

to these models by the law of one price. Specifically, for the 1201-state model, we solve the entire 1201 ridge regressions (A.5) (without lowering the number of states to a coarser model first and interpolating back to 1201-state model) to obtain the 1201×1201 AD price matrix $\mathbf{A}$. We then recover the time preference as well as the 1201-state marginal utilities and transition probabilities via (A.7). Table A.4 reports the risk-neutral and recovered moments of cross-sectional returns.

For the 150-state model, we employ the consolidated observable price data and solve (new) 150 ridge regressions (A.5) to obtain a 150×150 AD price matrix $\mathbf{A}$ and its dominant eigenvalue and eigenvector (which characterize the recovered time and risk preferences in the consolidated model).

Figure A.6 plots the time series of minimum and maximum marginal utilities of the consolidated model and the corresponding minimum and maximum marginal utilities of the full model within the states $\overline{j}_{\min}$ and $\overline{j}_{\max}$. We observe that the difference between $M_{j_{\min}}$ and $M_{j_{\max}}$ continues to persist over time. Moreover, $\overline{M}_{\overline{j}_{\min}}$ and $\overline{M}_{\overline{j}_{\max}}$ are outside the range of the corresponding $M_{j_{\min}}$ and $M_{j_{\max}}$ for most of the dates.

Table A.3: Variations in recovery inconsistencies

Panel A: Recovered marginal utilities		
	$\lvert\overline{M}_{\bar{j}_{\min}} - M_{j_{\text{med}}}\rvert$	$\lvert\overline{M}_{\bar{j}_{\max}} - M_{j_{\text{med}}}\rvert$
$\mathcal{C}_{\bar{j}_{\min}}$	0.67^{***}	
	(23.59)	
$\mathcal{C}_{\bar{j}_{\max}}$		0.01
		(0.23)
$\mathcal{C}_g$	0.27^{***}	0.85^{***}
	(7.16)	(41.46)

Panel B: Recovered transition probabilities, one-month and one-year ahead				
	$\lvert\overline{p}_{1;\,\bar{1}\,\bar{j}_{\min}} - p_{1;\,1\bar{j}_{\min}}\rvert$	$\lvert\overline{p}_{1;\,\bar{1}\,\bar{j}_{\max}} - p_{1;\,1\bar{j}_{\max}}\rvert$	$\lvert\overline{p}_{12;\,\bar{1}\,\bar{j}_{\min}} - p_{12;\,1\bar{j}_{\min}}\rvert$	$\lvert\overline{p}_{12;\,\bar{1}\,\bar{j}_{\max}} - p_{12;\,1\bar{j}_{\max}}\rvert$
$\mathcal{C}^P_{1\,;\bar{1}\,\bar{j}_{\min}}$	0.54^{***}			
	(16.57)			
$\mathcal{C}^P_{1\,;\bar{1}\,\bar{j}_{\max}}$		0.99^{***}		
		(179.19)		
$\mathcal{C}^P_{12\,;\bar{1}\,\bar{j}_{\min}}$			0.29^{***}	
			(7.73)	
$\mathcal{C}^P_{12\,;\bar{1}\,\bar{j}_{\max}}$				0.69^{***}
				(24.58)

Notes: This table reports the time-series correlations between the consistency measures and degrees of recovery inconsistencies for every Wednesday from January 5, 2000 to December 26, 2012. The local consistency measure $\mathcal{C}_{\bar{j}}$ for marginal utilities is the difference between the maximum and minimum marginal utilities associated with original states j that belong to $\bar{j}_{\max}$ or $\bar{j}_{\min}$. The global inconsistency measure $\mathcal{C}_g$ is the standard deviation of marginal utilities across all $S = 601$ states in the full model. The local consistency measure $\mathcal{C}^P_{\tau\,;\bar{1}\,\bar{j}}$ for transition probabilities of one-month ($\tau = 1$) and one-year ($\tau = 12$) horizons is the difference between the maximum and minimum transition probabilities of corresponding horizons starting from an original state belonging to the current consolidated state $\bar{1}$ to $\bar{j}_{\max}$ or $\bar{j}_{\min}$. t-statistics are reported in parentheses. * indicates significance at the 10% level; **, at the 5% level; and ***, at the 1% level.

Figure A.7 further plots the mean and median of relative probability differences (37) concerning 1201-state and 150-state models. These plots exhibit non-vanishing values persisting over time. These patterns of marginal utilities and probabilities are similar to Figures 1 and 2 (concerning 601-state and 150-state models), indicating robust inconsistencies in recovered marginal utilities and transition probabilities across various specifications.

To examine the variation of the recovery consistencies with measures quantifying the violation of the recovery consistency condition concerning 1201-state and 150-state models, we estimate the time-series correlations between consistency measures $\mathcal{C}_{\bar{j}}$, $\mathcal{C}_g$ (38) and recovered marginal utilities' inconsistency level, and between measures $\mathcal{C}^P_{1\,;\bar{1}\,\bar{j}}$, $\mathcal{C}^P_{12\,;\bar{1}\,\bar{j}}$ (39) and recovered

Table A.4: Summary statistics of risk-neutral and recovered moments

	Median	Std dev	Min	25th	75th	Max
Panel A: Risk-neutral moments						
Mean (%)	−2.11	4.10	−43.05	−3.81	−0.07	5.03
Volatility (%)	19.76	8.29	9.26	15.73	24.72	80.05
Skewness	−1.49	0.72	−6.55	−2.06	−1.09	−0.45
Kurtosis	9.10	7.69	3.83	6.34	14.19	14.19
Panel B: Recovered moments						
Mean (%)	11.15	5.12	−4.09	7.82	14.74	37.25
Volatility (%)	15.39	7.24	4.99	12.20	20.16	68.01
Skewness	−1.09	0.50	−6.08	−1.39	−0.85	−0.36
Kurtosis	6.70	4.17	3.69	5.30	8.88	81.90

Notes: This table reports the summary statistics of the risk-neutral and recovered moments of 30-day-to-maturity cross-sectional returns on S&P 500 for the 1201-state model. Returns are computed by considering all possible values of S&P 500 on the grid in the next period. Mean and volatility are annualized and reported as percentages. All moments are unconditional over the period of January 5, 2000 to August 30, 2023.

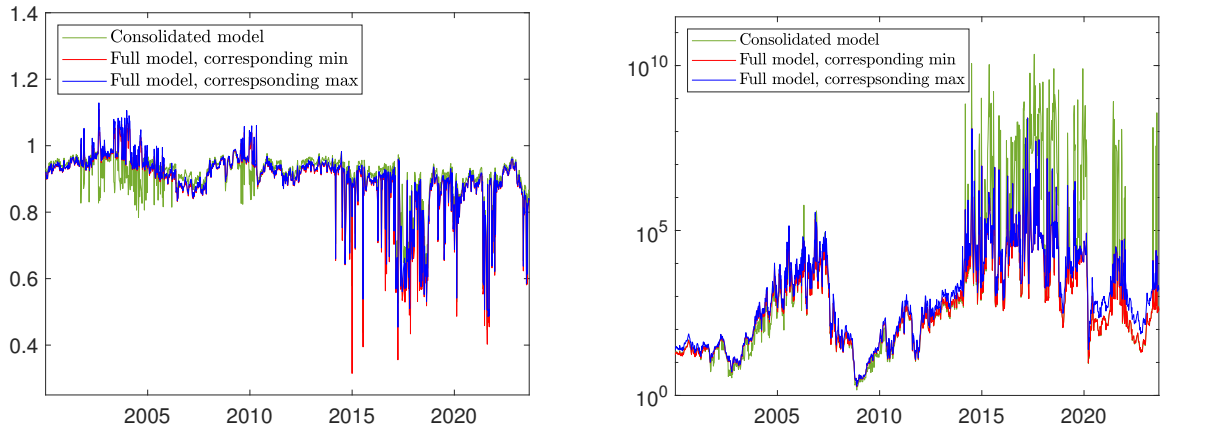

(a) Minimum marginal utilities of the consolidated model

(b) Maximum marginal utilities of the consolidated model

Figure A.6: Comparison of marginal utilities of the consolidated and full models

Notes: This figure plots the time series of the recovered minimum ($\overline{M}_{\bar{j}_{\min}}$) and maximum ($\overline{M}_{\bar{j}_{\max}}$) marginal utilities of the (150-state) consolidated model, along with the minimum ($M_{j_{\min}}$) and maximum ($M_{j_{\max}}$) marginal utilities among the original states of the (1201-state) model that correspond to the minimum ($j_{\min} \in \bar{j}_{\min}$) and maximum ($j_{\max} \in \bar{j}_{\max}$) marginal utilities states respectively in the consolidated model. Current state's marginal utility is normalized to one. The sample period is every Wednesday from January 5, 2000 to August 30, 2023.

transition probabilities' inconsistency level. Table A.5 presents the point estimates and the statistical significance of these correlations using data of the entire sample period January 5, 2000 to August 30, 2023. Most of these correlation estimates are positive and statistically significant

(p-value < 0.01), indicating that larger recovery inconsistencies tend to take place when the violation of consistency condition is more significant. These findings are similar to those reported in Table 3 in the main text (concerning 601-state and 150-state specifications), signifying the robustness of these theory-implied variations of recovery inconsistencies across various specifications.

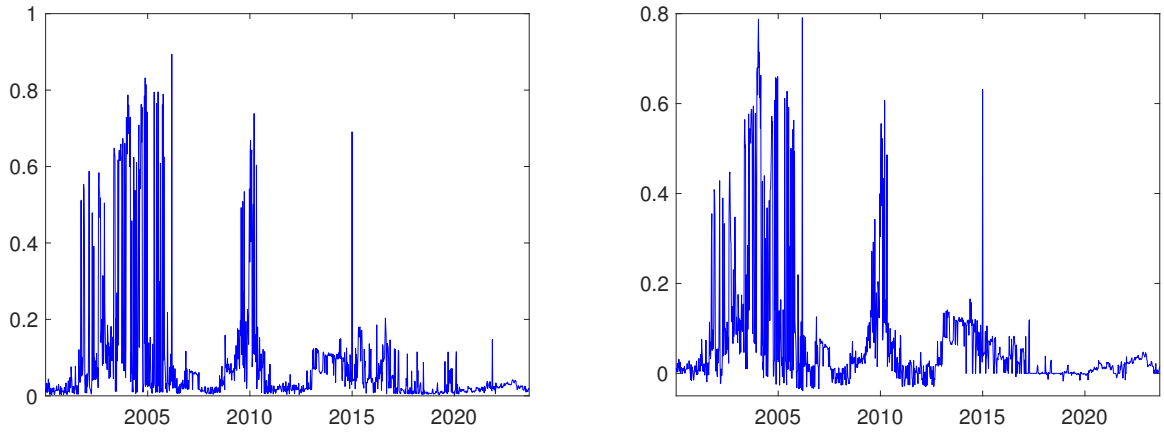

(a) Mean of absolute value of relative probability difference

(b) Median of relative probability difference

Figure A.7: Relative probability difference between the consolidated and full models

Notes: This figure plots the mean and median of the relative differences of the one-month recovered transition probabilities between the (150-state) consolidated and (1201-state) full models, starting from the current state to states in the consolidated model. Panel A plots the mean of the absolute values of the relative difference, and Panel B plots the median of the relative difference. The relative probability difference is defined as $\frac{\overline{p}_{\overline{1}\overline{j}} - \sum_{j\in\overline{j}} p_{1j}}{\sum_{j\in\overline{j}} p_{ij}}$, where $\overline{j} \in \overline{\mathcal{S}}$ and $j \in \mathcal{S}$, and $\overline{p}_{\overline{1}\overline{j}}$ and p_{1j} denote the recovered one-month transition probabilities from the current state of the consolidated and full models, respectively. The sample period is every Wednesday from January 5, 2000 to August 30, 2023.

Table A.5: Variations in recovery inconsistencies

Panel A: Recovered marginal utilities		
	$\lvert\overline{M}_{\overline{j}_{\min}} - M_{j_{\text{med}}}\rvert$	$\lvert\overline{M}_{\overline{j}_{\max}} - M_{j_{\text{med}}}\rvert$
$\mathcal{C}_{\overline{j}_{\min}}$	0.31^{***}	
	(11.32)	
$\mathcal{C}_{\overline{j}_{\max}}$		-0.01
		(-0.25)
$\mathcal{C}_g$	0.11^{***}	0.01
	(3.72)	(0.26)

Panel B: Recovered transition probabilities, one-month and one-year ahead				
	$\lvert\overline{p}_{1;\,\overline{1}\,\overline{j}_{\min}} - p_{1;\,1\overline{j}_{\min}}\rvert$	$\lvert\overline{p}_{1;\,\overline{1}\,\overline{j}_{\max}} - p_{1;\,1\overline{j}_{\max}}\rvert$	$\lvert\overline{p}_{12;\,\overline{1}\,\overline{j}_{\min}} - p_{12;\,1\overline{j}_{\min}}\rvert$	$\lvert\overline{p}_{12;\,\overline{1}\,\overline{j}_{\max}} - p_{12;\,1\overline{j}_{\max}}\rvert$
$\mathcal{C}^P_{1;\,\overline{1}\,\overline{j}_{\min}}$	0.61^{***}			
	(26.84)			
$\mathcal{C}^P_{1;\,\overline{1}\,\overline{j}_{\max}}$		0.41^{***}		
		(15.91)		
$\mathcal{C}^P_{12;\,\overline{1}\,\overline{j}_{\min}}$			0.94^{***}	
			(96.73)	
$\mathcal{C}^P_{12;\,\overline{1}\,\overline{j}_{\max}}$				0.37^{***}
				(13.93)

Notes: This table reports the time -series correlations between the consistency measures and degrees of recovery inconsistencies for every Wednesday from January 5, 2000 to August 30, 2023. The local consistency measure $\mathcal{C}_{\overline{j}}$ for marginal utilities is the difference between the maximum and minimum marginal utilities associated with original states j that belong to $\overline{j}_{\max}$ or $\overline{j}_{\min}$. The global inconsistency measure $\mathcal{C}_g$ is the standard deviation of marginal utilities across all $S = 1201$ states in the model. The local consistency measure $\mathcal{C}^P_{\tau;\,\overline{1}\,\overline{j}}$ for transition probabilities of one-month ($\tau = 1$) and one-year ($\tau = 12$) horizons is the difference between the maximum and minimum transition probabilities of corresponding horizons starting from an original state belonging to the current consolidated state $\overline{1}$ to $\overline{j}_{\max}$ or $\overline{j}_{\min}$. t-statistics are reported in parentheses. * indicates significance at the 10% level; **, at the 5% level; and ***, at the 1% level.

B Simulation and Calibration Analyses

This appendix presents recovery results and analysis for (i) a simulation setup, and (ii) a calibration setup. The setups are simple (simplified) to illustrate further aspects of the recovery consistency issue. The simulation analysis allows us to compare the recovered and the underlying market characteristics (the latter are known by simulation design). The calibration analysis allows us to examine the recovery inconsistency (overshooting or undershooting) behaviors under the calibrated U.S. aggregate consumption and stock market dynamics.

B.1 Simulation Analysis

By design, the simulation enables the knowledge of the underlying state specification, allowing us to compare and evaluate various subjective specifications and their recovery results against the underlying counterparts. Our simulation setup is guided by Proposition 1's finding that the heterogeneity among true underlying states, that are inadvertently and subjectively specified as a single state in the recovery process, gives rise to recovery inconsistencies. Specifically, we verify whether a larger heterogeneity of underlying states leads to a larger recovery inconsistency.

We first specify an underlying model of $S = 601$ states characterized by the time discount, marginal utilities, and transition probabilities among these states, which are the given inputs to the simulation setup (Footnote 6 below). These inputs are such that marginal utilities in the first 300 states exhibit a larger variation (i.e., heterogeneity) than those in the last 300 states. In contrast, the transition probability inputs from all underlying states exhibit a regular pattern (i.e., moderate variation). Such a simulation setup aims to focus on the effect of marginal utilities' heterogeneity on recovery results. We assume that the center state (numbered 301) is the current state. Following from these inputs, all AD prices in the underlying model can be determined.

Next, taking perspectives of two analysts, we consider two subjective specifications of $\overline{S} = 101$ consolidated states. In the first (uniformed) subjective specification, every 6 neighboring underlying states correspond to a consolidated state, while leaving the current state intact.[5] The second (adaptive) subjective specification features a finer (resp., coarser) state space partition

[5] That is, the current state (numbered 301) remains a single state in the uniformed subjective specification.

with 75 (resp., 25) consolidated states for the first (resp., the last) 300 underlying states, where the underlying marginal utilities are more (resp., less) heterogeneous. It also leaves the current state intact. As a result, while both subjective specifications have the same number of 101 consolidated states, the second one adapts better to the distribution of underlying marginal utilities in the simulation setup.[6]

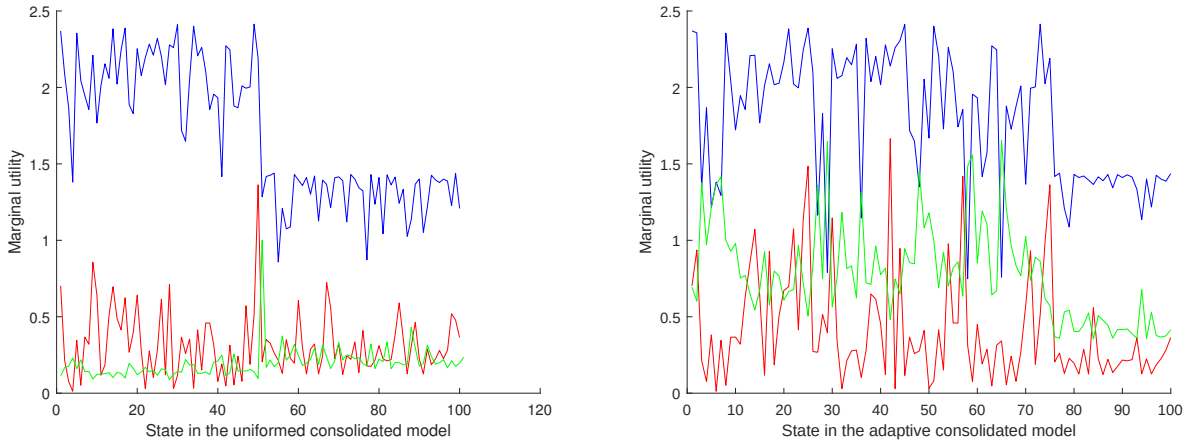

(a) Marginal utilities: Uniformed subjective state space specification.

(b) Marginal utilities: Adaptive subjective state space specification.

Figure B.8: Recovered marginal utilities in a simulation setup.

Notes: This figure plots the maximum (blue line) and minimum (red line) marginal utilities of of original underlying states that map into the consolidated state indicated in the horizontal axis. The green line plots the recovered marginal utilities for the corresponding consolidated states. Panel (a) concerns the uniformed subjective state specification, Panel (b) the adaptive subjective state specification. All marginal utilities are normalized by the marginal utility of the current state.

Figure B.8 presents the recovery results and their consistencies for the uniformed (Panel (a)) and adaptive (Panel (b)) subjective specifications. In both panels, for each consolidated state (horizontal axis), the blue (resp., red) line plots the maximum (resp., minimum) marginal utility (vertical axis) of the original underlying states that map into the consolidated state under consideration. The green line plots the recovered marginal utility for the consolidated model. Evidently, for most of the state space, the recovered marginal utility of the adaptive subjective specification (Panel (b)) is in-between the the minimum and maximum values of the corresponding

[6] Numerically, in the underlying market model, the min, median, max, mean and variance of marginal utilities for the first 300 original underlying states (normalized by the marginal utility of the current state) are respectively 0.0126, 1.1928, 2.4138, 1.2094 and 0.4812. The corresponding input values for the last 300 original states are 0.1223, 0.7655, 1.4396, 0.7810 and 0.1587. The corresponding input values for the overall 601 original states are 0.0126, 0.9424, 2.4138, 0.9952 and 0.3647. The min, median, max, mean and variance of the transition probabilities from the current state in the underlying model are respectively 2×10^{-6}, 0.0017, 0.0032, and 0.0017. The variance is 8×10^{-7}.

underlying marginal utilities. Whereas, the recovered marginal utility of the uniformed subjective specification (Panel (a)) is biased downward consistently in all states. This simulation setup illustrates that a more consistent recovery result is obtained for the adaptive specification as it deviates less from Proposition 1's recovery consistency condition. Put differently, when the preference dynamics of the underlying market model is more variable, our simulation analysis indicates a need for a finer (adaptive) state space specification to mitigate the recovery inconsistencies. In practical (non-simulation) settings, as the underlying state dynamics is not observed prior to the recovery implementation, such an adaptive subjective state space specification is elusive.

B.2 Calibration Analysis

Our calibration aims to capture stylized feature the U.S. aggregate consumption and stock market dynamics, examine the recovery inconsistency (overshooting or undershooting) direction and identify the responsible economic factors. For the clarity of the illustration and discussion, we adopt a simple but essential 3-state state space specification to capture an adverse, a normal, and a good state of the economy.

Setup: The analysis has two steps, namely the calibration and recovery steps. In the calibration step, we calibrate an endowment representative-agent economy with a constant relative risk aversion (CRRA) and underlying state space specification $\mathcal{S} = \{1, 2, 3\}$ to the stylized feature the U.S. aggregate consumption and stock market dynamics.[7] This calibration step provides us with an underlying model (i.e., underlying characteristics of state space probability distribution and preferences) matching the U.S. economy. In the recovery step, we recover the market model's characteristics using an analyst's subjective state space specification $\overline{\mathcal{S}} = \{\overline{1}, \overline{2}\}$ (see (B.2) below). For this recovery, we then only employ the prices generated by (but not the characteristics of) the underlying model constructed in the calibration step. Analyzing the recovered and underlying characteristics reveals the recovery inconsistency direction and the associated economic features. Details concerning these two steps are as follows.

[7] These three underlying states aim to model after three stylized states of the economy, namely, an adverse state 1 (associate with an elevated marginal utility), a normal state 2 (moderate marginal utility), and a good state (low marginal utility). See calibration results (B.1) below.

In the calibration step, as inputs to the underlying model $\mathcal{S}$, we use the U.S. household real consumption expenditure, S&P 500 index level, and 3-month Treasury Bill rate from 1985Q1 to 2022Q4 and at quarterly frequency. Our calibration employs the generalized method of moments (GMM) procedure to match five model-implied stationary moments with their counterparts in the data, namely, the expected consumption growth μ_c, the volatility of consumption growth σ_c, the risk-free rate r^f_{t+1}, the S&P 500 risk premium rx^s_t, and the volatility of S&P 500 return σ_s (detailed in Equation (B.8) below). Table B.6 presents the summary (non-annualized) statistics of the consumption and asset price inputs employed in our calibration. Since the U.S.

Variable	Mean	Std Dev	Min	25th	Median	75th	Max
Consumption growth	0.0068	0.0132	-0.0990	0.0037	0.0068	0.010	0.1038
Risk-free rate	0.0076	0.0063	-0.00003	0.0006	0.0073	0.0127	0.0223
Stock index return	0.0232	0.0676	-0.2356	-0.0132	0.0307	0.0642	0.1909
Risk premium	0.0156	0.0674	-0.2379	-0.0197	0.0203	0.0587	0.1782

Table B.6: Summary statistics of the consumption and asset price inputs to the calibration (reported moments are not annualized). Risk premium denotes the return of the stock index in excess of the risk-free rate (i.e., excess return).

consumption growth distribution clusters pronouncedly around the mean, we employ respectively 0.1th and 99th percentiles of the time-series consumption growth to delineate and calibrate the adverse (disaster) and good states, and the average consumption growth to calibrate the normal state. To calibrate basic asset price characteristics, we embed the three-state space $\mathcal{S}$ in a temporal setting of one period and two dates $\{t, t+1\}$. We employ a consumption-based asset pricing model (CCAPM) featuring a representative agent with CRRA $\gamma = 15$ and time discount factor $\delta = 0.98$ to price and calibrate the risk-free bond and the stock market (as a contingent claim on the aggregate consumption). Using a standard two-stage GMM estimation, this calibration then determines the underlying 3×3 one-period transition probability matrix $\mathbf{P}$ in the physical measure and the marginal utilities $\{M_i\}$, $i \in \mathcal{S} = \{1, 2, 3\}$, for the underlying model.[8] These calibrated underlying characteristics then imply the 3×3 one-period AD price matrix $\mathbf{A}$

[8] Recall that the marginal utilities are determined only up to a multiplicative constant.

via $A_{ij} = \delta \frac{M_j}{M_i} p_{ij}$, $i, j \in \{1, 2, 3\}$,

$$\text{(B.1)} \quad \mathbf{P} = \begin{bmatrix} 0.0425 & 0.4847 & 0.4727 \\ 0.0385 & 0.5840 & 0.3775 \\ 0.0192 & 0.5799 & 0.4009 \end{bmatrix}, \quad \begin{bmatrix} M_1 \\ M_2 \\ M_3 \end{bmatrix} = \begin{bmatrix} 4.7789 \\ 0.9029 \\ 0.6247 \end{bmatrix}, \quad \mathbf{A} = \begin{bmatrix} 0.0417 & 0.0898 & 0.0606 \\ 0.1999 & 0.5723 & 0.2559 \\ 0.1441 & 0.8215 & 0.3929 \end{bmatrix}.$$

Three observations on the calibrated model are in order. First, starting from any current state $i \in \{1, 2, 3\}$, the chance of reaching state 1 in the next period is much smaller than reaching the other two states, $p_{i1} \ll p_{i2}, p_{i2}$, $\forall i \in \{1, 2, 3\}$. Second, the marginal utility values satisfy $M_1 \gg M_2 > M_3$. These characteristics indicate three stylized economic states, namely, a rare disaster (adverse) state 1, a normal state 2 as, and a good state 3 (Footnote 7). Third, starting from any current state $i \in \{1, 2, 3\}$, the AD contract that pays off if the disaster state realizes next period is significantly cheaper than contracts that pays off if other two states realize, $A_{i1} \ll A_{i2}, A_{i3}$, $\forall i \in \{1, 2, 3\}$. Intuitively, while the adverse state 1 is undesirable (i.e., with a low consumption and a high marginality), its likelihood to realize next period is unconditionally very small. As a result, the required premium A_{i1}, $\forall i \in \{1, 2, 3\}$, to insure against such an adverse but highly unlikely event is low. For an assessment of the calibration, Table B.7 presents the calibration-implied versus actual (empirical) values for the annualized moments of the consumption and asset prices. Note that the stock index return volatility is lower, while the

Description	Model	Actual (empirical)
Mean consumption growth	0.0257	0.0273
Consumption growth volatility	0.0467	0.0264
Mean risk-free rate	0.0269	0.0303
Mean risk premium (stock)	0.0688	0.0625
Stock index return volatility	0.0487	0.1351

Table B.7: Calibration results of the consumption and asset price (annualized) moments. Risk premium denotes the return of the stock index in excess of the risk-free rate (i.e., excess return). The calibration model is estimated by a standard 2-stage GMM procedure, which employs moment equations listed in (B.8).

consumption growth volatility is higher, in the model than in the data. These numerical values result from the constraint to match the stock index risk premium in the calibration and data, reflecting the well-known equity risk premium puzzle for the current simple consumption-based asset pricing model (with CRRA $\gamma = 15$).

In the recovery step, we employ only asset prices generated from the implied one-period AD price matrix $\mathbf{A}$ in (B.1) but adapted to the subjective specification $\overline{\mathcal{S}}$ perceived by the analyst.[9] As discussed in the main text (see a similar procedure in (6)), the asset prices observed and perceived by the analyst are generated from $\mathbf{A}$ by the law of one price (no-arbitrage relationships) while consolidating the underlying $\mathcal{S}$ and subjective $\overline{\mathcal{S}}$ specifications,

$$\text{(B.2)} \qquad \left\{ \begin{array}{c} \textbf{Underlying specification:} \\ \mathcal{S} = \{1,2,3\} \end{array} \right. \longrightarrow \left\{ \begin{array}{c} \textbf{Subjective specification:} \\ \overline{\mathcal{S}} = \{\overline{1},\overline{2}\} \text{ with: } \quad \overline{1} = \{1,2\}, \quad \overline{2} = 3. \end{array} \right.$$

Without we analyze the direction of recovery inconsistencies of the subjective specification for two cases. In the first **Case (i)**, the analyst's perceived current state is the coupled state $\overline{1}$ (while the underlying current state is the normal state 2). In the second **Case (ii)**, the analyst's perceived current state is the single state $\overline{3}$ (while the underlying current state is the good state 3).

Case (i) – Current coupled state: The diagram in Figure B.9 illustrates the consolidation scheme between the underlying $\mathcal{S}$ and subjective $\overline{\mathcal{S}}$ specifications in this case, in which the analyst's perceived current state is the coupled state $\overline{1}$. Given this consolidation scheme and the law of one

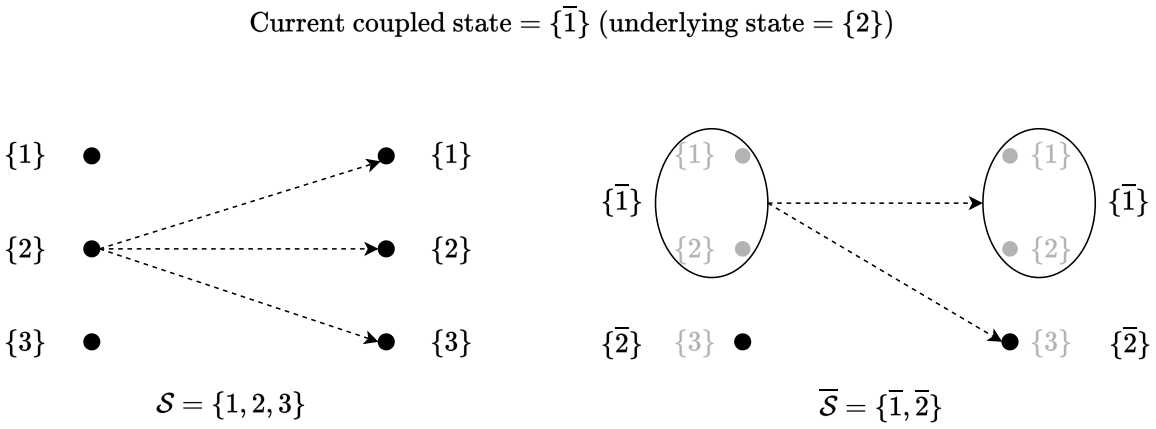

Figure B.9: Underlying (left panel) and consolidated (right panel) state space specifications associated with the consolidation scheme (B.2). The current underlying (true) state is 2, which is perceived as the coupled state $\overline{1}$ in the subjective specification by the analyst.

price, the one-period consolidated AD matrix perceived by the analysis is (a similar procedure is

[9] We do not use the underlying characteristics (transition probabilities or marginal utilities) in (B.1) in the recovery step because they are unobserved by the analyst.

presented in (6)),

$$\overline{\mathbf{A}} = \begin{bmatrix} 0.3602 & 0.1303 \\ 1.7082 & 0.6193 \end{bmatrix}.$$

The analyst then recovers the following time discount factor $\overline{\delta}$, marginal utilities $\{\overline{M}_{\overline{i}}\}$, and the one-period transition probability matrix $\overline{\mathbf{P}}$ in the subjective specification $\overline{\mathcal{S}}$

$$\text{(B.3)} \qquad \overline{\delta} = 0.979, \qquad \begin{bmatrix} \overline{M}_{\overline{1}} \\ \overline{M}_{\overline{2}} \end{bmatrix} = \begin{bmatrix} 4.8525 \\ 1.0219 \end{bmatrix}, \qquad \overline{\mathbf{P}} = \begin{bmatrix} 0.3680 & 0.6320 \\ 0.3675 & 0.6325 \end{bmatrix}.$$

Inconsistencies between the analyst's recovery results (B.3) and the underlying (B.1) and their magnitude and (undershooting or overshooting) direction can be seen by comparing their corresponding values (using the consolidation scheme in Figure B.9)

$$\text{(B.4)} \qquad \overline{\delta} - \delta = -0.001, \qquad \text{and} \qquad \begin{cases} \underbrace{\overline{p}_{t,t+1}(\overline{1},\overline{1})}_{0.3680} < \underbrace{p_{t,t+1}(2,1)}_{0.0385} + \underbrace{p_{t,t+1}(2,2)}_{0.5840}, \\ \underbrace{\overline{p}_{t,t+1}(\overline{1},\overline{1})}_{0.3680} < \underbrace{p_{t,t+1}(1,1)}_{0.0425} + \underbrace{p_{t,t+1}(1,2)}_{0.4847}. \end{cases}$$

Several observations on the comparative results (B.4) of the current numerical setting are in order. First, the inconsistency in the recovered time discount factor exists but is small and practically negligible. Second and in contrast, the inconsistency in the recovered transition probabilities is significant. Since the analyst perceives a current state $\overline{1}$, the analyst's recovered probability $\overline{p}_{t,t+1}(\overline{1},\overline{1})$ to remain in this coupled state next period significantly undershoots the corresponding underlying transition probability, whether we use as benchmark the transition probability (i) $p_{t,t+1}(2,1) + p_{t,t+1}(2,2)$ associated with the current underlying state 2, or (ii) $p_{t,t+1}(1,1)+p_{t,t+1}(1,2)$ associated with the current state 1 that is not the current underlying (true) state but might be in the analyst's perspective.[10]

To examine the relationship between this undershooting of the recovered the transition probability and the severity of the disaster state, we vary numerically the ratio of underlying marginal

[10] Since the current underlying (true) state is 2 while the analyst perceives a current coupled state $\overline{1} = \{1,2\}$ (Figure B.9), the analyst's perception is influenced by both the current (2) and non-current (1) underlying states. For robustness, our comparative analysis (B.4) considers both states 1 and 2 as the benchmark underlying state.

utilities in disaster and normal states $\frac{M_1}{M_2}$. Figure B.10 plots the difference $\overline{p}_{t,t+1}(\overline{1},\overline{1})-[p_{t,t+1}(2,1)+p_{t,t+1}(2,2)]$ (Left Panel (a)) and the difference $\overline{p}_{t,t+1}(\overline{1},\overline{1})-[p_{t,t+1}(1,1)+p_{t,t+1}(1,2)]$ (Right Panel (b)) between the one-period recovered and underlying transition probabilities against the ratio $\frac{M_1}{M_2}$. These

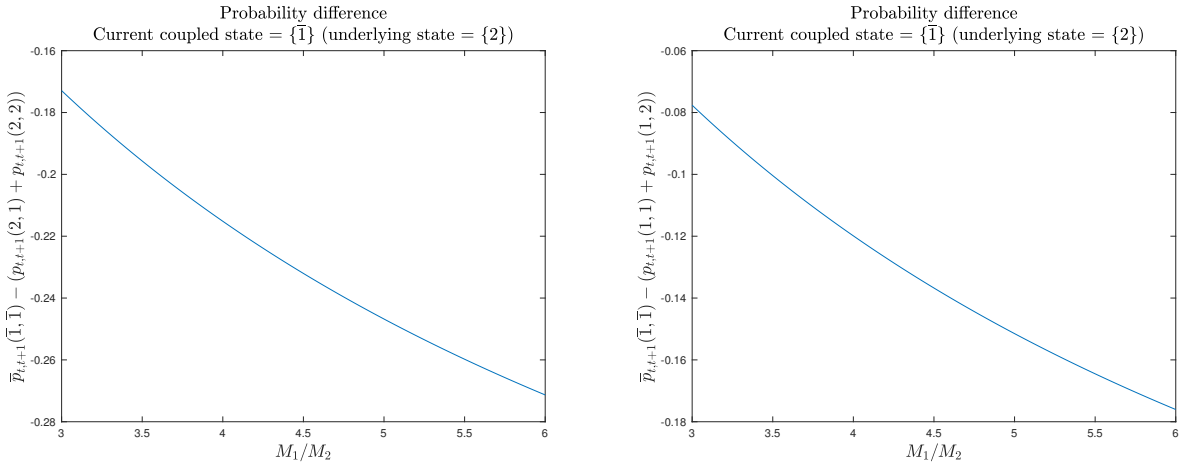

(a) (b)

Figure B.10: Probability differences. Panel (a): $\overline{p}_{t,t+1}(\overline{1},\overline{1}) - [p_{t,t+1}(2,1) + p_{t,t+1}(2,2)] < 0$. Panel (b): $\overline{p}_{t,t+1}(\overline{1},\overline{1}) - [p_{t,t+1}(1,1) + p_{t,t+1}(1,2)] < 0$

Notes: Panel (a) shows the difference between the recovered one-period transition probability $\overline{p}_{t,t+1}(\overline{1},\overline{1})$ in the subjective specification and the corresponding combined transition probabilities $[p_{t,t+1}(2,1)+p_{t,t+1}(2,2)]$ in the underlying (true) model versus the severity $\frac{M_1}{M_2}$ of the underlying adverse (disaster) state 1. Panel (b) shows the difference between $\overline{p}_{t,t+1}(\overline{1},\overline{1})$ and $[p_{t,t+1}(1,1)+p_{t,t+1}(1,2)]$ versus $\frac{M_1}{M_2}$. The current underlying (true) state is 2, which is perceived as the coupled state $\overline{1}$ in the subjective specification by the analyst as depicted in Figure B.9. A negative value of the difference: $\overline{p}_{t,t+1}(\overline{1},\overline{1})-[p_{t,t+1}(2,1)+p_{t,t+1}(2,2)] < 0$ (Panel (a)), or $\overline{p}_{t,t+1}(\overline{1},\overline{1})-[p_{t,t+1}(1,1)+p_{t,t+1}(1,2)] < 0$ (Panel (b)), indicates an undershooting of the transition probability recovered by the analyst.

plots show a robust undershooting of the recovered probability $\overline{p}_{t,t+1}(\overline{1},\overline{1})$ in the subjective specification for various values of the disaster state's severity, substantiating both undershooting relationships in (B.4) for a robust range of parameters. Next, Figure B.11 plots the difference $\overline{rx}^s_t(\overline{1}) - rx^s_t(2)$ between the recovered conditional stock market risk premium and the underlying counterpart. This difference in the conditional risk premia is computed from the underlying and recovery results and hence also captures the recovery inconsistencies and their direction.[11] The robust overshooting of the stock market risk premium exhibited in Figure B.11 reflects the fact that the current state $\overline{1}$ perceived by the analyst is an adverse state (while the true curren-

[11] The recovered conditional stock market risk premium $\overline{rx}^s_t(\overline{1})$ is computed using the recovered marginal utilities and probabilities (B.3) in the Euler pricing equation for the two-state (consolidated) CCAPM model $\{\overline{1},\overline{2}\}$ conditional on the consolidated current coupled state $\overline{1}$. The underlying conditional stock market risk premium $rx^s_t(2)$ is computed using the marginal utilities and probabilities (B.1) for the underlying three-state (calibrated) CCAPM model $\{1,2,3\}$ conditional on the underlying (true) current state 2.

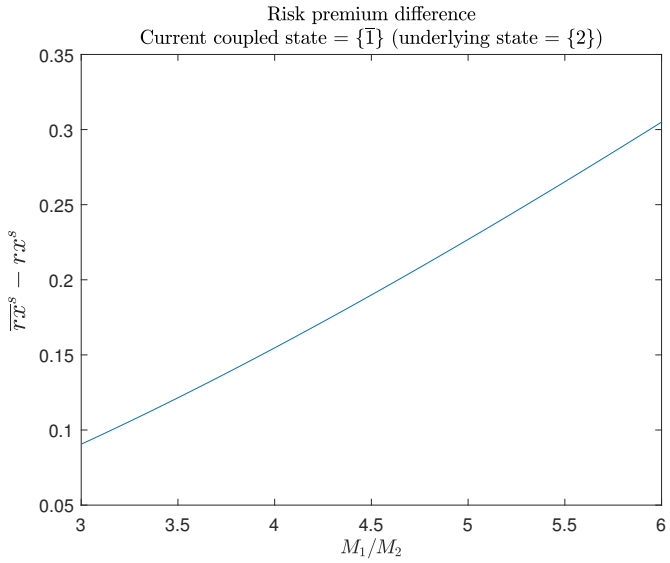

Figure B.11: This figure plots the difference between the conditional stock market risk premium $\overline{rx}_t^s(\bar{1})$ recovered using the subjective specification and its counterpart $rx_t^s(2)$ in the underlying (true) model versus the severity $\frac{M_1}{M_2}$ of the underlying disaster state 1. The current underlying (true) state is 2, which is perceived as the coupled state $\bar{1}$ in the subjective specification by the analyst as depicted in Figure B.9. A positive value of the difference, $\overline{rx}_t^s(\bar{1}) - rx_t^s(2) > 0$, indicates an overshooting of the conditional stock market risk premium recovered by the analyst.

t state 2 is normal state in the underlying model). This results in a elevated recovered current marginal utility $\overline{M}_{\bar{1}}$ (in relation to $\overline{M}_{\bar{2}}$ (B.3)) compared to the true current moderate marginal utility M_2 (in relation to M_1 and M_3). This suppresses the current stock price obtained by the analyst, compared to the (true) current stock price in the underlying model. The subjective undervaluation of the stock market then translates into an overshooting of the conditional risk premium of the stock market.

In summary of the current **Case (i)**, when the current (true) underlying state 2 belongs to a coupled state $\{\bar{1}\}$ in the subjective specification but the analyst's perceived current state is $\bar{1}$, such a scenario confounds the analyst's subjective current state with another underlying (but not actually current) adverse state 1. This confounding acts to elevate the (perceived) current marginal utility, and hence, lower the (perceived) current price of the insurances (AD assets) against the (perceived) disaster in state $\bar{1}$ happening at future periods τ and $\tau+1$. But as the underlying disaster is rare in the calibration of the U.S. economy, the likelihood of a disaster declines with horizon τ. As a result, the analyst currently perceives a cheaper insurance against the

disaster happening at $\tau+1$ than at τ, and therefore, necessarily infers an undervalued transition probability between the disaster state $\overline{1}$ at τ and at $\tau+1$. These economic features of the setting together explain the undershooting of the one-period probability $\overline{p}_{t,t+1}(\overline{1},\overline{1})$ (B.4) recovered by the analyst.

Case (ii) – Current single state: The diagram in Figure B.12 illustrates the consolidation scheme between the underlying $\mathcal{S}$ and subjective $\overline{\mathcal{S}}$ specifications. In this **Case (ii)**, the analyst's perceived current state is the single state $\overline{2}$, coinciding with the current underlying state 3. Given

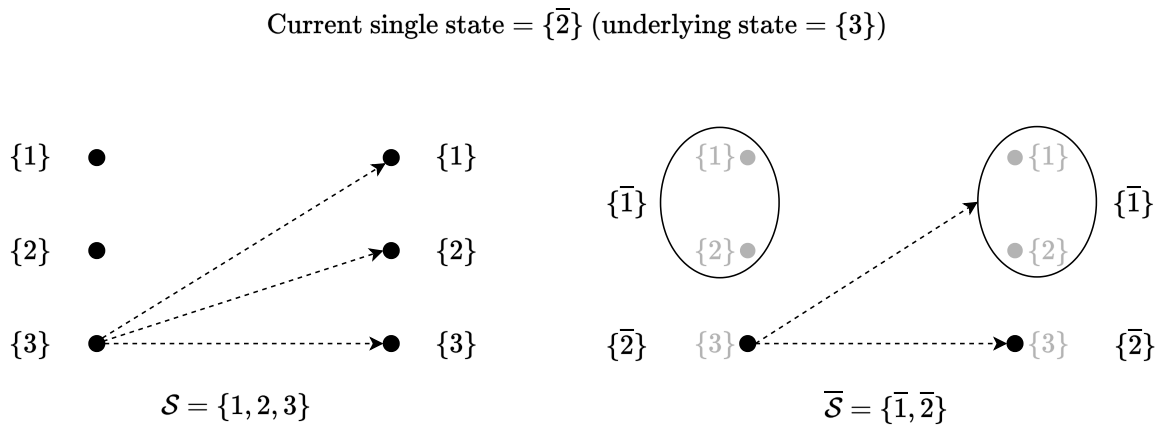

Figure B.12: Underlying (left panel) and consolidated (right panel) state space specifications associated with the consolidation scheme (B.2). The current underlying (true) state is 3, which is perceived as the single state $\overline{2}$ in the subjective specification by the analyst.

this consolidation scheme and the law of one price, the one-period consolidated AD matrix perceived by the analysis is

$$\overline{\mathbf{A}} = \begin{bmatrix} 0.2720 & 0.1034 \\ 1.9599 & 0.6960 \end{bmatrix}. \tag{B.5}$$

The analyst then recovers the following time discount factor $\overline{\delta}$, marginal utilities $\{\overline{M}_{\overline{i}}\}$, and the one-period transition probability matrix $\overline{\mathbf{P}}$ in the subjective specification $\overline{\mathcal{S}}$

$$\overline{\delta} = 0.9816, \qquad \begin{bmatrix} \overline{M}_{\overline{1}} \\ \overline{M}_{\overline{2}} \end{bmatrix} = \begin{bmatrix} 6.9342 \\ 1.0106 \end{bmatrix}, \qquad \overline{\mathbf{P}} = \begin{bmatrix} 0.2771 & 0.7229 \\ 0.2910 & 0.7090 \end{bmatrix}. \tag{B.6}$$

Inconsistencies between the analyst's recovery results (B.6) and the underlying (B.1) and their magnitude and (undershooting or overshooting) direction can be seen by comparing their corresponding values (using the consolidation scheme in Figure B.12)

$$\overline{\delta} - \delta = 0.0016, \quad \text{and} \quad \underbrace{\overline{p}_{t,t+1}(\overline{2},\overline{2})}_{0.7090} > \underbrace{p_{t,t+1}(3,3)}_{0.4009} \tag{B.7}$$

These results for the current single state show the inconsistency in both the recovered time discount factor and transition probabilities. While the time discount factor's inconsistency is small and practically negligible, the inconsistency in the recovered transition probabilities is significant, similar to the earlier findings (B.4) for the current coupled state. However, in contrast to (B.4), the analyst's recovered probability $\overline{p}_{t,t+1}(\overline{2},\overline{2})$ to remain in the current state $\{\overline{2}\}$ next period significantly overshoots the (true) underlying transition probability $p_{t,t+1}(3,3)$ in (B.7). This change in the recovery inconsistency direction indicates the relevance of the current state (being single or coupled) in the recovery process.

To examine the relationship between this overshooting of the recovered the transition probability and the severity of the disaster state, we vary numerically the ratio of underlying marginal utilities in disaster and normal states $\frac{M_1}{M_2}$. Figure B.13 plots the difference $\overline{p}_{t,t+1}(\overline{2},\overline{2}) - p_{t,t+1}(3,3)$ between the one-period recovered and underlying transition probabilities against the ratio $\frac{M_1}{M_2}$. This plot shows a robust overshooting of the recovered probability $\overline{p}_{t,t+1}(\overline{2},\overline{2})$ in the subjective specification for various values of the disaster state's severity, substantiating the overshooting relationship (B.7) for a robust range of parameters.

Next, Figure B.14 plots the difference $\overline{rx}^s_t(\overline{2}) - rx^s_t(3)$ between the recovered conditional stock market risk premium and the underlying counterpart. This difference in the conditional risk premia is computed from the underlying and recovery results and hence also captures the recovery inconsistencies and their direction.[12] Similar to Figure B.11, the difference in conditional stock market risk premia across the recovered and underlying models are results of the recovery in-

[12] Per Figure B.12, the recovered conditional stock market risk premium $\overline{rx}^s_t(\overline{2})$ is computed using the recovered marginal utilities and probabilities (B.6) for the two-state (consolidated) CCAPM model $\{\overline{1},\overline{2}\}$ conditional on the consolidated current coupled state $\overline{2}$. The underlying conditional stock market risk premium $rx^s_t(3)$ is computed using the marginal utilities and probabilities (B.1) in the Euler equation for the underlying three-state (calibrated) CCAPM model $\{1,2,3\}$ conditional on the underlying (true) current state 3.

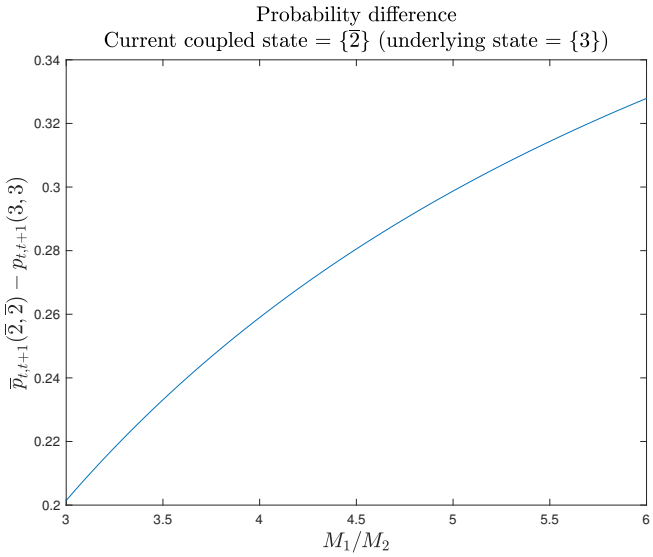

Figure B.13: This figure plots the difference between the recovered one-period transition probability $\overline{p}_{t,t+1}(\overline{2},\overline{2})$ in the subjective specification and the corresponding transition probability $p_{t,t+1}(3,3)$ in the underlying (true) model versus the severity $\frac{M_1}{M_2}$ of the underlying disaster state 1. The current underlying (true) state is 3, which is perceived as the single state $\overline{2}$ in the subjective specification by the analyst as depicted in Figure B.12. A positive value of the difference, $\overline{p}_{t,t+1}(\overline{2},\overline{2}) - p_{t,t+1}(3,3) > 0$, indicates an overshooting of the transition probability recovered by the analyst.

consistencies (the relative magnitude of current marginal utilities and transition probabilities starting from current states in consolidated and underlying models, in particular).

In summary of the current **Case (ii)**, when the current state is a single good state 3, the analyst's subjective specification of the current state $\overline{2}$ is correct, i.e., $\overline{2} \equiv 3$. This assures that the analyst correctly observes the current price of the insurance against the event of remaining in the good state at $\tau+1$, or $\overline{A}_{\tau+1;\overline{2}\,\overline{2}} = A_{\tau+1;33}$. The U.S. economy calibrated model's adverse (rare disaster) state $1 \in \overline{1}$ features a declining disaster's insurance price with the horizon, $\overline{A}_{\tau+1;\overline{2}\,\overline{1}} < \overline{A}_{\tau;\overline{2}\,\overline{1}}$. Therefore, to counter this outsized contribution of the τ-period insurance price $\overline{A}_{\tau;\overline{2}\,\overline{1}}$ to the correctly observed $\tau+1$-period contingent price $\overline{A}_{\tau+1;\overline{2}\,\overline{2}}$, the analyst necessarily infers an undervalued one-period (from τ to $\tau+1$) asset price $\overline{A}_{\overline{1}\,\overline{2}}$, or equivalently, an overvalued complementary price $\overline{A}_{\overline{2}\,\overline{2}}$.[13] The latter asset overvaluation amounts to an overshooting of the corresponding

[13] First, note that the contribution of the τ-period AD asset price $\overline{A}_{\tau;\overline{2}\,\overline{1}}$ to the $\tau+1$-period AD asset price $\overline{A}_{\tau+1;\overline{2}\,\overline{2}}$ is via the product $\overline{A}_{\tau;\overline{2}\,\overline{1}}\overline{A}_{\overline{1}\,\overline{2}}$. When $\overline{A}_{\tau+1;\overline{2}\,\overline{2}}$ is correctly observed, a (perceived) overvaluation of $\overline{A}_{\tau;\overline{2}\,\overline{1}}$ by an analyst is necessarily accompanied (and countered) by a (perceived) undervaluation of $\overline{A}_{\overline{1}\,\overline{2}}$ by the same analyst. Second, the perceived AD prices $\overline{A}_{\overline{1}\,\overline{2}}$ and $\overline{A}_{\overline{2}\,\overline{2}}$ are mutually complementary.

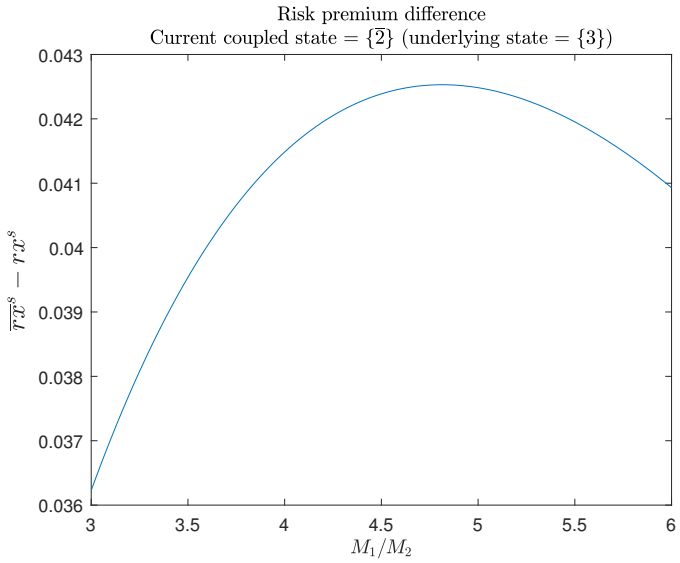

Figure B.14: This figure plots the difference between the conditional stock market risk premium $\overline{rx}_t^s(\overline{2})$ recovered using the subjective specification and its counterpart $rx_t^s(3)$ in the underlying (true) model versus the severity $\frac{M_1}{M_2}$ of the underlying disaster state $\{1\}$. The current underlying (true) state is $\{3\}$, which is perceived as the single state $\{\overline{2}\}$ in the subjective specification by the analyst as depicted in Figure B.12. A positive value of the difference, $\overline{rx}_t^s(\overline{2}) - rx_t^s(3) > 0$, indicates an overshooting of the conditional stock market risk premium recovered by the analyst.

probability $\overline{p}_{t,t+1}(\overline{2},\overline{2})$ recovered by the analyst. These features together therefore explain the overshooting of the one-period transition probability (B.7).

Moment equations for calibration parameter estimation: We employ the 2-stage GMM procedure to estimate the parameters for the calibration model, which is a stationary CCAPM model with 3 states. We match the following moments to the data.

(B.8) Average consumption growth:
$$\mu_c = \mathbb{E}_t\left[\frac{c_{t+1}}{c_t} - 1\right]$$

(B.9) Consumption growth volatility:
$$\sigma_c^2 = \mathbb{E}_t\left[\left(\frac{c_{t+1}}{c_t} - 1 - \mu_c\right)^2\right]$$

(B.10) Risk premium of stock:
$$rx_t^s = -(1 + r_{t+1}^f) Cov_t\left(\Lambda_{t+1}, r_{t+1}^s\right)$$

(B.11) Stock return volatility:
$$\sigma_s^2 = \mathbb{E}_t\left[\left(\frac{c_{t+1}}{\mathbb{E}_t\left[\Lambda_{t+1} c_{t+1}\right]} - 1 - (rx_t^s + r_{t+1}^f)\right)^2\right]$$

(B.12) Risk-free rate:
$$\frac{1}{1 + r_{t+1}^f} = \mathbb{E}_t\left[\Lambda_{t+1}\right].$$

Note that in our estimation, all quantities on the RHS of the above equations are taken from the 3-state model while all quantities on the LHS are from the actual data.

Define g to be a vector containing the 5 moment conditions

$$g = \begin{bmatrix} \mathbb{E}_t\left[\frac{c_{t+1}}{c_t} - 1\right] - \mu_c \\ \mathbb{E}_t\left[\left(\frac{c_{t+1}}{c_t} - 1 - \mu_c\right)^2\right] - \sigma_c^2 \\ -(1 + r^f_{t+1})Cov_t\left(\Lambda_{t+1}, r^s_{t+1}\right) - rx^s_t \\ \mathbb{E}_t\left[\left(\frac{c_{t+1}}{\mathbb{E}_t[\lambda_{t+1}c_{t+1}]} - 1 - (rx^s_t + r^f_{t+1})\right)^2\right] - \sigma_s^2 \\ \mathbb{E}_t\left[\Lambda_{t+1}\right] - \frac{1}{1+r^f_{t+1}} \end{bmatrix},$$

where the expectation is over the stationary probabilities p_{ss}. Given the weight matrix W, we choose transition probabilities to minimize $J = g'Wg$ subject to constraints $0 \leq p_{ij} \leq 1$ and $p_{13} = 1 - p_{11} - p_{12}$, $p_{23} = 1 - p_{21} - p_{22}$, $p_{33} = 1 - p_{31} - p_{32}$. The standard two-stage GMM estimation results are presented in Table B.7.

C Technical Derivations and Analysis

We present a derivation of the necessary and sufficient condition for the recovery consistency in Appendix C.1 and the persistence of the recovery consistency issue in Appendix C.2 using Vandermonde matrix's analytical properties.

C.1 Recovery Consistency's Necessary and Sufficient Condition: A Derivation

This appendix presents a proof of the necessary and sufficient condition for the recovery consistency (Proposition 1). The proof addresses separately whether the current state is a single or a coupled state.

Case 1 - Single Current State: We consider an original specification of $\mathcal{S} = \{1, \cdots, S\}$ and a consolidated specification $\overline{\mathcal{S}} = \{\overline{1}, \cdots, \overline{j}, \cdots, \overline{S}\}$, which are adopted by two analysts. To simplify the exposition, we consider the following mapping (or consolidation scheme) between the two specifications: $\overline{1} = 1, \overline{2} = 2, \cdots, \overline{K} = K$, and $\overline{S} = \{K+1, \cdots, S\}$, as steps of the derivation for a general mapping is similar. Suppose that the current state is the single state $\overline{1}$ for the second (consolidated) analyst, and 1 for the first (original) analyst.

In the first direction of the proof (i.e., proving the sufficient condition), we assume consistent recoveries under both specifications. As a result, the following no-arbitrage conditions on observed price data must be satisfied for the two consistent specifications:

$$A_{\tau+1;1i} = \sum_{j=1}^{S} A_{\tau;1j} A_{ji}, \quad \forall i \in \mathcal{S} \text{ and } \forall \tau \in \{1, 2, 3, \cdots\} \tag{C.1}$$

$$\overline{A}_{\tau+1;\overline{1}\,\overline{i}} = \sum_{\overline{j}=\overline{1}}^{\overline{S}} \overline{A}_{\tau;\overline{1}\,\overline{j}} \overline{A}_{\overline{j}\,\overline{i}}, \quad \forall \overline{i} \in \overline{\mathcal{S}} \text{ and } \forall \tau \in \{1, 2, 3, \cdots\} \tag{C.2}$$

$$\overline{A}_{\tau;\overline{1}\,\overline{i}} = \sum_{j \in \overline{i}} A_{\tau;1j}, \quad \forall \overline{i} \in \overline{\mathcal{S}} \text{ and } \forall \tau \in \{1, 2, 3, \cdots\}. \tag{C.3}$$

The above equation system holds for any horizon τ in the future. However, AD price matrices $\mathbf{A}$ and $\overline{\mathbf{A}}$ contain a fixed number of components to be solved for, resulting in an over-identified

equation system. In particular, we substitute (C.3) into (C.2) and obtain

$$\sum_{j\in\bar{i}} A_{\tau+1;1j} = \sum_{\bar{j}=\bar{1}}^{\overline{S}} \left(\sum_{k\in\bar{j}} A_{\tau;1k} \right) \overline{A}_{\bar{j}\,\bar{i}}, \quad \forall\, \bar{i} \in \overline{\mathcal{S}} \text{ and } \forall \tau \in \{1,2,3,\cdots\}. \tag{C.4}$$

The equation system, (C.1) and (C.4), has an infinite number of equations but only $S^2+(K+1)^2$ unknowns. Hence, in order for the system to have a solution, the components in $\overline{\mathbf{A}}$ must satisfy

$$\overline{A}_{\bar{i}\,\bar{j}} = \sum_{j\in\bar{j}} A_{ij}, \quad \forall \bar{i} = i \in \{1,\cdots,K\} \text{ and } \bar{j} \in \overline{\mathcal{S}} \tag{C.5}$$

$$\overline{A}_{\overline{S}\,\bar{j}} = \sum_{j\in\bar{j}} A_{ij}, \quad \forall i \in \overline{S} \text{ and } \bar{j} \in \overline{\mathcal{S}}, \tag{C.6}$$

so that by summing up the equations (C.1) in states $i \in \overline{S}$ we obtain (C.4).

Given that the AD price matrix $\mathbf{A}$ of the original specification $\mathcal{S}$ satisfies (C.5) and (C.6), the right eigenvector, $\mathbf{x}^{(1,R)} = \left[x_1^{(1,R)},\cdots,x_S^{(1,R)}\right]'$, associated with the largest and positive eigenvalue δ will satisfy the following form:

(C.7)

$$\begin{bmatrix} A_{11} & \cdots & A_{1K} & A_{1,K+1} & \cdots & A_{1S} \\ \vdots & \ddots & \vdots & \vdots & \ddots & \vdots \\ A_{K1} & \cdots & A_{KK} & A_{K,K+1} & \cdots & A_{KS} \\ A_{K+1,1} & \cdots & A_{K+1,K} & A_{K+1,K+1} & \cdots & A_{K+1,S} \\ \vdots & \ddots & \vdots & \vdots & \ddots & \vdots \\ A_{S1} & \cdots & A_{SK} & A_{S,K+1} & \cdots & A_{SS} \end{bmatrix} \begin{bmatrix} x_1^{(1,R)} \\ \vdots \\ x_K^{(1,R)} \\ x_{K+1}^{(1,R)} = \overline{x}_{\overline{S}}^{(1,R)} \\ \vdots \\ x_S^{(1,R)} = \overline{x}_{\overline{S}}^{(1,R)} \end{bmatrix} = \delta \begin{bmatrix} x_1^{(1,R)} \\ \vdots \\ x_K^{(1,R)} \\ x_{K+1}^{(1,R)} = \overline{x}_{\overline{S}}^{(1,R)} \\ \vdots \\ x_S^{(1,R)} = \overline{x}_{\overline{S}}^{(1,R)} \end{bmatrix},$$

which implies the marginal utilities satisfy $M_i = M_k$, for all i and k belonging to the same coupled state. From the formula of recovered probabilities in (2), it follows that $p_{i\bar{h}} = p_{k\bar{h}}$, $\forall i,k \in \bar{j}$ and $\bar{j},\bar{h} \in \overline{\mathcal{S}}$.

Next, we prove the other direction (i.e., proving the necessary condition). We assume that the inputs of the original specification satisfy $M_i = M_k, p_{i\bar{h}} = p_{k\bar{h}}$, $\forall i,k \in \bar{j}$, and $\bar{j},\bar{h} \in \overline{\mathcal{S}}$. According

to (2), the original AD price matrix $\mathbf{A}$ satisfy

$$\sum_{j\in\overline{j}} A_{ij} = \sum_{j\in\overline{j}} A_{kj}, \quad \forall i,k \in \overline{S} \text{ and } \overline{j} \in \overline{\mathcal{S}}. \tag{C.8}$$

Since our primary analysis concerns consistency, we take $\mathcal{S}$ as the underlying specification in the current thought experiment. Consequently, we have $\mathbf{A}_{\tau+1} = \mathbf{A}_\tau \mathbf{A}$ holds for all horizon τ. No-arbitrage restriction of trade assets gives (C.3). These conditions together with (C.8) imply that $\overline{\mathbf{A}}_{\tau+1} = \overline{\mathbf{A}}_\tau \overline{\mathbf{A}}$ also holds for all τ and thus we obtain (C.5) and (C.6). Consequently, employing (2), we have

$$\overline{\delta} = \delta; \qquad \frac{\overline{M}_{\overline{j}}}{M_j} = \frac{\overline{M}_{\overline{1}}}{M_1}, \ \forall\, \overline{j} = j \in \{1,\cdots,K\};$$

$$\overline{p}_{t,t+1}(\overline{1},\overline{j}) = p_{t,t+1}(1,j), \ \forall\, \overline{j} = j \in \{1,\cdots,K\}, \ \forall t; \tag{C.9}$$

$$\overline{p}_{t,t+1}(\overline{1},\overline{S}) = \sum_{j=K+1}^{S} p_{t,t+1}(1,j), \ \forall t; \qquad \frac{\overline{M}_{\overline{S}}}{\overline{M}_{\overline{1}}} = \sum_{j=K+1}^{S} \frac{p_{t,t+1}(1,j)}{\sum_{i=K+1}^{S} p_{t,t+1}(1,i)} \frac{M_j}{M_1}, \ \forall t.$$

That is, all consistency conditions are satisfied, establishing the recovery consistency for the case of single current state.

Case 2 - Coupled current state: We consider an original specification of $\mathcal{S} = \{1,\cdots,S\}$ and a consolidated specification $\overline{\mathcal{S}} = \{\overline{1},\overline{K+1},\cdots,\overline{S-1},\overline{S}\}$, which are adopted by two analysts. The mapping (or consolidation scheme) between the two specifications is as follows: $\overline{1} = \{1,\cdots,K\}$, $\overline{K+1} = K+1$, $\overline{K+2} = K+2$, $\cdots\{\overline{S-1}\} = S-1$, and $\overline{S} = S$. Suppose that the current state is the coupled state $\overline{1}$ for the second (consolidated) analyst and 1 for the first (original) analyst.

In the first direction of the proof (i.e., proving the sufficient condition), we assume consistent recoveries under both specifications. As a result, the same no-arbitrage conditions (C.1)–(C.3) for Case 1 on observed price data must be satisfied for the two consistent specifications. We again obtain the equation system (C.1) and (C.4). In order for the system to have a solution, the

components in $\overline{\mathbf{A}}$ must satisfy

$$\overline{A}_{\overline{1}\,\overline{j}} = \sum_{j \in \overline{j}} A_{ij}, \quad \forall i \in \overline{1} \text{ and } \overline{j} \in \overline{\mathcal{S}}, \tag{C.10}$$

$$\overline{A}_{\overline{i}\,\overline{j}} = \sum_{j \in \overline{j}} A_{ij}, \quad \forall\, \overline{i} = i \in \{K+1, \cdots, S\} \text{ and } \overline{j} \in \overline{\mathcal{S}}, \tag{C.11}$$

so that by summing up the equations (C.1) in states $i \in \overline{1}$ we obtain (C.4).

Given that the AD price matrix $\mathbf{A}$ of the original specification $\mathcal{S}$ satisfies (C.10) and (C.11), the right eigenvector, $\mathbf{x}^{(1,R)} = [x_1^{(1,R)}, \cdots, x_S^{(1,R)}]'$, associated with the largest and positive eigenvalue δ will satisfy the following form:

(C.12)

$$\begin{bmatrix} A_{11} & \dots & A_{1K} & A_{1,K+1} & \dots & A_{1S} \\ \vdots & \ddots & \vdots & \vdots & \ddots & \vdots \\ A_{K1} & \dots & A_{KK} & A_{K,K+1} & \dots & A_{KS} \\ A_{K+1,1} & \dots & A_{K+1,K} & A_{K+1,K+1} & \dots & A_{K+1,S} \\ \vdots & \ddots & \vdots & \vdots & \ddots & \vdots \\ A_{S1} & \dots & A_{SK} & A_{S,K+1} & \dots & A_{SS} \end{bmatrix} \begin{bmatrix} x_1^{(1,R)} = \overline{x}_{\overline{1}}^{(1,R)} \\ \vdots \\ x_K^{(1,R)} = \overline{x}_{\overline{1}}^{(1,R)} \\ x_{K+1}^{(1,R)} \\ \vdots \\ x_S^{(1,R)} \end{bmatrix} = \delta \begin{bmatrix} x_1^{(1,R)} = \overline{x}_{\overline{1}}^{(1,R)} \\ \vdots \\ x_K^{(1,R)} = \overline{x}_{\overline{1}}^{(1,R)} \\ x_{K+1}^{(1,R)} \\ \vdots \\ x_S^{(1,R)} \end{bmatrix}$$

which implies the marginal utilities satisfy $M_i = M_k$, for all i and k belonging to the same coupled state. From the formula of recovered probabilities in (2), it follows that $p_{i\overline{h}} = p_{k\overline{h}}$, $\forall i, k \in \overline{j}$ and $\overline{j}, \overline{h} \in \overline{\mathcal{S}}$.

Next, we prove the other direction (i.e., proving the necessary condition). We assume that the inputs of the original specification satisfy $M_i = M_k, p_{i\overline{h}} = p_{k\overline{h}}$, $\forall i, k \in \overline{j}$, and $\overline{j}, \overline{h} \in \overline{\mathcal{S}}$. According to (2), the original AD price matrix $\mathbf{A}$ satisfy

$$\sum_{j \in \overline{j}} A_{ij} = \sum_{j \in \overline{j}} A_{kj}, \quad \forall i, k \in \overline{1} \text{ and } \overline{j} \in \overline{\mathcal{S}}. \tag{C.13}$$

Since our primary analysis concerns consistency, we take $\mathcal{S}$ as the underlying specification in the thought experiment. Consequently, we have $\mathbf{A}_{\tau+1} = \mathbf{A}_\tau \mathbf{A}$ holds for all horizon τ. No-

arbitrage restriction of traded assets gives (C.3). These conditions together with (C.13) imply that $\overline{\mathbf{A}}_{\tau+1} = \overline{\mathbf{A}}_{\tau}\overline{\mathbf{A}}$ also holds for all τ and thus we obtain (C.10) and (C.11). Consequently, employing (2), we have

$$
\begin{aligned}
&\overline{\delta} = \delta; \qquad \overline{p}_{t,t+1}(\overline{1},\overline{1}) = \sum_{j=1}^{K} p_{t,t+1}(1,j),\ \forall t; \\
&\overline{p}_{t,t+1}(\overline{1},\overline{j}) = p_{t,t+1}(1,j)\frac{1-\sum_{i=1}^{K} p_{t,t+1}(1,i)}{1-\sum_{i=1}^{K}\frac{M_i}{M_1}p_{t,t+1}(1,i)},\ \forall\, \overline{j} = j \in \{K+1,\cdots,S\},\ \forall t; \\
&\frac{\overline{M}_{\overline{j}}}{\overline{M}_{\overline{1}}} = \frac{M_j}{M_1}\frac{1-\sum_{i=1}^{K} p_{t,t+1}(1,i)}{1-\sum_{i=1}^{K}\frac{M_i}{M_1}p_{t,t+1}(1,i)},\ \forall\, \overline{j} = j \in \{K+1,\cdots,S\},\ \forall t.
\end{aligned}
\tag{C.14}
$$

That is, all consistency conditions are satisfied, implying the recovery consistency for the case of coupled current state. Together with the derivation above for the case of single current state, this establishes Proposition 1.

C.2 Recovery Convergence: A Derivation

This appendix presents a derivation of the non-convergence (persistence) property of the recovery consistency issue (Proposition 2). The derivation first obtains explicit expressions for the inverses of AD price matrices, before relating their the spectral gaps (eigenvalue distributions) to the persistence property of recovery inconsistencies.

Inverses of AD Price Matrices: We first relate AD price matrices to Vandermonde matrix, whose inverse is known analytically, before applying this technique to derive the recovered results, their consistency and convergence properties.[14] Recall from Section 3 that the recovery inconsistencies originate from the inconsistency of the perturbative component $\overline{\mathbf{B}}$ of the one-period AD price matrix. As a result, a quantitative analysis of the recovery inconsistencies relies on an explicit inversion of the price matrix $\overline{\mathbf{A}}_{0\tau}^{-1}$. In fact, $\overline{\mathbf{A}}_{0\tau}^{-1}$ and $\overline{\mathbf{B}}$ feature predominantly in the divergence of the recovered time (18) and risk (22) preferences.

To obtain $\overline{\mathbf{A}}_{0\tau}^{-1}$ explicitly, we first express every row $\mathbf{A}_{0\tau i,:}$ of $\mathbf{A}_{0\tau}$ (resp., every row $\overline{\mathbf{A}}_{0\tau\overline{i},:}$ of $\overline{\mathbf{A}}_{0\tau}$) as a linear combination of the unperturbed left eigenvectors $\{\mathbf{x}_0^{(k,L)}\}$, $k \in \{1,\ldots,S\}$ (resp., $\{\overline{\mathbf{x}}_0^{(\overline{k},L)}\}$, $\overline{k} \in \{1,\ldots,\overline{S}\}$), because these eigenvectors span the space of $1\times S$ (resp., $1\times\overline{S}$) row

[14] For completeness, a digression on Vandermonde matrix system is presented in (C.29) and (C.30) below.

vectors,

$$\text{(C.15)}\qquad \begin{cases} \mathbf{A}_{0\tau i,:} = \sum_{k=1}^{S} \gamma_{ik}\, \mathbf{x}^{(k,L)}, \\ \text{or in matrix form } \mathbf{A}_{0\tau} = \mathbf{\Gamma}\, \mathbf{X}^{L}, \end{cases} \qquad \begin{cases} \overline{\mathbf{A}}_{0\tau \bar{i},:} = \sum_{\bar{k}=\bar{1}}^{\overline{S}} \overline{\gamma}_{\bar{i}\bar{k}}\, \overline{\mathbf{x}}^{(\bar{k},L)}, \\ \text{or in matrix form } \overline{\mathbf{A}}_{0\tau} = \overline{\mathbf{\Gamma}}\, \overline{\mathbf{X}}^{L}, \end{cases}$$

where $\mathbf{\Gamma}$ and $\overline{\mathbf{\Gamma}}$ are matrices of respective coefficients $\{\gamma_{ik}\}$ and $\{\overline{\gamma}_{\bar{i}\bar{k}}\}$. Since right and left eigenvectors are orthonormal, $\mathbf{X}_0^L \mathbf{X}_0^R = \mathbb{1}_{S\times S}$ and $\overline{\mathbf{X}}_0^L \overline{\mathbf{X}}_0^R = \mathbb{1}_{\overline{S}\times\overline{S}}$, the coefficient matrices are $\mathbf{\Gamma} = \mathbf{A}_{0\tau}\mathbf{X}^R$ and $\overline{\mathbf{\Gamma}} = \overline{\mathbf{A}}_{0\tau}\overline{\mathbf{X}}^R$. Using the recursive construction (3) of the unperturbed τ-period AD matrices $\mathbf{A}_{0\tau} = \mathbf{A}_{0\tau-1}\mathbf{A}_0$ and $\overline{\mathbf{A}}_{0\tau} = \overline{\mathbf{A}}_{0\tau-1}\overline{\mathbf{A}}_0$, and the fact that columns of matrices $\mathbf{X}_0^R$ and $\overline{\mathbf{X}}_0^R$ are right eigenvalues of one-period AD price matrices $\mathbf{A}_0$ and $\overline{\mathbf{A}}_0$, we obtain explicit expressions for the coefficient matrices[15]

$$\mathbf{\Gamma} = \underbrace{\begin{bmatrix} \delta_0^{(1)} & \dots & \delta_0^{(S)} \\ \vdots & \ddots & \vdots \\ \left[\delta_0^{(1)}\right]^S & \dots & \left[\delta_0^{(S)}\right]^S \end{bmatrix}}_{\equiv \mathbf{D}_S} \underbrace{\begin{bmatrix} x_{01}^{(1,R)} & \dots & 0 \\ \vdots & \ddots & \vdots \\ 0 & \dots & x_{01}^{(S,R)} \end{bmatrix}}_{\equiv \mathbf{Diag}\left(X_{01}^{(R)}\right)} = \underbrace{\mathbf{D}_S}_{S\times S}\, \underbrace{\mathbf{Diag}\left(X_{01}^{(R)}\right)}_{S\times S},$$

(C.16)

$$\overline{\mathbf{\Gamma}} = \underbrace{\begin{bmatrix} \delta_0^{(1)} & \dots & \delta_0^{(\overline{S})} \\ \vdots & \ddots & \vdots \\ \left[\delta_0^{(1)}\right]^{\overline{S}} & \dots & \left[\delta_0^{(\overline{S})}\right]^{\overline{S}} \end{bmatrix}}_{\equiv \overline{\mathbf{D}}_{\overline{S}}} \underbrace{\begin{bmatrix} \overline{x}_{01}^{(1,R)} & \dots & 0 \\ \vdots & \ddots & \vdots \\ 0 & \dots & \overline{x}_{01}^{(\overline{S},R)} \end{bmatrix}}_{\equiv \mathbf{Diag}\left(\overline{X}_{01}^{(R)}\right)} = \underbrace{\overline{\mathbf{D}}_{\overline{S}}}_{\overline{S}\times\overline{S}}\, \underbrace{\mathbf{Diag}\left(\overline{X}_{01}^{(R)}\right)}_{\overline{S}\times\overline{S}},$$

where diagonal matrix $\mathbf{Diag}(X_{01}^{(R)})$ (resp., $\mathbf{Diag}(\overline{X}_{01}^{(R)})$) contains the first component of the unperturbed right eigenvectors $\mathbf{x}_0^{(k,R)}$, $k \in \{1,\dots,S\}$ (resp., $\overline{\mathbf{x}}_0^{(\bar{k},R)}$, $\bar{k} \in \{1,\dots,\overline{S}\}$). The k-th row of matrix $\mathbf{D}_S$ (resp., $\overline{\mathbf{D}}_{\overline{S}}$) as defined in the above expressions contains the k-th exponent of the eigenvalues $\{\delta_0^{(1)},\dots,\delta_0^{(S)}\}$ (resp., $\{\delta_0^{(1)},\dots,\delta_0^{(\overline{S})}\}$). Therefore, $\mathbf{D}_S$ and $\overline{\mathbf{D}}_{\overline{S}}$ are Vandermonde matrices (see the digression (C.29) and (C.30) below), whose inverses, $\mathbf{D}_S^{-1}$ and $\overline{\mathbf{D}}_{\overline{S}}^{-1}$, have known closed-form expressions. Specifically, the element $(1,i)$ of the inverse Vandermonde matrix

[15] Recall that the dominant unperturbed eigenspaces are consistent, hence $\delta_0^{(1)} = \bar{\delta}_0^{(1)} = \delta_0$ as noted below (17). To arrive at these expressions, recall the convention that the current state is 1. As a result, the first row of observable price matrix $\mathbf{A}_{0\tau}$ (3) contains the current one-period AD prices, $\mathbf{A}_{0\tau;1:} = \mathbf{A}_{01:}$, the second row $\mathbf{A}_{0\tau;2:} = \mathbf{A}_{01:}\mathbf{A}_0$, and so on to the S-th row $\mathbf{A}_{0\tau;S:} = \mathbf{A}_{01:}\mathbf{A}_0^{S-1}$. The product $\mathbf{A}_{0\tau}\mathbf{X}_0^R$ then is composed of various rows of the form $\mathbf{A}_{01:}\mathbf{A}_0^k\mathbf{X}_0^R$, $k \in \{0,\dots,S-1\}$, resulting in (C.16).

$\left[\overline{\mathbf{D}}_{\overline{S}}^{-1}\right]$ is (e.g., Man (2017))

$$\text{(C.17)} \qquad \left[\overline{\mathbf{D}}_{\overline{S}}^{-1}\right]_{1i} = \frac{\left(\delta_0^{(1)}\right)^{\overline{S}-i} + a_1\left(\delta_0^{(1)}\right)^{\overline{S}-i-1} + \ldots + a_{\overline{S}-i-1}\left(\delta_0^{(1)}\right) + a_{\overline{S}-i}}{\delta_0^{(1)}\prod_{j\neq 1}^{\overline{S}}(\delta_0^{(1)} - \delta_0^{(j)})}, \quad i \in \{1,\ldots,\overline{S}\},$$

(C.18)

$$a_0 = 1, \quad a_1 = -\sum_j^{\overline{S}} \delta_0^{(j)}, \quad a_2 = \sum_{j\neq m}^{\overline{S}} \delta_0^{(j)}\,\delta_0^{(m)}, \quad \ldots, \quad a_{\overline{S}-1} = (-1)^{\overline{S}-1}\prod_j^{\overline{S}} \delta_0^{(j)}, \quad a_h = 0, \forall h < 0.$$

Substituting the expressions (C.16) of $\mathbf{\Gamma}$ and $\overline{\mathbf{\Gamma}}$ into (C.15) yields the inverse matrices $\overline{\mathbf{A}}_{0\tau}^{-1} = \overline{\mathbf{X}}^R\,\overline{\mathbf{\Gamma}}^{-1} = \overline{\mathbf{X}}^R\mathbf{Diag}\left(\frac{1}{\overline{X}_{01}^{(R)}}\right)\overline{\mathbf{D}}_{\overline{S}}^{-1}$ and $\mathbf{A}_{0\tau-} = \mathbf{\Gamma}_-\mathbf{X}^L = \mathbf{D}_{S-}\,\mathbf{Diag}\left(X_{01}^{(R)}\right)\mathbf{X}^L$, which transform the divergence (18) in analysts' recovered time preferences (in the first order of ε) into

$$\overline{\delta}^{(1)}(\varepsilon) - \delta^{(1)}(\varepsilon) \;\sim\; \left[\overline{\mathbf{x}}_0^{(1,L)}\,\overline{\mathbf{A}}_{0\tau}^{-1}\mathbf{A}_{0\tau-} \;-\; \mathbf{x}_0^{(1,L)}\right]\,\mathbf{B}^+\,\overline{\mathbf{x}}_0^{(1,R)}$$

$$\text{(C.19)} \qquad = \left[\overline{\mathbf{x}}_0^{(1,L)}\,\overline{\mathbf{X}}^R\,\mathbf{Diag}\left(\frac{1}{\overline{X}_{01}^{(R)}}\right)\overline{\mathbf{D}}_{\overline{S}}^{-1}\,\mathbf{D}_{S-}\,\mathbf{Diag}\left(X_{01}^{(R)}\right)\mathbf{X}^L \;-\; \mathbf{x}_0^{(1,L)}\right]\,\mathbf{B}^+\,\overline{\mathbf{x}}_0^{(1,R)}.$$

Note that the $\overline{S}$ eigenvalues $\{\delta_0^{(k)}\}$, $\in \{1,\ldots,\overline{S}\}$, in matrix $\overline{\mathbf{D}}_{\overline{S}}$ (C.15) are also in matrix $\mathbf{D}_S$, and the $\overline{S}$ first components $\{\overline{x}_{01}^{(k,R)}\}$, $k \in \{1,\ldots,\overline{S}\}$ in matrix $\mathbf{Diag}(\overline{X}_{01}^{(R)})$ are also in matrix $\mathbf{Diag}(X_{01}^{(R)})$ because the unperturbed component is consistent by construction. The cancellation of these quantities in (C.19) yields an explicit decomposition for the divergence in the recovered time preferences[16]

$$\overline{\delta}^{(1)}(\varepsilon) - \delta^{(1)}(\varepsilon) \;\sim\; \sum_{k=\overline{S}+1}^{S} \underbrace{\left(\sum_{i=1}^{\overline{S}} \left[\overline{\mathbf{D}}_{\overline{S}}^{-1}\right]_{1i}\left[\delta_0^{(k)}\right]^i \frac{x_{01}^{(k,R)}}{x_{01}^{(1,R)}}\right)}_{\equiv C_{1k}} \mathbf{x}_0^{(k,L)}\,\mathbf{B}^+\,\overline{\mathbf{x}}_0^{(1,R)}$$

[16] Because the $\overline{S}\times S$ matrix $\mathbf{D}_{S-}$ is obtained by dropping $(S-\overline{S})$ extra rows (not needed for the recovery in $\overline{\mathcal{S}}$) of the $S\times S$ matrix $\mathbf{D}_S$, the matrix product $\overline{\mathbf{D}}_{\overline{S}}^{-1}\,\mathbf{D}_{S-}$ can be separated into two blocks. The left block is the identity matrix $\mathbb{1}_{\overline{S}\times\overline{S}}$ that helps to cancel term $\mathbf{x}_0^{(1,L)}$ in (C.19). The remaining (right) block retains the last $(S-\overline{S})$ columns of matrix $\mathbf{D}_S$. Further, the orthonormality between right and left eigenvectors implies $\overline{\mathbf{x}}_0^{(1,L)}\,\overline{\mathbf{X}}^R = (1,0,\ldots,0)$ which retains only the first row of $\overline{\mathbf{D}}_{\overline{S}}^{-1}$ in the resulting divergence (C.20).

$$= \sum_{k=\overline{S}+1}^{S} C_{1k}\ \mathbf{x}_0^{(k,L)}\ \mathbf{B}^+\ \overline{\mathbf{x}}_0^{(1,R)}, \tag{C.20}$$

where $\left[\overline{\mathbf{D}}_{\overline{S}}^{-1}\right]_{1i}$ is the element $(1,i)$ of the inverse Vandermonde matrix $\left[\overline{\mathbf{D}}_{\overline{S}}^{-1}\right]$ (C.17).

Compared to the qualitative expression (18), the explicit decomposition (C.20) offers deeper quantitative insights into factors driving the inconsistencies in the recovered time preferences. First, only the couplings between the dominant eigenvector $\overline{\mathbf{x}}_0^{(1,R)}$ and extra eigenvectors $\mathbf{x}_0^{(k,L)}$, $k \in \{\overline{S}+1,\ldots,S\}$, contribute to the inconsistencies. This is because the couplings between the dominant and the lower eigenvectors $\mathbf{x}_0^{(k,L)}$, $k \in \{1,\ldots,\overline{S}\}$, are present and common in the recovery results for both original ($\mathcal{S}$) and consolidated ($\overline{\mathcal{S}}$) specifications, hence are canceled out in the divergence of the two recovery results (Footnote 16). In the special case of consistent perturbative components, $\mathbf{x}_0^{(k,L)}\ \mathbf{B}^+ = 0$ for every (extra) state $k \in \{\overline{S}+1,\ldots,S\}$, the couplings with the extra eigenvectors $\mathbf{x}_0^{(k,L)}$ vanish and the recovery consistency is preserved, $\overline{\delta}^{(1)}(\varepsilon) = \delta^{(1)}(\varepsilon)$.

Second, the couplings between the dominant eigenvector and extra eigenvectors $\{\mathbf{x}_0^{(k,L)}\}$ are scaled by corresponding factors $\{C_{1k}\}$, $k \in \{\overline{S}+1,\ldots,S\}$ in the divergence (C.20). Being linear combinations of the elements (C.17) of the inverse Vandermonde matrix, these factors are explicit and shed light on how recovery inconsistencies vary with analyst's subjective specification $\overline{\mathcal{S}}$. Elements $\left\{\left[\overline{\mathbf{D}}_{\overline{S}}^{-1}\right]_{1i}\right\}$, $i \in \{1,\ldots,\overline{S}\}$, are rational functions of the eigenvalues $\{\delta_0^{(j)}\}$, $j \in \{1,\ldots,\overline{S}\}$, so are the scaling factors $\{C_{1k}\}$, $k \in \{\overline{S}+1,\ldots,S\}$. For a finer subjective specification $\overline{\mathcal{S}}$, i.e. a larger number of coupled states $\overline{S}$, the denominators of $\overline{\mathbf{D}}_{\overline{S}}^{-1}$'s (and the scaling factors) are polynomials of higher orders in the eigenvalues $\prod_{j\neq 1}^{\overline{S}}(\delta_0^{(1)} - \delta_0^{(j)})$. As a result, when the eigenvalues of the underlying one-period AD price matrix $\mathbf{A}_0$ are distributed closely (i.e., a dense spectrum or small spectral gap), a finer specification $\overline{\mathcal{S}}$ may be associated with larger scaling factors (i.e., rational functions with larger numbers of poles). We note that a partial fraction decomposition does not mitigate the issue that the magnitudes of the scaling factors, or the degree and number of poles of the denominators of $\overline{\mathbf{D}}_{\overline{S}}^{-1}$'s and $\{C_{1k}\}$, increase with a finer $\overline{\mathcal{S}}$ (a larger $\overline{S}$) when the eigenvalues are similar. To see this in an analogous example, note that the

partial fraction decomposition generates the identity,

$$\text{(C.21)}\quad \frac{1}{\left(x-\delta_0^{(2)}\right)\left(x-\delta_0^{(3)}\right)} = \frac{a}{x-\delta_0^{(2)}} + \frac{b}{x-\delta_0^{(3)}}, \quad \text{with:} \quad a=\frac{1}{\delta^{(3)}-\delta^{(2)}}, \quad b=\frac{1}{\delta^{(2)}-\delta^{(3)}}.$$

When $x=\delta_0^{(1)}$ in this example, the identity becomes

$$\text{(C.22)}\quad \frac{1}{\left(\delta_0^{(1)}-\delta_0^{(2)}\right)\left(\delta_0^{(1)}-\delta_0^{(3)}\right)} = \frac{1}{\left(\delta_0^{(3)}-\delta_0^{(2)}\right)\left(\delta_0^{(1)}-\delta_0^{(2)}\right)} + \frac{1}{\left(\delta_0^{(2)}-\delta_0^{(3)}\right)\left(\delta_0^{(1)}-\delta_0^{(3)}\right)}.$$

That is, all terms on both sides of this equality are of the same order, each has two poles. In the general case of inconsistent perturbative components, the couplings $\mathbf{x}_0^{(k,L)}\ \mathbf{B}^+\ \overline{\mathbf{x}}_0^{(1,R)}$, $k\in\{\overline{S}+1,\ldots,S\}$, are non-zero (and unconstrained by the consistency requirement). When scaled by larger factors $\{C_{1k}\}$ associated with a finer subjective specification $\overline{\mathcal{S}}$, these couplings may produce a larger divergence (C.20), i.e., larger recovery inconsistencies.

A comparison of the divergences in the recovered risk preferences' loadings (22) and in the recovered time preferences (18) indicates that an explicit expression for the former can be obtained in an identical procedure, i.e., replacing C_{1k} in (C.20) by C_{hk}, and $\left[\overline{\mathbf{D}}_{\overline{S}}^{-1}\right]_{1i}$ in (C.17) by $\left[\overline{\mathbf{D}}_{\overline{S}}^{-1}\right]_{hi}$, where $h\in\{2,\ldots,\overline{S}\}$. The resulting explicit expressions for the recovered risk preferences then implicate similar quantitative findings on the sources driving the inconsistencies in the recovered marginal utilities.

In summary, the analysts' recovery results remain divergent as long as their recovery specifications remain inconsistent with each other. The perturbative setup demonstrates that the divergence between an analyst's recovery results and the underlying is scaled by rational functions of the AD price matrix's eigenvalues. The analyst's finer subjective specification suppresses the degree of these rational functions, which is the difference between the degrees of the polynomials in the numerator and denominator of a rational function. As a result, when the eigenvalues are distributed closely, a finer subjective specification may actually increase the divergence, hence the inconsistencies, of the recovery results. This is because a dense spectrum of the AD price matrix implies that higher eigenspaces perturb and distort the dominant (recovery) one more strongly.

Spectral Gaps of AD Price Matrices: Consider the eigenproblem of AD price matrices $\mathbf{A}(\varepsilon)$ and $\overline{\mathbf{A}}(\varepsilon)$ (14) in the perturbative setup,

(C.23)

$$\mathbf{A}(\varepsilon)\,\mathbf{x}^{(k,R)}(\varepsilon) = \delta^{(k)}(\varepsilon)\,\mathbf{x}^{(k,R)}(\varepsilon), \text{ with } \begin{cases} \mathbf{A}(\varepsilon) = \mathbf{A}_0 + \varepsilon\mathbf{B} \\ \delta^{(k)}(\varepsilon) = \delta_0^{(k)} + \varepsilon\Delta\delta^{(k)}, & k \in \{1,\ldots,S\}, \\ \mathbf{x}^{(k,R)}(\varepsilon) = \mathbf{x}_0^{(k,R)} + \varepsilon\Delta\mathbf{x}^{(k,R)}, \end{cases}$$

and

(C.24)

$$\overline{\mathbf{A}}(\varepsilon)\,\overline{\mathbf{x}}^{(k,R)}(\varepsilon) = \overline{\delta}^{(k)}(\varepsilon)\,\overline{\mathbf{x}}^{(k,R)}(\varepsilon), \text{ with } \begin{cases} \overline{\mathbf{A}}(\varepsilon) = \overline{\mathbf{A}}_0 + \varepsilon\overline{\mathbf{B}} \\ \overline{\delta}^{(k)}(\varepsilon) = \overline{\delta}_0^{(k)} + \varepsilon\Delta\overline{\delta}^{(k)}, & k \in \{1,\ldots,\overline{S}\}, \\ \overline{\mathbf{x}}^{(k)}(\varepsilon) = \overline{\mathbf{x}}_0^{(k)} + \varepsilon\Delta\overline{\mathbf{x}}^{(k)}, \end{cases}$$

Substituting the perturbative expansions in the second part into the first part of (C.23), matching terms linear in ε, multiplying to the left of the resulting equation by the unperturbed k-th left (row) eigenvector $\mathbf{x}_0^{(k,L)}$, and employing the orthonormality between left and right eigenvectors, yield the eigenvalues (i.e., spectrum) of the AD matrix $\mathbf{A}(\varepsilon)$ associated with the original specification (and similarly for the spectrum of the AD matrix $\overline{\mathbf{A}}(\varepsilon)$),

(C.25)

$$\begin{cases} \delta^{(k)}(\varepsilon) = \delta_0^{(k)} + \varepsilon\,\mathbf{x}_0^{(k,L)}\,\mathbf{B}\,\mathbf{x}_0^{(k,R)}, \\ k \in \{1,\ldots,S\}, \end{cases} \qquad \begin{cases} \overline{\delta}^{(k)}(\varepsilon) = \overline{\delta}_0^{(k)} + \varepsilon\,\overline{\mathbf{x}}_0^{(k,L)}\,\overline{\mathbf{B}}\,\overline{\mathbf{x}}_0^{(k,R)}, \\ k \in \{1,\ldots,\overline{S}\}. \end{cases}$$

Since the unperturbed components of the perturbative setup (12) are consistent, the two spectra share $\overline{S}$ unperturbed components of their eigenvalues

(C.26)

$$\delta_0^{(k)} = \overline{\delta}_0^{(k)}, \qquad \forall k \in \{1,\ldots,\overline{S}\}.$$

The distances from the k-th eigenvalue to the dominant (first) eigenvalue (or, spectral gaps) in the original and consolidated spectra are

$$\delta^{(k)}(\varepsilon) - \delta^{(1)}(\varepsilon) = \left[\delta_0^{(k)} - \delta_0^{(1)}\right] + \varepsilon\left[\mathbf{x}_0^{(k,L)}\,\mathbf{B}\,\mathbf{x}_0^{(k,R)} - \mathbf{x}_0^{(1,L)}\,\mathbf{B}\,\mathbf{x}_0^{(1,R)}\right], \quad \forall k \in \{1,\ldots,S\},$$

$$\overline{\delta}^{(k)}(\varepsilon) - \overline{\delta}^{(1)}(\varepsilon) = \left[\overline{\delta}_0^{(k)} - \overline{\delta}_0^{(1)}\right] + \varepsilon\left[\overline{\mathbf{x}}_0^{(k,L)}\,\overline{\mathbf{B}}\,\overline{\mathbf{x}}_0^{(k,R)} - \overline{\mathbf{x}}_0^{(1,L)}\,\overline{\mathbf{B}}\,\overline{\mathbf{x}}_0^{(1,R)}\right], \quad \forall k \in \{1,\ldots,\overline{S}\}.$$

Since these spectral gaps share identical unperturbed components (C.26) for $k \in \{1,\ldots,\overline{S}\}$, their relative spectral gaps for these eigenvalues are linear in ε. Up to the multiplicative constant of ε, the relative gaps are[17]

$$RG^{(k)} \equiv \left[\overline{\delta}^{(k)}(\varepsilon) - \overline{\delta}^{(1)}(\varepsilon)\right] - \left[\delta^{(k)}(\varepsilon) - \delta^{(1)}(\varepsilon)\right]$$

$$\sim \left(\overline{\mathbf{x}}_0^{(k,L)}\,\overline{\mathbf{B}}\,\overline{\mathbf{x}}_0^{(k,R)} - \overline{\mathbf{x}}_0^{(1,L)}\,\overline{\mathbf{B}}\,\overline{\mathbf{x}}_0^{(1,R)}\right) - \left(\mathbf{x}_0^{(k,L)}\,\mathbf{B}\,\mathbf{x}_0^{(k,R)} - \mathbf{x}_0^{(1,L)}\,\mathbf{B}\,\mathbf{x}_0^{(1,R)}\right) \tag{C.27}$$

$$= \left(\overline{\mathbf{x}}_0^{(k,L)}\,\overline{\mathbf{B}}\,\overline{\mathbf{x}}_0^{(k,R)} - \mathbf{x}_0^{(k,L)}\,\mathbf{B}\,\mathbf{x}_0^{(k,R)}\right) - \left(\overline{\mathbf{x}}_0^{(1,L)}\,\overline{\mathbf{B}}\,\overline{\mathbf{x}}_0^{(1,R)} - \mathbf{x}_0^{(1,L)}\,\mathbf{B}\,\mathbf{x}_0^{(1,R)}\right), \qquad k \in \{2,\ldots,\overline{S}\}.$$

We now employ the general identity $\overline{\mathbf{B}} = \overline{\mathbf{A}}_{0\tau}^{-1}\,\mathbf{A}_{0\tau-}\mathbf{B}^{+}$ (15) and the consistency property of the unperturbed right eigenvectors $\mathbf{x}_0^{(k,R)}$ and $\overline{\mathbf{x}}_0^{(k,R)}$, which share relevant identical components, to reduce $\mathbf{B}\,\mathbf{x}_0^{(k,R)}$ to $\mathbf{B}^{+}\,\overline{\mathbf{x}}_0^{(k,R)}$, for $k \in \{2,\ldots,\overline{S}\}$, as in (11). As a result, up to the multiplicative constant of ε, the relative spectral gaps of AD price matrices $\overline{\mathbf{A}}$ and $\mathbf{A}$ can be written (similar to (18))

$$RG^{(k)} \equiv \left[\overline{\delta}^{(k)}(\varepsilon) - \overline{\delta}^{(1)}(\varepsilon)\right] - \left[\delta^{(k)}(\varepsilon) - \delta^{(1)}(\varepsilon)\right]$$

$$\sim \underbrace{\left[\overline{\mathbf{x}}_0^{(k,L)}\,\overline{\mathbf{A}}_{0\tau}^{-1}\mathbf{A}_{0\tau-} - \mathbf{x}_0^{(k,L)}\right]}_{\text{unperturbed \& consistent factor}}\underbrace{\mathbf{B}^{+}\,\overline{\mathbf{x}}_0^{(k,R)}}_{\text{perturbative factor}} - \underbrace{\left[\overline{\mathbf{x}}_0^{(1,L)}\,\overline{\mathbf{A}}_{0\tau}^{-1}\mathbf{A}_{0\tau-} - \mathbf{x}_0^{(1,L)}\right]}_{\text{unperturbed \& consistent factor}}\underbrace{\mathbf{B}^{+}\,\overline{\mathbf{x}}_0^{(1,R)}}_{\text{perturbative factor}}, \tag{C.28}$$

for all $k \in \{2,\ldots,\overline{S}\}$. Two observations concerning these relative spectral gaps are in order. While the first shows that both recovery inconsistencies and non-vanishing relative spectral gaps originate from different retentions of information in two inconsistent specifications, the second shows the difference between recovery inconsistencies and relative spectral gaps.

First observation: In the special case where the perturbative components $\mathbf{B}$ and $\overline{\mathbf{B}}$ of AD price matrices are consistent, we have $\mathbf{A}_{0\tau-}\mathbf{B}^{+} = \overline{\mathbf{A}}_{0\tau}\overline{\mathbf{B}}$, and $\mathbf{x}_0^{(k,L)}\mathbf{B}^{+} = \overline{\mathbf{x}}_0^{(k,L)}\overline{\mathbf{B}}$, for all $k \in \{1,\ldots,\overline{S}\}$. As a result, both terms on the RHS of (C.28) vanish, reducing to relative spectral gaps $RG^{(k)} = 0$, $\forall k \in \{1,\ldots,\overline{S}\}$ as information about the underlying market model is preserved by consistent

[17] That is, the multiplicative constant ε is omitted from the right-hand side of (C.27) for notational and exposition simplicities.

perturbative components $\mathbf{B}$ and $\overline{\mathbf{B}}$. In the general case where the perturbative components of AD price matrices are not consistent with each other, $\mathbf{B}$ and $\overline{\mathbf{B}}$ are not constrained by consistency conditions. Their exogeneity imply that both terms on the RHS of (C.28) do not vanish in general. Furthermore, due to this exogeneity, a finer consolidated specification $\mathcal{S}$ does not unambiguously increase or decrease the correlation between the consistent and inconsistent factors in each of the two terms on the RHS of (C.28). Intuitively, a finer $\mathcal{S}$ does not necessarily reduce the relative spectral gaps $RG^{(k)}$, $k \in \{2, \ldots, \overline{S}\}$, because information about the underlying market model is not preserved by inconsistent perturbative components $\mathbf{B}$ and $\overline{\mathbf{B}}$.

Second observation: We examine and compare inconsistencies in recovered marginal utilities (21) versus relative spectral gaps of AD price matrices (C.28). Since the unperturbed eigenvalues $\{\delta_0^{(k)}\}$, $k \in \{1, \ldots, S\}$, and $\{\overline{\delta}_0^{(k)}\}$, $k \in \{1, \ldots, \overline{S}\}$, appear explicitly in (21), an important factor to the recovery inconsistencies of marginal utilities is the unpaired terms among the two sums in (21) (indexed by $k \in \{\overline{S}+1, \ldots, S\}$, associated with the original specification). Whereas, since the relative spectral gaps (C.28) concern the comparison of the spectral gaps of AD price matrices, they are about the paired eigenvalues (indexed by $k \in \{1, \ldots, \overline{S}\}$), which differ only in their perturbative components (see (C.26)). As a result, a finer specification affects the recovery inconsistencies in marginal utilities in two channels: (i) the divergence of the paired numerators $\overline{\mathbf{x}}_0^{(k,L)} \overline{\mathbf{B}} \overline{\mathbf{x}}_0^{(1,R)}$ and $\mathbf{x}_0^{(k,L)} \mathbf{B} \mathbf{x}_0^{(1,R)}$, $k \in \{1, \ldots, \overline{S}\}$ in (21) due to inconsistent perturbative components of AD price matrices, and (ii) the change in the number of unpaired terms (unpaired contributions) among the two sums in (21). In contrast, a finer specification affects the relative spectral gaps of AD price matrices (C.28) in the first channel as discussed in the first observation above.

Altogether, these results derive and quantify the non-convergence property of the recovery consistency issue summarized in Proposition 2.

A digression on the Vandermonde matrix: To relate the Vandermonde matrix to the recovery setting, we recall a well-known application of this matrix (and its inverse). This application concerns the exact fitting of a $(n-1)-$degree polynomial $f(x)$ that passes through n given points $\{(x_0, y_0) \ldots (x_{n-1}, y_{n-1})\}$. The fitting "recovers" n unknown coefficients $\{a_0, \ldots, a_{n-1}\}$ of poly-

nomial $f(x)$ via an equation system

(C.29) Vandermonde system:
$$\begin{cases} a_0 + a_1 x_0 + a_2 x_0^2 + \ldots + a_{n_1} x_0^{n-1} &= y_0, \\ a_0 + a_1 x_1 + a_2 x_1^2 + \ldots + a_{n_1} x_1^{n-1} &= y_1, \\ \vdots & \\ a_0 + a_1 x_{n-1} + a_2 x_{n-1}^2 + \ldots + a_{n_1} x_{n-1}^{n-1} &= y_{n-1}, \end{cases}$$

or in matrix form

(C.30)
$$[a_0 \;\; a_1 \;\; \ldots \;\; a_{n-1}] \underbrace{\begin{bmatrix} 1 & 1 & \ldots & 1 \\ x_0 & x_1 & \ldots & x_{n-1} \\ \vdots & \vdots & \ddots & \vdots \\ x_0^{n-1} & x_1^{n-1} & \ldots & x_{n-1}^{n-1} \end{bmatrix}}_{\text{Vandermonde matrix}} = [y_0 \;\; y_1 \;\; \ldots \;\; y_{n-1}] .$$

From this follows a unique solution for the coefficients, $\{a_k\}$, $k \in \{0, \ldots, n-1\}$ from x's and y's coordinates.

A change of notation relates this equation system to our recovery setting (C.16). After replacing S with n, and $\delta_0^{(k+1)}$ by x_k (for $k \in \{0, \ldots, S-1\}$), the matrix product $\mathbf{D}_S$ **Diag** $\left(\frac{1}{\delta_0^{(1)}}, \frac{1}{\delta_0^{(2)}}, \ldots, \frac{1}{\delta_0^{(S)}} \right)$ (where $S \times S$ matrix $\mathbf{D}_S$ is given (C.16)) becomes the $n \times n$ Vandermonde matrix on the LHS of the system (C.30). Since the analytical expression for the inverse of the Vandermonde matrix is known, the analytical expression for the inverse matrix $[\mathbf{D}_S]^{-1}$ is also known. The same holds for $\overline{\mathbf{D}}_{\overline{S}}$ in (C.16), which yields explicit expressions for its elements $\left[\overline{\mathbf{D}}_{\overline{S}}^{-1}\right]_{1i}$ (C.17).